

Lecture 4: Non linear parameter estimation problems: tools for enhancing metrological objectives

B. Rémy, S. André, D.Maillet¹

¹ LEMTA, Université de Lorraine & CNRS, Vandœuvre-lès-Nancy, France

E-mail: benjamin.remy@univ-lorraine.fr
stephane.andre@univ-lorraine.fr
denis.maillet@univ-lorraine.fr

Abstract. The aim of this lecture is to present a methodology for enhancing the estimation of parameters in the case on Non-Linear Parameter Estimation problem (NLPE). After some definitions and vocabulary precisions, useful tools to investigate NLPE problems will be introduced. Different techniques will be proposed for tracking for instance the true degree of freedom of a given estimation problem (Correlation, Rank of sensitivity matrix, SVD, ..) and enhancing the estimation of particular parameters by using either Reduced model or Model with fixed parameters. The reduced model can be unbiased or biased. We will present a technique allowing to check whether a model is biased or not. We will show how it is possible to use the residuals plot for evaluating the systematic error on the parameters estimated through a biased model. Different examples in thermal metrology will be presented for illustrating all these points.

List of acronyms:

- **NLPE:** Non Linear Parameter Estimation
- **PEP:** Parameter Estimation Problem
- **MBM:** Model-Based Metrology
- **SVD:** Singular Value Decomposition
- **OLS:** Ordinary Least Squares
- **SNR:** Signal-to-Noise Ratio

Scope

1. Foreword
2. Some definitions and vocabulary precisions
3. Useful tools to investigate NLPE problems
 - 3.1 Sensitivities
 - 3.2 Variance/Correlation matrix
 - 3.3 Ill-conditioned PEP and strategies for tracking true degrees of freedom
 - 3.3.1 Pathological example of ill-conditioning resulting from correlated parameters

- 3.3.2 Rank of the sensitivity matrix.
 - 3.3.3 Generalization: use of SVD to track PEP degrees of freedom
 - 3.3.3.1 Parameterizing a NLPE problem around the nominal values of its parameters
 - 3.3.3.2 Reminder of the Singular Value Decomposition of a rectangular matrix
 - 3.3.3.3 Singular Value Decomposition of the scaled sensitivity matrix
 - 3.3.3.4 Non linear ordinary least square estimator and SVD
 - 3.3.3.5 Mean quadratic estimation error and singular values
 - 3.3.3.6 Residuals analysis and signature of the presence of a bias in the metrological process
 - 4. Enhancing the performances of estimation
 - 4.1 Dimensional analysis or natural parameters: case of coupled conduction/radiation flash experiment
 - 4.2 Reducing the PEP to make it well-conditioned: case of thermal characterization of a deposit
 - 4.3 Note on the change of parameters
 - 5. Models with different numbers of parameters: the hot wire case
 - 5.1 Different models for thermal characterization by the hot wire method
 - 5.1.1 The standard hot wire model: model 0
 - 5.1.2 The finite hot wire model: model 1
 - 5.1.3 The semi-infinite hot wire model: model 2
 - 5.2 Sensitivity study
 - 5.3 Model Reduction using fewer parameters
 - 6. Design optimization: flash experiment for thermal characterization of a liquid
 - 6.1 Modelling
 - 6.2 Solution
 - 6.3 Sensitivity study
 - 6.4 Simplified study with a two-parameter model
 - 6.5 Change in the definition of the parameters
 - 7. Taking the bias into account to reduce the variances on estimated parameters: case of the flash method
 - 7.1 Modelling
 - 7.2 Estimation with no bias
 - 7.3 Estimation with a bias: whole domain approach
 - 7.4 Estimation with a bias: use of a variable estimation time interval
 - 7.5 Correction of the bias using a variable estimation time interval: application to the flash method
 - 8. Conclusion
- References

1. Foreword

The Non Linear Parameter Estimation problem has been the subject of numerous lectures during the past METTI schools (see [1] Thermal Measurements and Inverse Techniques, edited by Helcio R.B. Orlande, Olivier Fudym, Denis Maillet, Renato M. Cotta, Series: Heat Transfer, CRC Press, 770 p, 2011). This text aims first at gathering in a synthetic way the basic notions and tools that can be used practically to analyse NLPE problems in engineering and science.

At the same time, it provides new insights about the tools available to:

- (i) enhance our knowledge about parameter identifiability in a given problem (which parameters can be really estimated in a given experiment and which precision can be achieved ?),
- (ii) track the origin of pitfalls in PEP,
- (iii) offer new perspectives for enhancing the quality of MBM in a general way.

2. Some definitions and vocabulary precisions

Performances of contemporary metrology, that is material characterization, are not the result of the enhancement of the technology of measuring instruments only. They are rather the consequence of the significant progresses accomplished in the field of Inverse Problems solving, especially when it is based on a very large amount of data. These are provided by new tools and by the facilities now available for numerical acquisition of experimental signals (CCD detectors allowing for 2D/3D numerical data and high frequency time resolution). Understanding the conditions for which parameters can be estimated from the model/measurements pair constitutes also a key point for reaching a high quality estimation.

Measuring a physical quantity β_j requires a specific experiment allowing for this quantity to "express itself as much as possible" (notion of sensitivity). This experiment requires a system onto which inputs $u(t)$ are applied (stimuli) and whose outputs $y(t)$ are collected (observations). t is the explanatory variable: it corresponds to time for a purely dynamical experiment. A model M is required to mathematically express the dependence of the system's response with respect to quantity β_j and to other additional parameters β_k ($k \neq j$): $y_{mo} = \eta(t, \beta, u)$. Many candidates may exist for function η - depending on the degree of complexity reached for modelling the physical process - which may exhibit different mathematical structure - depending for example on the type of method used to solve the model equations. Once this model is established, the physical quantities in vector β acquire the status of model parameters. This model (called knowledge model if it is derived from physical laws and/or conservation principles) is initially established in a direct formulation. Knowing inputs $u(t)$ and the value taken by parameter β , the output(s) can be predicted.

The linear or non linear character of the model has to be determined:

- A Linear model with respect to its Inputs (LI structure) is such as:

$$y_{mo}(t, \beta, \alpha_1 u_1 + \alpha_2 u_2) = \alpha_1 y_{mo}(t, \beta, u_1) + \alpha_2 y_{mo}(t, \beta, u_2) \quad (1)$$

- A Linear model with respect to its parameters (LP structure) is such as:

$$y_{mo}(t, \alpha_1 \beta_1 + \alpha_2 \beta_2, u) = \alpha_1 y_{mo}(t, \beta_1, u) + \alpha_2 y_{mo}(t, \beta_2, u) \quad (2)$$

In a metrological problem referred here as MBM, observations of the outputs will be provided by measurements. The inverse problem consists in making the direct problem work backwards with the objective of getting (extracting) β from $y_{mo}(t, \beta, u)$ for given inputs and observations y . This is an identification process. The difficulty stems here from two points:

- Measurements y are subjected to random perturbations (intrinsic noise ϵ) which in turn will generate perturbed estimated values $\hat{\beta}$ of β , even if the model is perfect: this constitutes an estimation problem.
- the mathematical model may not correspond exactly to the reality of the experiment. Measuring the value of β in such a condition leads to a biased estimation

$Bias = E(\hat{\beta}) - \beta^{true}$: this corresponds to an identification problem (which model η to use ?) associated to an estimation problem (how to estimate β for a given model?).

The estimation/identification process basically tends to make the model match the data (or the contrary). This is made by using some mathematical "machinery" aiming at reducing some gap (distance or norm)

$$r(\beta) = y - y_{mo}(t, \beta, u) \tag{3}$$

One of the obvious goal of NLPE studies is then to be able to assess the performed estimation through the calculation of the variances $V(\hat{\beta})$ of the estimators of the different parameters. If the probabilistic distribution law of the noise is known, this allows to give the order of magnitude of confidence bounds for the estimates. NLPE problems require the use of Non Linear statistics for studying such properties of the estimates.

Because of the two above-mentioned drawbacks of MBM, the estimated or measured value of a parameter β_j will be considered as "good" if it is not biased and if its variance is minimum. Quantifying the bias and variance is also helpful to determine which one of two rival experiments is the most appropriate for measuring the searched parameter (Optimal design). In case of multiple parameters (vector β) and NLPE problems, it is also helpful to determine which components of vector β are correctly estimated in a given experiment.

3. Useful tools to investigate NLPE problems

3.1. Sensitivities

The central role of the sensitivity matrix in PEP has been shown in the preceding lecture (Lecture 2). In the case of a single output signal y with m sampling points for the explanatory variable t and for a model involving n parameters, the sensitivity matrix is ($m \times n$) defined as

$$S_{ij} = \left. \frac{\partial y_{mo}(t_i; \beta^{nom})}{\partial \beta_j} \right|_{t, \beta_k \text{ for } k \neq j} \tag{4}$$

As the problem is NL, the sensitivity matrix has only a local meaning. It is calculated for a given nominal parameter vector β^{nom} .

If the model has a LP structure, this means that the sensitivity matrix is independent from β . It can be expressed as (Lecture 2)

$$y_{mo}(t, \beta) = \sum_{j=1}^n S_j(t) \beta_j \tag{5}$$

The sensitivity coefficient $S_j(t)$ to the j^{th} parameter β_j corresponds to the j^{th} column of matrix S . The primary way of getting information about the identifiability of the different parameters is to analyse and compare the sensitivity coefficients through graphical observations. This is possible only when considering reduced sensitivity coefficients S_j^* (sometimes called "scaled" sensitivity coefficients) because the parameters of a model do not have in general the same units.

$$S_j^* = \beta_j S_j = \beta_j \left. \frac{\partial y_{mo}(t; \boldsymbol{\beta}^{nom})}{\partial \beta_j} \right|_{t, \beta_k \text{ pour } k \neq j} = \left. \frac{\partial y_{mo}(t; \boldsymbol{\beta}^{nom})}{\partial (\ln \beta_j)} \right|_{t, \beta_k \text{ pour } k \neq j} \quad (6)$$

or

$$\mathbf{S}^* = \mathbf{S} \mathbf{R} \quad (7)$$

with \mathbf{R} the square diagonal matrix whose diagonal is composed of the components β_j of $\boldsymbol{\beta}$.

TOOL Nr1: A superimposed plot of reduced sensitivity coefficients $S_j^*(t)$ gives a first idea about the most influential parameter for a given model (largest magnitude) and about possible correlations (sensitivity coefficients following the same evolution).

Example: Measurement of thermophysical properties of a coating layer through the Flash method using thermal contrast principle (Number of parameters $n = 2$).

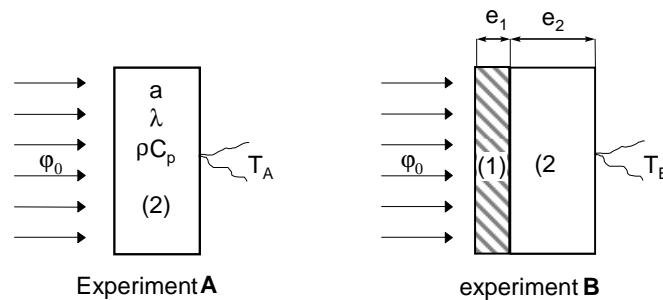


Figure 1 : Basis of the “ thermal contrast ” method

The thermal contrast method requires the repetition of two "flash" experiments **A** and **B** (**Figure 1**). The first one is operated on the substrate only (index (2)) whose thermophysical properties are known. The second experiment is performed on the two-layered sample (index (1)/(2)). In both cases, one records the rear face temperature evolutions. The thermograms so obtained are normalized with respect to their maximum and the difference of the scaled thermograms T_A and T_B is computed to produce the thermal contrast thermogram. This latter is a function of the thermophysical properties of the coating (1) and of the substrate (2) through two parameters:

$$K_1 = \frac{e_1}{e_2} \sqrt{\frac{a_2}{a_1}} \quad \text{and} \quad K_2 = \sqrt{\frac{\lambda_1 \rho_1 c_1}{\lambda_2 \rho_2 c_2}}$$

The observable (contrast curve) and the reduced sensitivity coefficients to K_1 and K_2 are plotted in **Figure 2**. They show (i) that the sensitivities have the same order of magnitude as the signal (a good thing) but unfortunately (ii) these sensitivities appear to be totally correlated (a bad thing). In this case, this simple plot shows that sensitivities to K_1 and K_2 are likely proportional and therefore that the identifiability of both parameters is impossible. This example will be more thoroughly modelled and studied in section 4 of this lecture.

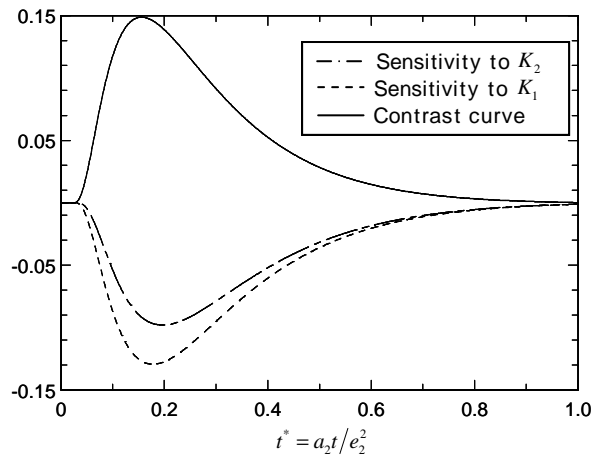


Figure 2 : Reduced sensitivity coefficients for $K_1 = 0.1$ and $K_2 = 1.36$

3.2. Variance/Correlation matrix

To go further and to investigate more deeply the PEP, the statistics of the estimator must be analysed. This can be made when (i) an estimator has been chosen (that is, a method to derive estimated values for the different parameters from the experimental signal), and (ii) the statistical properties of noise $\boldsymbol{\varepsilon}$ are known (according to experimentally founded observations).

Considering the noise on the experimental signal, we assume it unbiased (perfect measurement with ideal sensor), having additive character and a probability law with 0 mean and constant variance σ^2 which correspond to

$$y_i = y_{mo}(t_i; \boldsymbol{\beta}) + \varepsilon_i \quad ; \quad E(\boldsymbol{\varepsilon}) = \mathbf{0} \quad ; \quad \text{cov}(\boldsymbol{\varepsilon}) = \sigma^2 \mathbf{I}_m \quad (8)$$

where \mathbf{I}_m is the identity matrix of size m (number of measurement points).

According to Beck's taxonomy (see [2] p. 134 and chapter VII), these assumptions correspond to the set "1111—11" with the following additional precisions: nonstochastic independent explanatory variable (time), and no prior information for the parameters.

The OLS estimator $\hat{\boldsymbol{\beta}}_{OLS}$ minimizes the least square sum, which gives, for the j^{th} equation

$$J_{OLS}(\boldsymbol{\beta}) = \mathbf{r}^T(\mathbf{t}; \boldsymbol{\beta}, \mathbf{u}) \mathbf{r}(\mathbf{t}; \boldsymbol{\beta}, \mathbf{u}) = \|\mathbf{r}(\mathbf{t}; \boldsymbol{\beta}, \mathbf{u})\|^2 = \sum_{i=1}^m (y_i - y_{mo}(t_i; \boldsymbol{\beta}, \mathbf{u}))^2 \quad (9)$$

where

$$\mathbf{r}(\mathbf{t}; \boldsymbol{\beta}, \mathbf{u}) = \mathbf{y} - \mathbf{y}_{mo}(\mathbf{t}; \boldsymbol{\beta}, \mathbf{u}) \quad (10)$$

are defined as the residuals.

The estimator is produced thanks to a minimization process i.e. when the j^{th} equations

$$\partial J_{OLS}(t, \hat{\boldsymbol{\beta}}_{OLS}) / \partial \beta_j = 0 \quad (j = 1 \dots n) \quad (11)$$

are verified. The OLS estimator can be proved unbiased which means that the statistical mean of repeated estimated values $\hat{\boldsymbol{\beta}}$ is equal to the exact parameter vector $\boldsymbol{\beta}$.

Lecture 2 describes the behaviour of such an estimator for a LP model where the calculations can be fully completed.

In the case of a NL structure, the minimum is found through an iterative process using local linearity (Gauss-Newton algorithm basically, see [3]) of the form:

$$\hat{\beta}_{OLS}^{(k+1)} = \hat{\beta}_{OLS}^{(k)} + \left(\mathbf{S}^{(k)T} \mathbf{S}^{(k)} \right)^{-1} \mathbf{S}^{(k)T} \left(\mathbf{y} - \mathbf{y}_{mo}(\hat{\beta}_{OLS}^{(k)}) \right) \quad (12)$$

(See the corresponding relation in Lecture 2).

The iterative process (12) requires to compute the inverse of matrix $\mathbf{S}^T \mathbf{S}$. Therefore, this latter must offer good enough conditioning through repeated iterations, which is possible if the sensitivity coefficients are non zero and linearly independent. Without any specialized and dedicated tools, this iterative process can be stopped when the residuals norm $\mathbf{r}^T \mathbf{r}$ is of the same order of magnitude as the measurement noise, that is when:

$$J_{OLS}(\hat{\beta}^{(k)}) \approx m \sigma^2 \quad (13)$$

At convergence, the standard deviation of the error made for the estimated parameters can be evaluated thanks to the (symmetrical) **estimated** covariance matrix of the estimator. It characterizes the precision that can be reached on the estimated parameters (its inverse is sometimes named the precision matrix) and depends on the statistical assumptions that can be made on the data. In view of an OLS estimator, this matrix is

$$\text{cov}(\hat{\beta}) \equiv \begin{bmatrix} \text{var}(\hat{\beta}_1) & \text{cov}(\hat{\beta}_1, \hat{\beta}_2) & \cdots & \text{cov}(\hat{\beta}_1, \hat{\beta}_n) \\ \text{cov}(\hat{\beta}_1, \hat{\beta}_2) & \text{var}(\hat{\beta}_2) & & \text{cov}(\hat{\beta}_2, \hat{\beta}_n) \\ \vdots & \vdots & \ddots & \vdots \\ \text{cov}(\hat{\beta}_1, \hat{\beta}_n) & \text{cov}(\hat{\beta}_2, \hat{\beta}_n) & \cdots & \text{var}(\hat{\beta}_n) \end{bmatrix} \approx \sigma^2 \left(\mathbf{S}^T(\hat{\beta}) \mathbf{S}(\hat{\beta}) \right)^{-1} \quad (14)$$

It depends obviously on the level of the Signal-to-Noise Ratio (SNR) and brings into play the inverse of the $\mathbf{S}^T \mathbf{S}$ matrix, already pointed as a decisive operation for a troubleless estimation. Matrix $\mathbf{S}^T \mathbf{S}$, which is also called the Fisher's information matrix with assumptions (8) and under the additional hypothesis of a Gaussian noise, depends on the number of measurement points and of their distribution along the estimation interval, which, by the way, may be optimised if necessary [2]. The diagonal coefficients are the squares of the estimated standard deviation of each parameter $\sigma_{\hat{\beta}_i}^2$. They quantify the error that one can expect through inverse estimation. This is true if the assumptions made for the noise are consistent with the experiment. The problem being NLP, retrieving these optimum bounds through a statistical analysis may depend on the starting guesses made to initialize the estimation algorithm. This matrix can also be an indicator for detecting possible correlations between the parameters. An estimation of the correlation matrix is calculated according to

$$\mathbf{cor}(\hat{\beta}) \approx \begin{bmatrix} 1 & \rho_{ij} & \cdots \\ \rho_{ij} & 1 & \cdots \\ \vdots & \vdots & \ddots \end{bmatrix} \text{ all terms being the result of } \rho_{ij} = \frac{\text{cov}(\hat{\beta}_i, \hat{\beta}_j)}{\sqrt{\sigma_{\hat{\beta}_i}^2 \sigma_{\hat{\beta}_j}^2}} \quad (15)$$

The correlation coefficients (off-diagonal terms) correspond to a quantification of the correlation existing between the two estimations of parameters β_i and β_j and, more precisely, between their errors. They vary between -1 and 1. They are global quantities (in some sense, “averaged” over the considered identification interval, the whole $[0, t]$ here). Gallant [4] suggested that difficulty in computation may be encountered when the common logarithm of the ratio of the largest to smallest eigenvalues of **cor** exceeds one-half the number of significant decimal digits used by the computer.

A more practical hybrid matrix representation **Vcor** can be constructed. It gathers the diagonal terms of the **covariance** matrix (more precisely their square root, normalized by the value of the estimated parameter) and the off-diagonal terms of the **correlation** matrix.

$$\mathbf{Vcor}(\hat{\beta}) \approx \begin{bmatrix} \sqrt{\text{var}(\hat{\beta}_1)} / \hat{\beta}_1 & \rho_{12} & \dots \\ \rho_{21} & \sqrt{\text{var}(\hat{\beta}_2)} / \hat{\beta}_2 & \dots \\ \vdots & \vdots & \ddots \end{bmatrix} \tag{16}$$

TOOL Nr2: Matrix $\mathbf{Vcor}(\hat{\beta})$ gives a quantitative point of view about the identifiability of the parameters. The diagonal gives a kind of measurement (minimal bound!) of the error made on the estimated parameters (due to the sole stochastic character of the noise, supposed unbiased). The off-diagonal terms (correlation coefficients) are generally of poor interest because of their too global character. Values very close to ± 1 may explain very large variances (errors) on the parameters through a correlation effect.

NB: Another matrix, **rcov** ($\hat{\beta}$) defined in equation (52b) further on, is also very useful for assessing the quality of a potential inversion. Its diagonal coefficients are the squares of those of **Vcor** ($\hat{\beta}$), but its off-diagonal coefficients are different.

Example: Here are two **V_{cor}** matrix taken from [1]. They were obtained for the same NLPE problems and for the same given set of nominal values of the $n = 3$ parameters but considering two different observables **A** and **B** (two different locations of the temperature measurements).

$\mathbf{Vcor}_A(\hat{\beta}) \approx \begin{bmatrix} 0.027 & 0.994 & -0.999 \\ \square & 0.0066 & -0.989 \\ \square & \square & 0.029 \end{bmatrix}$ <p>3. Observable A</p>	$\mathbf{Vcor}_B(\hat{\beta}) \approx \begin{bmatrix} 0.0002 & -0.38 & 0.63 \\ \square & 0.0008 & -0.93 \\ \square & \square & 0.0042 \end{bmatrix}$ <p>4. Observable B</p>
---	--

In the case of observable **A**, a high variance (nearly 3% for a one standard deviation error !) is observed for parameters β_1 and β_3 and explained by a high degree of correlation between them ($\rho_{13} = 0.999$). Observable **A** can clearly not be used for estimating these parameters. On the contrary, observable **B** offers good identifiability for all parameters (small variances) and does not show any risk of correlations.

3.3. *Ill-conditioned PEP and strategies for tracking true degrees of freedom*

3.3.1. Pathological example of ill-conditioning resulting from correlated parameters.

The good identifiability of parameters can be related to the local convexity of the cost functional $J_{OLS}(\boldsymbol{\beta})$ in the hyper-parameter space. In case of correlated parameters, one obvious consequence is that many possible local minima will exist and make estimation algorithms fail. The discussion that follows here is taken from an example of inverse estimation in a case of coupled radiative-conductive heat transfer [5]. The thermal characterization of a semi-transparent material implies at least three basic parameters: the thermal diffusion characteristic time $t_d = e^2/a$, the dimensionless optical thickness τ_0 and the dimensionless Planck number N (explanations to follow in section 4.1) and so $\boldsymbol{\beta} = [t_d, \tau_0, N]^T$. The estimation of the three parameters in this NLP problem may be difficult for some range of values of parameters τ_0 and N where matrix $V_{cor}(\hat{\boldsymbol{\beta}})$ shows that a high degree of correlation between these two parameters exists, whereas the value of parameter t_d remains unconcerned.

A plot of the OLS criterium $J_{OLS}(\boldsymbol{\beta})$ in the 2D space (τ_0, N) for a given t_d value and a given noise σ (Figure 3) makes the consequence of such bad conditioning quite clear.

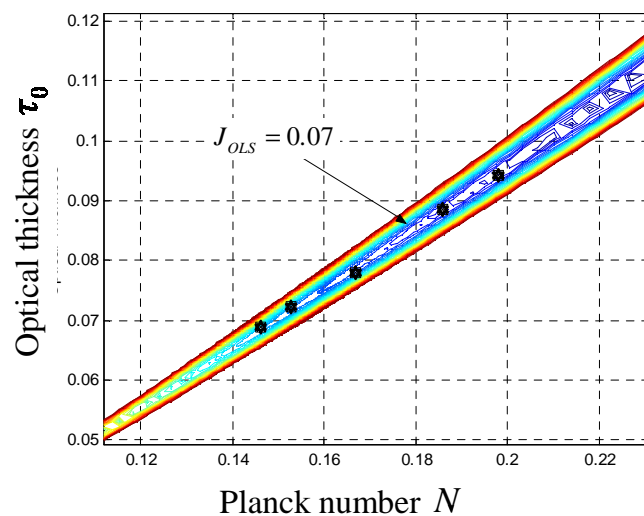


Figure 3 : Level sets for $J_{OLS}(\boldsymbol{\beta})$ in the (τ_0, N) parameter space

All level sets draw a very narrow valley oriented along a line which graphically corresponds to the relation $N \cong 2\tau_0$. A 3D plot would show that the central line of this valley does really correspond to a descending slope and hence that no real minima can be found. The level set indicated in the figure corresponds to exactly $J_{OLS} = 0.07 = m\sigma^2$. Trying to make the iterative optimization algorithm working below this limit for the stopping criterion is useless. In other words, the larger the noise, the higher the stopping level-set should be.

In the present case, this will not change the identifiability criterion. Depending on the initial guesses for the parameters, the deterministic algorithm will find different minima and different parameter

estimates (**Table 1** : Example of local minima found $\hat{\beta}$, case Nr 1,2,3). The big dots in **Figure 3** and the local minimum Nr 4 given in **Table 4** have been obtained with a stochastic algorithm (Simulated Annealing) proving that when the problem is ill-conditioned, stochastic algorithms are of little help for a correct estimation process (as it is usually believed).

Such behavior is more likely the result of a model which is not suitable with respect to the physics involved. In the present case, it is interesting to note in Table 1 that all local minima that were found follows the relation $N(\tau_0 + 1)/\tau_0 = Constant$.

In fact, an approximate modeling for conductive-radiative transfer in optically thin media can be shown to be more pertinent and more parsimonious. It makes naturally arise the notion of radiative resistance R_r which can be expressed as $R_r = N(\tau_0 + 1)/\tau_0$. This resistance is the appropriate parameter in this limiting behavior and prove that there is no way to identify independently τ_0 and N (Many different pair are able to produce the same value for R_r .)

Parameter vector components	Local Minima (found using either deterministic or stochastic algorithms)			
	N°1	N°2	N°3	N°4
a (10^7 m ² /s)	5.2	4.9	5.85	4.8
N	0.6	0.74	0.16	0.82
τ_0	0.38	0.5	0.07 ₆	0.56
$R_r = \frac{N_{Pl}}{\tau_0}(\tau_0 + 1)$	2.18	2.22	2.26	2.28

Table 1 : Example of local minima found $\hat{\beta}$

TOOL Nr3: For an independent noise with known standard deviation and for a given model, it may be interesting to look at the level-set representation of the optimisation criterion in appropriate cut-planes (for given pair of parameters if $n > 3$), and compare it with the minimum achievable criterium given by $J = m\sigma^2$, where m is the number of measurements.

3.3.2. Rank of the sensitivity matrix.

We focus here on the scaled (or reduced) sensitivity matrix (6 and 7). This (m, n) matrix is composed of n column vectors, the reduced sensitivity coefficients \mathbf{S}_j^*

$$\mathbf{S}^* = [\mathbf{S}_1^* \quad \mathbf{S}_2^* \quad \dots \quad \mathbf{S}_n^*] \quad \text{with} \quad \mathbf{S}_j^* = \beta_j \left. \frac{\partial \eta(\mathbf{t}; \boldsymbol{\beta}^{nom})}{\partial \beta_j} \right|_{\mathbf{t}, \beta_k \text{ for } k \neq j} \quad (17)$$

and where \mathbf{t} is a column vector composed by all the m times of measurement:

$$\mathbf{t} = [t_1 \ t_2 \ \dots \ t_m]^T \tag{18}$$

These n column vectors \mathbf{S}_j^* are in fact just the components of a set of n vectors $\vec{\mathbf{S}}_j^*$ in a m -dimension vector space. One can recall here that this set of vector $\Sigma = \{ \vec{\mathbf{S}}_1^*, \vec{\mathbf{S}}_2^*, \dots, \vec{\mathbf{S}}_n^* \}$ is linearly independent only if:

$$\sum_{j=1}^n \alpha_j \mathbf{S}_j^* = \mathbf{0} \Rightarrow \alpha_j = 0 \text{ for any } j \text{ with } 1 \leq j \leq n \tag{19}$$

This means that a linear combination of all these m vectors is equal to zero only if all its coefficients (the α_j 's here) are equal to zero. If it is not the case, system Σ is linearly dependent. Let us note that the presence of a null vector in the set of vectors Σ makes it linearly dependent: such a null vector $\vec{\mathbf{S}}_j^*$ would correspond here to a parameter that has no influence on the variation of the model output, (the very specific case of a parameter β_j equal to zero is discarded here).

So, if the set is dependent, one has to remove one vector $\vec{\mathbf{S}}_j^*$ from the original set Σ and try again to test the independence condition (19) with the $n-1$ remaining vectors. This can be made with the n possible choices for the vector $\vec{\mathbf{S}}_j^*$ that is removed from set Σ . If one finds one such independent set of $n-1$ vectors, the rank of the set is $n-1$. In the opposite case, one has to test the independence with $n-2$ vectors and so on... The rank r of Σ is the larger number of vectors for an independent subset of Σ that can be formed with the n original vectors.

In order to illustrate this, we will assume that $m = n = 2$ and we assume that the model is linear. This corresponds to two observations of a model with two parameters β_1 and β_2 . This leads to the set of two sensitivity vectors $\Sigma = \{ \vec{\mathbf{S}}_1^*, \vec{\mathbf{S}}_2^* \}$ from which the situations shown in Figure 4 can be considered:

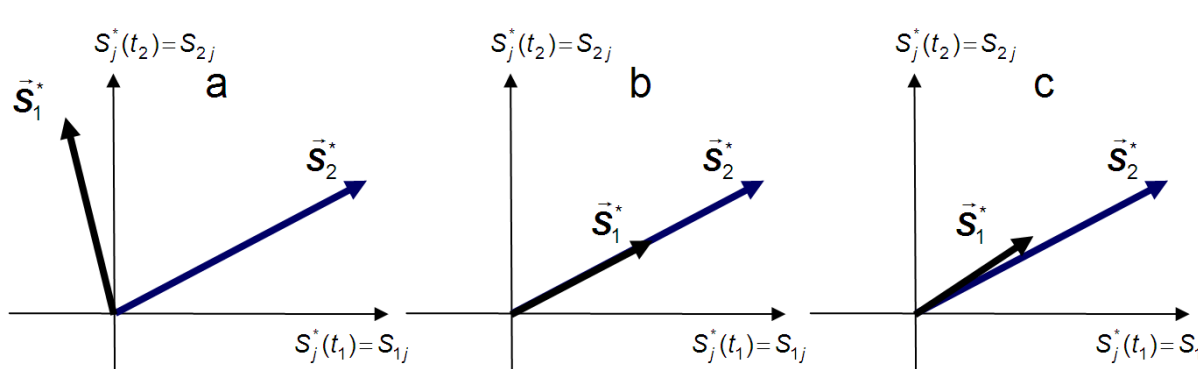


Figure 4 : *Reduced sensitivity vectors:*

a - independent sensitivities ($r = n = 2$) **b** - dependent sensitivities **c** - nearly dependent sensitivities

Case **a** corresponds to linearly independent sensitivity coefficients: the rank of Σ is equal to 2. It is also the rank of the reduced sensitivity matrix \mathbf{S}^* and hence the rank of the sensitivity matrix, since $\mathbf{S}^* = \mathbf{S} \mathbf{R}$ (where \mathbf{R} is the square diagonal matrix with two diagonal coefficients β_1 and β_2 according to equation 7). One can say that the observations of the model output provides two degrees of freedom since two parameters can be estimated.

Case **b** demonstrates a pathological nature of the sensitivity coefficients: they are proportional, with $\bar{\mathbf{S}}_2^* = 2 \bar{\mathbf{S}}_1^*$ (one sees that the choice $\alpha_1 = 2$ and $\alpha_2 = -1$ in (19) allows to show that the set of vectors Σ is not independent) and estimation of both coefficients is not possible anymore. In this case, the rank of \mathbf{S}^* and hence the rank of \mathbf{S} is $r = 1$ and the determinant of the information matrix $\mathbf{S}^T \mathbf{S}$ is equal to zero. This means that the explicit value of $\hat{\beta}_{OLS}$, in the linear case and with a noise of spherical covariance matrix, which requires an inversion of this information matrix is not possible. The same is true for the calculation of the variance-covariance matrix of $\hat{\beta}_{OLS}$: the observations of the model output provide only one degree of freedom and only one parameter can be estimated, if the value of the other one is known.

Case **c** lies in between: the two reduced sensitivity vectors are nearly proportional $\bar{\mathbf{S}}_2^* \approx 2 \bar{\mathbf{S}}_1^*$. Even if the mathematical rank is still equal to 2 (the previous equality is not an exact one), one guesses that the number of degrees of freedom is somewhere between one and two and a more refined statistical analysis, taking into account the noise level in the measurements, has to be implemented.

Let us note that it is possible to test the presence of two nearly proportional vectors in set Σ , in the very general case, with of course a number of parameters less or equal to the number of observations ($n \leq m$), by testing the assumption $\bar{\mathbf{S}}_k^* - c_{kj} \bar{\mathbf{S}}_j^* = \text{or} \approx \vec{0}$, where c_{kj} is a proportionality constant: a plot of $\mathbf{S}_k^*(t_j)$ as a function of $\mathbf{S}_j^*(t_j)$, for the m common values t_j of the independent variable where observations are available (parametric representation of a curve) shows whether the plots gather on the $\mathbf{S}_k^*(t) = c_{kj} \mathbf{S}_j^*(t)$ line or not.

As an example of this type of representation, **Figure 5** illustrates the case taken from [1] of a 1D rear face transient response of a low insulating sample (conductivity λ) sandwiched between two very thin copper layers. The knowledge model (RDM1 in [1]) assumes pure thermal resistance for the insulating layer and pure known capacities for the copper layers. The front face is stimulated by a Dirac pulse of energy Q (J.m^{-2}) and with a heat loss coefficient h ($\text{W.m}^{-2} \text{K}^{-1}$) equal on its two faces: the sensitivities to the three parameters Q , λ and h seem to be qualitatively independent, but only in terms of two by two linear dependencies: this does not mean that the rank of the reduced sensitivity matrix (if only these three parameters are looked for) is equal to three, because three by three linear dependencies may be possible.

This aspect, a possible dependency between the three sensitivity coefficients, is studied in **Figure 6**, for the same experimental design: a linear combination of the form $\bar{\mathbf{S}}_3^* - c_1 \bar{\mathbf{S}}_1^* - c_2 \bar{\mathbf{S}}_2^* = \text{or} \approx \vec{0}$ is looked for between the three sensitivity coefficients (for $\beta_1 = Q$, $\beta_2 = h$ and $\beta_3 = \lambda$) and a linear OLS estimation is made using the $\mathbf{S}_1^*(t_j)$'s and the $\mathbf{S}_2^*(t_j)$'s as the new independent variables and the $\mathbf{S}_3^*(t_j)$'s as new observations. The corresponding $\mathbf{S}_3^*(t_j)$ values are plotted as a function of the recalculated values (optimal linear combination) of the corresponding

model, $\hat{c}_1 S_1^* (t_i) + \hat{c}_2 S_2^* (t_i)$: since the corresponding curve is very close to the first bisecting line, a *qualitative* 3 by 3 possible linear dependency is detected.

However one can wonder how close it should be to impede the estimation of the three parameters: this has to be confirmed by a calculation of the covariance or V_{cor} matrix of the corresponding estimations, as explained in 3.2.

So, we will focus here on non linear parameter estimation problems where local linearization concepts as well as a Singular Value Decomposition of matrix deserve to be introduced.

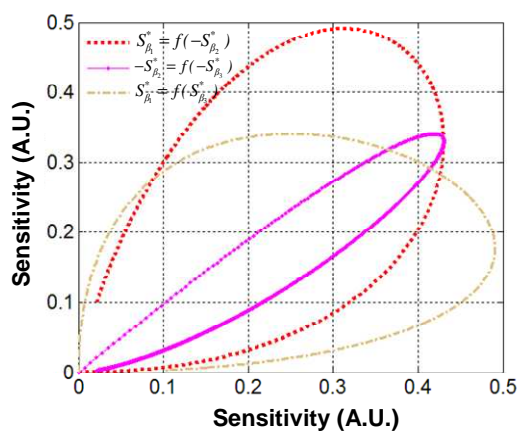


Figure 5 : Sensitivities plotted by pairs

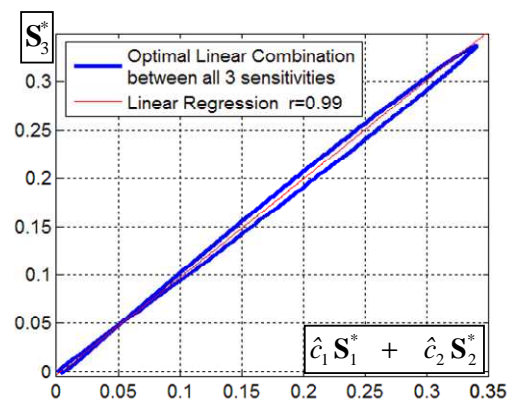


Figure 6 : Evidence of Linear Combination between all three parameters

3.3.3. Generalization : Use of SVD to track PEP degrees of freedom

It has been shown previously (see Lecture 2) that the question of identifiability of the parameters of a model relies on the condition number of the information matrix $(S^T S)$. However a systematic tool for tracking down hidden correlations is lacking. Such a tool will be presented now to circumvent this problem. Ultimately it will allow determining which parameters it is wise to exclude from the estimation (metrological) process, in order to get better estimates of the remaining ones.

In the next section two sequential steps will be presented.

First, in order to use all the tools available for linear estimation (see Lecture 2) on which the iterative OLS estimation (12) is based, the differential dy_{mo} of the model will be calculated around a reference point β^{nom} , that is a nominal value of the parameter vector for which a sensitivity analysis has been carried out (see previous sections) and the original parameter vector β will be made dimensionless using the components of β^{nom} : a reduced parameter vector x with a well-defined norm will be constructed.

Second, Singular Value Decomposition (SVD) will be applied to the reduced sensitivity matrix of the "tangent" local linearized model around β^{nom} , the ultimate goal being the determination the r

parameters that can be estimated in a problem with n original parameters (with $n \geq r$), when the levels of the measurement noise and measurement magnitude are known (SNR).

The non linear model $y_{mo}(t, \boldsymbol{\beta})$ is still considered here with m available measurements.

3.3.3.1. *Parameterizing a non-linear parameter estimation problem around the nominal values of its parameters*

The following one-output non linear model is considered here:

$$y_{mo} = \eta(t; \boldsymbol{\beta}) \tag{20}$$

where $\boldsymbol{\beta}$ is the column vector of the n parameters, of size $(n, 1)$, y_{mo} its (scalar) output at time t and η is a scalar function on t . If m observations of y_{mo} are available for times t_i , one can use a column vector notation:

$$\mathbf{y}_{mo} = \boldsymbol{\eta}(t; \boldsymbol{\beta}) \tag{21}$$

where \mathbf{y}_{mo} is the output vector of the model, of dimensions $(m, 1)$ and t the column vector of the m times of observation. $\boldsymbol{\eta}(\cdot)$ is a vector function whose values belong to R^m .

Since the model is non linear, it will be written under a differential form, in the neighbourhood of a reference point $\boldsymbol{\beta}^{nom}$, which corresponds to a *nominal* value, where a sensitivity study has been already implemented. This allows to use a local linearity :

$$d\mathbf{y}_{mo} = \mathbf{S}(t; \boldsymbol{\beta}^{nom}) d\boldsymbol{\beta} \quad \text{with} \quad S_{ij} = \left. \frac{\partial \eta(t_i; \boldsymbol{\beta}^{nom})}{\partial \beta_j} \right|_{t, \beta_k \text{ for } k \neq j} \tag{22}$$

Let us note that in the notation $d\mathbf{y}_{mo}$, the column vector t of the measurement times has been "frozen". S is the sensitivity matrix.

$$\mathbf{S} = [\mathbf{s}_1 \quad \mathbf{s}_2 \quad \dots \quad \mathbf{s}_n] \quad \text{with} \quad \mathbf{s}_j = \left. \frac{\partial \boldsymbol{\eta}(t; \boldsymbol{\beta}^{nom})}{\partial \beta_j} \right|_{t, \beta_k \text{ for } k \neq j} \tag{23}$$

In (22), the column vector $d\mathbf{y}_{mo}$ has a norm, because all its m components have the same physical unit. However, such is not the case for column vector $d\boldsymbol{\beta}$, which is only a column matrix composed of n parameters whose physical dimensions are not necessarily the same: $d\beta_1$ is a very small variation in the neighbourhood of β_1^{nom} , which can be a thermal conductivity λ . $d\beta_2$ a very small variation around β_2^{nom} , which can be a volumetric heat capacity ρc and so on ...

So $d\boldsymbol{\beta}$ is not really a vector belonging to any vector space of dimension n , but a simple collection of n parameters.

In order to transform it into a real vector, a normalization of all its elements is necessary. The components of $\boldsymbol{\beta}^{nom}$ will be used for that purpose. A new dimensionless parameter \mathbf{x} is introduced.

Its components are defined by:

$$x_j = \ln \left(\beta_j / \beta_j^{nom} \right) \quad (24)$$

And its nominal value is equal to zero:

$$\mathbf{x}^{nom} = \mathbf{0} = [0 \ 0 \ \dots \ 0]^T \quad (25)$$

In the neighbourhood of $\boldsymbol{\beta}^{nom}$, each component of \mathbf{x} is equal to the relative variation of the corresponding component of $\boldsymbol{\beta}$ around its nominal value (first order series expansion):

$$x_j = \ln \left(\beta_j / \beta_j^{nom} \right) = \ln \left(1 + \frac{\beta_j - \beta_j^{nom}}{\beta_j^{nom}} \right) \approx \frac{\beta_j - \beta_j^{nom}}{\beta_j^{nom}} \quad (26)$$

The new parameter vector \mathbf{x} is written the following way :

$$\mathbf{x} = \ln \left(\mathbf{R}_{nom}^{-1} \boldsymbol{\beta} \right) \approx \mathbf{R}_{nom}^{-1} \left(\boldsymbol{\beta} - \boldsymbol{\beta}^{nom} \right) \quad (27)$$

with :

$$\mathbf{R}_{nom} = \begin{bmatrix} \beta_1^{nom} & 0 & \dots & 0 \\ 0 & \beta_2^{nom} & \ddots & 0 \\ \vdots & \ddots & \ddots & \vdots \\ 0 & 0 & \dots & \beta_n^{nom} \end{bmatrix} \quad (28)$$

With this definition, the differential $d\mathbf{x}$ of \mathbf{x} is the logarithmic differential of $\boldsymbol{\beta}$:

$$d\mathbf{x} = [dx_1 \ dx_2 \ \dots \ dx_n]^T \quad \text{with} \quad dx_j = \frac{d\beta_j}{\beta_j^{nom}} \approx \frac{d\beta_j}{\beta_j} = d\ln(\beta_j) \quad (29)$$

Let us note that the very last equality is only valid in the neighbourhood of $\boldsymbol{\beta}^{nom}$. It can also be written in a column vector notation :

$$d\mathbf{x} = \mathbf{R}_{nom}^{-1} d\boldsymbol{\beta} \approx \mathbf{R}^{-1} d\boldsymbol{\beta} \quad (30)$$

where \mathbf{R} is the square diagonal matrix whose diagonal is composed of the components of $\boldsymbol{\beta}$, in the same way as (28) for the definition of \mathbf{R}_{nom} starting from $\boldsymbol{\beta}^{nom}$.

Equation (22) is rewritten in order to make $d\mathbf{x}$ appear :

A double change of basis, in the measurements domain and in the parameter domain, using the matrices of the left \mathbf{U} and right \mathbf{V} , in the SVD of \mathbf{S}^* written for $\mathbf{K} = \mathbf{S}^*$ yields :

$$\mathbf{S}^* = \mathbf{U} \mathbf{W} \mathbf{V}^T \quad (33)$$

Matrix \mathbf{V} is used as a (square) change of matrix basis and it transforms the differential of the reduced parameter vector $d\mathbf{x}$ into a new differential vector $d\mathbf{p}$, where \mathbf{p} can be called the diagonal parameter vector, of dimensions $(n, 1)$.

Matrix \mathbf{U} allows to change the differential observation vector $d\mathbf{y}_{mo}$ of dimensions $(m, 1)$ into a differential vector $d\mathbf{z}_{mo}$ of smaller length, where \mathbf{z}_{mo} can be called the diagonal observation vector, of dimensions $(n, 1)$.

$$d\mathbf{y}_{mo} = \mathbf{U} d\mathbf{z}_{mo} \quad \text{and} \quad d\mathbf{x} = \mathbf{V} d\mathbf{p} \quad (34 \text{ a,b})$$

Let us note here that the reduction of the length of the observation vector (m observations for $d\mathbf{y}_{mo}$ and only n components in $d\mathbf{z}_{mo}$ stems from the fact that the $(m-n)$ singular eigenvectors \mathbf{U}_k not present in matrix \mathbf{U} corresponds to null singular values w_k (for $k > n$).

Use of equations (32) and (33) to (34), together with the property $\mathbf{U}^T \mathbf{U} = \mathbf{V}^T \mathbf{V} = \mathbf{I}_n$, allows to get the equivalent of the differential model (31a) in the double transformed space:

$$d\mathbf{z}_{mo} = \mathbf{W} d\mathbf{p} \quad (35)$$

This equation corresponds to a diagonalization of the model in \mathbb{R}^n , and one gets then, component by component:

$$dp_k = \frac{1}{w_k} dz_{mo,k} \quad \text{for} \quad k = 1, 2, \dots, n \quad (36)$$

Combining (34a, b) and (35) yields:

$$d\mathbf{x} = \mathbf{V} \mathbf{W}^{-1} \mathbf{U}^T d\mathbf{y}_{mo} = \mathbf{S}^{*+} d\mathbf{y}_{mo} \quad (37)$$

where $\mathbf{S}^{*+} = \mathbf{V} \mathbf{W}^{-1} \mathbf{U}^T$ is the pseudo-inverse, or inverse of Moore-Penrose, of the scaled (rectangular) sensitivity matrix \mathbf{S}^* .

Combination of the preceding equations leads to a relationship between $d\boldsymbol{\beta}$ and $d\mathbf{y}_{mo}$:

$$d\boldsymbol{\beta} = \mathbf{R}_{nom} \mathbf{V} \mathbf{W}^{-1} \mathbf{U}^T d\mathbf{y}_{mo} \quad (38)$$

and an integration can be implemented to give the relationship between the diagonal and original sets of parameters in a column vector form:

$$\mathbf{p} = \mathbf{V}^T \mathbf{x} = \mathbf{V}^T \ln(\mathbf{R}_{nom}^{-1} \boldsymbol{\beta}) \approx \mathbf{V}^T \mathbf{R}_{nom}^{-1} (\boldsymbol{\beta} - \boldsymbol{\beta}^{nom}) \quad \text{because} \quad \mathbf{p}^{nom} = \mathbf{V}^T \mathbf{x}^{nom} = \mathbf{0} \quad (39)$$

The transformed observation vector can be expressed:

$$\mathbf{z}_{mo} = \mathbf{U}^T (\mathbf{y}_{mo} - \mathbf{y}_{mo}(\boldsymbol{\beta}^{nom})) = \mathbf{W} \mathbf{p} \quad \text{because} \quad \mathbf{z}_{mo}^{nom} = \mathbf{W} \mathbf{p}^{nom} = \mathbf{0} \quad (40)$$

Combining (39) and (40) yields:

$$\mathbf{p} = \mathbf{V}^T \ln(\mathbf{R}_{nom}^{-1} \boldsymbol{\beta}) = \mathbf{W}^{-1} \mathbf{U}^T (\mathbf{y}_{mo} - \mathbf{y}_{mo}(\boldsymbol{\beta}^{nom})) \Rightarrow \boldsymbol{\beta} = \mathbf{R}_{nom} \exp(\mathbf{V} \mathbf{W}^{-1} \mathbf{U}^T (\mathbf{y}_{mo} - \mathbf{y}_{mo}(\boldsymbol{\beta}^{nom}))) \quad (41)$$

An approximation of this expression in the neighbourhood of $\boldsymbol{\beta}^{nom}$ is available:

$$\boldsymbol{\beta} \approx \mathbf{R}_{nom} \left[\mathbf{1} + \mathbf{V} \mathbf{W}^{-1} \mathbf{U}^T (\mathbf{y}_{mo} - \mathbf{y}_{mo}(\boldsymbol{\beta}^{nom})) \right] = \boldsymbol{\beta}^{nom} + \mathbf{R}_{nom} \mathbf{V} \mathbf{W}^{-1} \mathbf{U}^T (\mathbf{y}_{mo} - \mathbf{y}_{mo}(\boldsymbol{\beta}^{nom})) \quad (42)$$

where $\mathbf{1}$ is the column vector of length n whose coefficients are equal to unity.

3.3.3.4. Non linear ordinary least square estimator and SVD

It is interesting to compare diagonal equation (36) that shows the interest of an inversion in the left and right singular spaces with the OLS estimator (12) of parameter $\boldsymbol{\beta}$. So, if the first order approximation in the neighbourhood of $\boldsymbol{\beta}^{nom}$ is considered, the difference between measurements and model outputs can be expressed with the *residual* vector defined in (10), and \mathbf{r}_{lin} the linearized form of this difference vector:

$$\mathbf{r}(\boldsymbol{\beta}) = \mathbf{y} - \mathbf{y}_{mo}(\boldsymbol{\beta}) \approx \mathbf{r}_{lin}(\boldsymbol{\beta}) = \mathbf{y} - \mathbf{y}_{mo}(\boldsymbol{\beta}^{nom}) - \mathbf{S}(\boldsymbol{\beta}^{nom}) (\boldsymbol{\beta} - \boldsymbol{\beta}^{nom}) \quad (43)$$

The least squares sum J_{OLS} can be written as a quadratic form J^\diamond , using the fact that $J_{OLS} = J_{OLS}^T$ (scalar) :

$$J(\boldsymbol{\beta}) = \mathbf{r}^T(\boldsymbol{\beta}) \mathbf{r}(\boldsymbol{\beta}) \approx J^\diamond(\boldsymbol{\beta}) = (\mathbf{y} - \mathbf{y}_{mo}(\boldsymbol{\beta}^{nom}))^T (\mathbf{y} - \mathbf{y}_{mo}(\boldsymbol{\beta}^{nom})) + (\boldsymbol{\beta} - \boldsymbol{\beta}^{nom})^T \mathbf{S}^T(\boldsymbol{\beta}^{nom}) \mathbf{S}(\boldsymbol{\beta}^{nom}) (\boldsymbol{\beta} - \boldsymbol{\beta}^{nom}) - 2(\boldsymbol{\beta} - \boldsymbol{\beta}^{nom})^T \mathbf{S}^T(\boldsymbol{\beta}^{nom}) (\mathbf{y} - \mathbf{y}_{mo}(\boldsymbol{\beta}^{nom})) \quad (44)$$

When the minimum is reached, one gets:

$$\frac{dJ^\diamond}{d\boldsymbol{\beta}} = 0 \quad \Rightarrow \quad \mathbf{S}^T(\boldsymbol{\beta}^{nom}) \mathbf{S}(\boldsymbol{\beta}^{nom}) (\hat{\boldsymbol{\beta}} - \boldsymbol{\beta}^{nom}) = \mathbf{S}^T(\boldsymbol{\beta}^{nom}) (\mathbf{y} - \mathbf{y}_{mo}(\boldsymbol{\beta}^{nom})) \quad (45)$$

which leads to an approximation of the OLS estimator:

$$\hat{\boldsymbol{\beta}} - \boldsymbol{\beta}^{nom} = (\mathbf{S}^T(\boldsymbol{\beta}^{nom}) \mathbf{S}(\boldsymbol{\beta}^{nom}))^{-1} \mathbf{S}^T(\boldsymbol{\beta}^{nom}) (\mathbf{y} - \mathbf{y}_{mo}(\boldsymbol{\beta}^{nom})) \quad (46)$$

This is exactly the same equation as the iterative algorithm (12), with $\hat{\boldsymbol{\beta}} = \hat{\boldsymbol{\beta}}_{OLS}^{(k+1)}$ and $\boldsymbol{\beta}^{nom} = \hat{\boldsymbol{\beta}}_{OLS}^{(k)}$. One shows, using (31b) and (33) :

$$\left(\mathbf{S}^T(\boldsymbol{\beta}^{nom}) \mathbf{S}(\boldsymbol{\beta}^{nom}) \right)^{-1} \mathbf{S}^T(\boldsymbol{\beta}^{nom}) = \mathbf{R}_{nom} \mathbf{V} \mathbf{W}^{-1} \mathbf{U}^T \quad (47)$$

The least square estimator (46), with the diagonal parameter \mathbf{p} and the experimental diagonal signal \mathbf{z} in their new bases, can be written thanks to (47) :

$$\hat{\mathbf{p}} = \mathbf{W}^{-1} \mathbf{z} \quad \text{with} \quad \mathbf{z} = \mathbf{U}^T (\mathbf{y} - \mathbf{y}_{mo}(\boldsymbol{\beta}^{nom})) \quad (48a, b)$$

Equation (48a) is diagonal. Use of (46) and (47) provides a new expression for the OLS estimator of $\boldsymbol{\beta}$:

$$\hat{\boldsymbol{\beta}} = \mathbf{R}^{nom} \left(\mathbf{1} + \mathbf{V} \mathbf{W}^{-1} \mathbf{U}^T (\mathbf{y} - \mathbf{y}_{mo}(\boldsymbol{\beta}^{nom})) \right) \quad (49)$$

This expression is the same as relationship (42) that links $\boldsymbol{\beta}$ and $\mathbf{y}_{mo}(\boldsymbol{\beta})$: these corresponding two values are simply replaced by the linearized OLS estimator $\hat{\boldsymbol{\beta}}$ and by measurements \mathbf{y} respectively.

The linearized OLS estimator of the reduced parameter vector $\hat{\boldsymbol{x}}$ stems directly from (49):

$$\hat{\boldsymbol{x}} = \left(\mathbf{S}^{*T}(\boldsymbol{\beta}^{nom}) \mathbf{S}^*(\boldsymbol{\beta}^{nom}) \right)^{-1} \mathbf{S}^{*T}(\boldsymbol{\beta}^{nom}) (\mathbf{y} - \mathbf{y}_{mo}(\boldsymbol{\beta}^{nom})) \quad (50)$$

3.3.3.5. Mean quadratic estimation error and singular values

With the noise properties defined in (8), the variance-covariance of the linearized OLS estimator $\hat{\boldsymbol{\beta}}$ given by equation (46), can be written thanks to (31b) and (33) :

$$\begin{aligned} \text{cov}(\hat{\boldsymbol{\beta}}) &= \sigma^2 \left(\mathbf{S}^T(\boldsymbol{\beta}^{nom}) \mathbf{S}(\boldsymbol{\beta}^{nom}) \right)^{-1} = \sigma^2 \left(\mathbf{R}_{nom}^{-1} \mathbf{S}^{*T} \mathbf{S}^* \mathbf{R}_{nom}^{-1} \right)^{-1} \\ &= \sigma^2 \mathbf{R}_{nom} \left(\mathbf{S}^{*T} \mathbf{S}^* \right)^{-1} \mathbf{R}_{nom} = \sigma^2 \mathbf{R}_{nom} \mathbf{V} \mathbf{W}^{-2} \mathbf{V}^T \mathbf{R}_{nom} \end{aligned} \quad (51)$$

This expression is valid if the difference between $\hat{\boldsymbol{\beta}}$ and $\boldsymbol{\beta}^{nom}$ is small: it is always the case near convergence of algorithm (12) where $\boldsymbol{\beta}^{nom}$ can be redefined as $\boldsymbol{\beta}^{nom} = \hat{\boldsymbol{\beta}}_{OLS}^{(k)}$ and with $\hat{\boldsymbol{\beta}} = \hat{\boldsymbol{\beta}}_{OLS}^{(k+1)}$.

The expression of the variance-covariance matrix of $\hat{\boldsymbol{x}} = \mathbf{R}_{nom}^{-1} \hat{\boldsymbol{\beta}}$ becomes:

$$\text{cov}(\hat{\boldsymbol{x}}) = \mathbf{R}_{nom}^{-1} \text{cov}(\hat{\boldsymbol{\beta}}) \left(\mathbf{R}_{nom}^{-1} \right)^T = \sigma^2 \mathbf{V} \mathbf{W}^{-2} \mathbf{V}^T \quad (52a)$$

The first relationship in equation (52a) allows to calculate the reduced covariance matrix of $\hat{\boldsymbol{\beta}}$, $\text{rcov}(\hat{\boldsymbol{\beta}})$, whose diagonal coefficients are the reduced variances of the estimators of each parameter, using the nominal values of the parameters as scaling factors:

$$\text{rcov}(\hat{\boldsymbol{\beta}}) = \text{cov}(\hat{\boldsymbol{x}}) = \begin{bmatrix} \sigma_{\hat{\beta}_1}^2 / (\beta_1^{nom})^2 & \text{cov}(\hat{\beta}_1, \hat{\beta}_2) / (\beta_1^{nom} \beta_2^{nom}) & & \text{cov}(\hat{\beta}_1, \hat{\beta}_n) / (\beta_1^{nom} \beta_n^{nom}) \\ & \sigma_{\hat{\beta}_2}^2 / (\beta_2^{nom})^2 & & \\ & & \ddots & \\ \text{Symmetric} & & & \sigma_{\hat{\beta}_n}^2 / (\beta_n^{nom})^2 \end{bmatrix} = \sigma^2 (\mathbf{S}^T \mathbf{S})^{-1} \quad (52b)$$

where $\sigma_{\hat{\beta}_j}$ is the standard deviation of $\hat{\beta}_j$. The square roots of the diagonal terms of this matrix, $\sigma_{\hat{\beta}_j} / \beta_j^{nom}$, can be considered as a measure of the relative error made for each parameter and caused by presence of noise in the measurements \mathbf{y} .

It is very interesting to calculate the trace of this matrix, which is equal to the sum of the variances of the different components of $\hat{\boldsymbol{x}}$:

$$\begin{aligned} \text{Tr}(\text{cov}(\hat{\boldsymbol{x}})) &\equiv \sum_{j=1}^n \sigma_{x_j}^2 = \sum_{j=1}^n (\sigma_{\beta_j} / \beta_j^{nom})^2 \\ \Rightarrow \sum_{j=1}^n (\sigma_{\beta_j} / \beta_j^{nom})^2 &= \sigma^2 \text{Tr}(\mathbf{V} \mathbf{W}^{-2} \mathbf{V}^T) = \sum_{k=1}^n \frac{\sigma^2}{w_k^2} \sum_{i=1}^n V_{ik}^2 \end{aligned} \quad (53)$$

where σ_{x_j} is the standard deviation of the estimate of reduced parameter x_j and σ_{β_j} the corresponding one for β_j . Since the right singular vectors have a unit norm ($\|\mathbf{V}_k\|^2 = \sum_{i=1}^n V_{ik}^2 = 1$), this last equation becomes :

$$\text{Tr}(\text{cov}(\hat{\boldsymbol{x}})) = \sum_{j=1}^n (\sigma_{\beta_j} / \beta_j^{nom})^2 = \sigma^2 \sum_{k=1}^n \frac{1}{w_k^2} \quad (54)$$

In order to get a good estimation (in percents) of all the parameters of the model, the quadratic mean of the relative standard deviations of their estimates m_q should be smaller than a given level $m_{q\max}$ (NB: subscript q corresponds here to the quadratic mean of the normalized standard deviations) :

$$m_q = \left(\frac{1}{n} \sum_{j=1}^n (\sigma_{\beta_j} / \beta_j^{nom})^2 \right)^{1/2} = \sigma \left(\frac{1}{n} \sum_{k=1}^n \frac{1}{w_k^2} \right)^{1/2} \leq m_{q\max} \quad (55)$$

One of the objectives of the "inverter" (the person in charge of the inversion) is to get a relative error m_q , expressed in term of quadratic mean, lower than an upper threshold $m_{q\max}$ equal to a few percents. This means that as soon as the number n of parameters that have to be estimated becomes large, the singular values w_k of the corresponding reduced sensitivity matrix decrease, which increases the error. This increase of the error is proportional to the standard deviation of the noise. This standard deviation has the same unit as the output of the signal and the same is true for the

singular values which do not depend on the structure of the model (function η) only, but also on the intensity of the stimulation (in a problem where the output is related to a field: temperature, concentration, ...) and on the choice of the "times" of observation \mathbf{t} .

Both a lower and an upper level can also be constructed for the criterion of global relative error m_q defined in (55), using the smaller singular value w_n :

$$\frac{1}{\sqrt{n}} \frac{\sigma}{w_n} \leq m_q = \left(\frac{1}{n} \sum_{j=1}^n (\sigma_{\beta_j} / \beta_j^{nom})^2 \right)^{1/2} \leq \frac{\sigma}{w_n} \quad (56)$$

This clearly shows that a too large value for the ratio σ / w_n , between the standard deviation of the measurement noise and the smaller singular value of the reduced sensitivity matrix $\mathbf{S}^*(\boldsymbol{\beta}^{nom})$, can make the estimation of the whole set of parameters «explode». In that case, one of the β_j parameters (the parameter "supposed to be known", β_{sk}) has to be removed from the original set of parameters to be estimated. This will lead to a new parameter vector $\boldsymbol{\beta}'$ to be estimated, of smaller dimensions ($n-1, 1$), with a better (smaller) associated m_q criterion (lower average dispersion) but with the apparition of a bias on its $n-1$ estimates, because of the biased value of the removed parameter β_{sk} that will be fixed to its nominal value that is different from its exact value (see Lecture 2).

TOOL Nr4: The SVD of the normalized sensitivity matrix calculated for nominal values of parameter vector $\boldsymbol{\beta}$ can bring valuable information to quantify the real identifiability of the parameters, once the level of noise known.

3.3.4. Residuals analysis and signature of the presence of a bias in the metrological process

One way to analyse the results of the estimation process is to calculate the residuals (equation 10) at convergence. When conditions (8) are fulfilled, it can be easily shown that the expectancy of the residuals curve $\mathbf{r}(\mathbf{t}, \hat{\boldsymbol{\beta}})$ is equal to a null function:

$$\mathbf{E}(\mathbf{r}) = \mathbf{E} \left[y_i - y_{mo}(t_i, \hat{\boldsymbol{\beta}}) \right] = \mathbf{E} \left[\mathbf{S}(\boldsymbol{\beta} - \hat{\boldsymbol{\beta}}) \right] = \mathbf{E} \left[-\mathbf{S}(\mathbf{S}^T \mathbf{S})^{-1} \mathbf{S}^T \boldsymbol{\varepsilon} \right] = -\mathbf{S}(\mathbf{S}^T \mathbf{S})^{-1} \mathbf{S}^T \mathbf{E}(\boldsymbol{\varepsilon}) \quad (57)$$

Since $\mathbf{E}(\boldsymbol{\varepsilon}) = \mathbf{0}$, $\mathbf{E}(\mathbf{r}) = \mathbf{0}$ which means that if the model used for describing the experiment is appropriate, the residuals curve is "unsigned" (unbiased theoretical model). On the contrary, "signed" residuals can be considered as the signature of some biased estimation.

The bias can stem from different causes such as:

- (i) the a priori decision that some parameters of the model are known and therefore fixed at some given value (maybe measured by another experiment). As active parameters in the PEP, they can alter the estimates of the remaining unknown parameters.

- (ii) Experimental imperfections which makes the model idealized with respect to the reality of the phenomena.

The existence of a bias means that a systematic and generally unknown inconsistency exists between the model and the experimental data.

We give here an example taken from [1] and already studied in section 3.3.2 above. It concerns the simulation of a flash experiment applied to a three-layer medium: two highly capacitive and conductive coatings and a central layer made of a material with very poor conductivity (highly insulating material) and heat capacity (aerogel material). This system can be modelled through some function $T^{rear} = y_{mo}(t, \boldsymbol{\beta})$. An artificial bias is introduced under the form of a linear drift superimposed to the output simulated observations. It corresponds practically to a linear deviation of the signal from the equilibrium situation before the experiment starts. A noise respecting equations (8) is also added to the simulation of the measurements so that we have at each time t_k :

$$y_k = y_{mo}^{drift}(t_k, \boldsymbol{\beta}) + \varepsilon_k = y_{mo}(t_k; \boldsymbol{\beta}) - b_y(t_k) + \varepsilon_k \quad (58a)$$

Model $y_{mo}(t, \boldsymbol{\beta})$ used for direct modelling is exact if no drift is present in the experiment. However, in the opposite case, it becomes biased, since it does not accounts the presence of this drift. The output bias b_y above is defined by:

$$b_y(t_k) \equiv y_{mo}(t_k, \boldsymbol{\beta}) - y_{mo}^{drift}(t_k, \boldsymbol{\beta}) \quad (58b)$$

Let us note that in this definition, the drift model is the reference one ($y_{mo}^{exact} = y_{mo}^{drift}$) and the preceding thermal model is the biased one ($y_{mo}^{biased} = y_{mo}$).

This model used for parameter estimation is ill-conditioned: some correlation exists between the parameters (Case $n=3$ corresponding to the correlation existing between parameters shown in **Figure 5** and **Figure 6**). **Figure 7** below shows:

- the simulated rear face noisy output of the system, with the drift (dotted curve)
- the rear face recalculated output using the biased estimate $\hat{\boldsymbol{\beta}}$ (solid line curve)
- the drift of the model output (function $-b_y(t)$) introduced. At the final time of the experiment ($t_f = 1000s$), the magnitude of the drift represents less than 4% of the maximum level of the signal.
- the residuals curve (with the noise, and after subtraction of the noise)

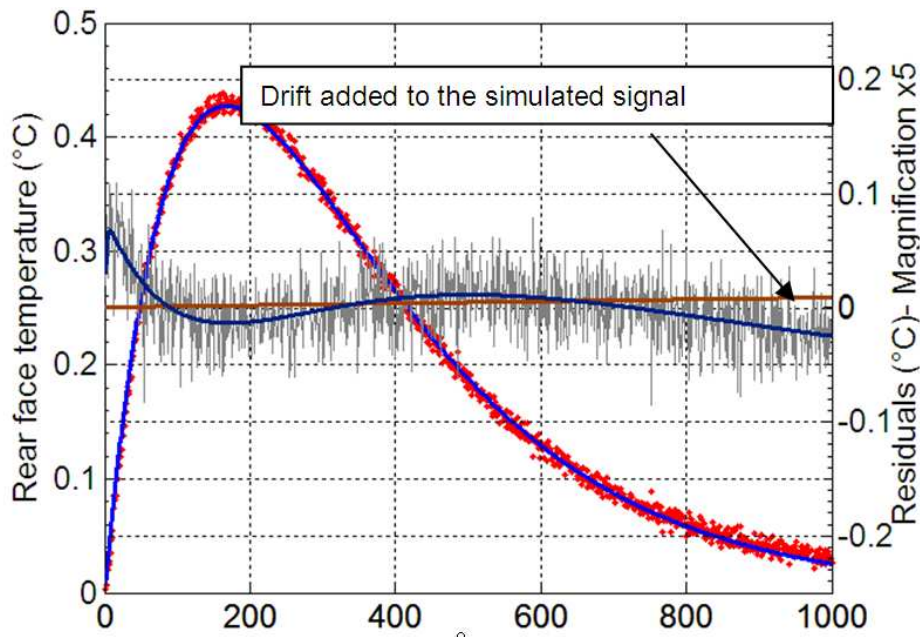


Figure 7 : Signed character of "post-estimation" residuals in the presence of a bias and using a badly conditioned PEP

The "signed" character of the residuals is obvious (oscillation around zero with a much smaller frequency than the noise). The three parameters estimated using these biased "measurements" has led to expectancies of the parameter estimates with respectively a -18% , -7.5% , $+19\%$ difference with respect to the exact input values. These differences are not of stochastic origin (caused by noise only) but result from the introduction of the bias. One possibility for the experimenter who wants to check whether his estimations are biased or not, is to observe the output of the inversion process for varying identification ranges of the independent variable.

For example, we can vary the identification time interval. If a bias affects the data when compared to the modelling, then the estimations will vary, depending on the selected identification interval. This is what can be observed in **Table 2** where three identifications have been performed for three different time intervals [0-70s], [0-150s], [0-300s]. In this case we have used a more refined model than the one used for **Figure 7** and thus a more badly-conditioned PEP. In this table both thermal properties of the insulating material (thermal conductivity and thermal diffusivity) were estimated from the biased data. Obviously with such a material, the small heat capacity makes a good estimation of this parameter difficult, but sadly (because of a lack of sensitivity) this also affects the estimation of the second parameter. The thermal diffusivity and conductivity estimated from the data of **Figure 7** depend strongly on the identification intervals. The values can change within a factor of 60% or 170% in that case.

Time Interval	70 s	150 s	300 s
a (m^2/s)	3.76.10-6	3.22.10-6	2.21.10-6
λ ($W/m \cdot ^\circ C$)	0.031	0.064	0.084

Table 2 : Influence of the existence of some bias on the parameter estimates for a badly conditioned problem

TOOL Nr5: The "post-estimation" residuals have to be analysed carefully to check the potential existence of a bias of systematic origin. Its magnitude can be compared to the standard deviation of the white noise of the sensor in order to check whether this bias may introduce too large confidence intervals for the estimates (with respect to the pure stochastic estimation of the variances of parameter estimates in the absence of any bias). Invariant estimates for different identification intervals suggest that the bias is acceptable. In the opposite case, strategies must be implemented, either to change the nature of the estimation problems (reduction of the initial goals) or to use residuals to give a fair quantitative evaluation of confidence bounds of the estimates. Some hints on that topic will be given in the next sections.

4. Enhancing the performances of estimation

Some tools have been given above: they can help the experimenter to gain insight into its metrological problem. They can lead to a conclusion of failure: the problem is ill-conditioned regarding the estimation of the interesting parameters. This means that the parameters we initially wish to measure will actually never be estimated accurately. Two strategies are possible: recognizing that the initial goal is in vain, or modifying the problem through physical thinking to make it well-posed or adequately conditioned even by changing the goals themselves (number of parameters to estimate). Quoting J.V.Beck: "the problem of nonidentifiability can be avoided, through either the use of a different experiment or a smaller set of parameters that are identifiable". This position emerges from the well-known parsimony "principle" (see <http://en.wikipedia.org/wiki/Parsimony>) which in the field of science could be summarized by this sentence : "trying to perfectly recover reality is indeed very easy, when one adds parameters to each others so that it connects-the-dots". There is much more to learn and to retrieve from the distance maintained between a model and the observations it is supposed to match. The resulting consequence is that any minimization algorithm is a good one because the problem is well defined. This section will now proceed to give additional tools to work out badly conditioned problems with special analysis regarding the role of known versus unknown parameters.

4.1 Dimensional analysis or natural parameters: case of coupled conduction/radiation flash experiment

Through the preceding sections, the reader should have been convinced of the importance of notions like the pertinence of a model (good representation of reality, controlled origins of bias), the application of a parsimony principle, that is to adapt one's metrological objective by making the "quality" of the available information match the degree of complexity of the model.

A reduced model, seen as a model with a reduced number of parameters, has to be considered first in the light of Dimensional Analysis. The principles of Dimensional Analysis in Engineering precisely relies on the construction of "appropriate" natural parameters (the Pi-groups) emerging from the rank determination of the dimensional matrix of all physical quantities involved in the problem with respect to a basis of "base" quantities [6].

If we consider the heat transfer problem in a semi-transparent material like glass, coupled conduction and radiation transfers must be considered. Material parameters involve classical thermophysical properties of the opaque material (thermal conductivity λ , specific heat ρc) with the additional parameters accounting for radiative transfer : the absorption (extinction coefficient) β (m^{-1}), the level of temperature of the material T_0 (in Kelvin) which rules the magnitude of radiation emission, the

Stefan-Boltzman constant σ_{SB} , the refractive index n , and the inner emissivities ε_i of the boundaries (no units - opaque coatings of the glass slab are considered here).

Let us assume that a flash experiment is planned, with an absorbed heat density Q . In order to study the possibilities for a transient thermal characterization technique of such materials (which parameters can be measured with this experiment ?), the model will give the rear face temperature response of the slab (thickness e) as the following function:

$$y_{mo} = T_{rear}^{flash}(t, e, Q, \rho c, \lambda, \beta, \sigma_{SB}, T_0, \varepsilon_i, n) \quad (59)$$

Practicing a "blind" Dimensional Analysis leads to the construction of a new function depending on a new set of parameters:

$$y_{mo} = T_{rear}^{*flash} = \frac{T_{rear}^{flash} - T_0}{T_0^*} \left(t^* = at / e^2, \tau_0 = \beta e, N = \frac{\lambda \beta}{n^2 \sigma T_0^3}, T_0^* = Q / \rho c e, \varepsilon_i \right) \quad (60)$$

which naturally produces 4 pi-groups governing heat transfer inside the sample, with a reduction of the number of initial parameters of the model from 10 to 5.

Another classical example deals with conductive and convective mechanisms of transfer which appear jointly in problems of heat transfer within boundary layers. Solving the Inverse Heat Conduction Problem in order to get a heat exchange coefficient estimation will require the introduction of the classical Reynolds, Nusselt and Prandtl numbers.

4.2 Reducing the PEP to make it well-conditioned: case of thermal characterization of a deposit

➤ **Model:** Case of the contrast method

The method of the thermal contrast already presented in **Section 3.1** consists in making two "flash" experiments in order to estimate the thermal properties of the coating layer, denoted (1) in **Figure 8** below (the same as **Figure 1**). We will now on detail the modelling already presented briefly in section 3.1, in order to be able to find out which parameters of the model can be really estimated, in this non linear parameter estimation problem.

Let us remind that the first flash experiment is carried out on the substrate denoted (2), which allows characterization of the substrate in terms of diffusivity (the thermal capacity of the substrate is measured by another facility). The second flash experiment is performed on the two-layer material denoted (1)/(2).

In both cases, the variation of the rear-face temperature T with time, called thermogram, is measured. By taking the difference of these thermograms T_A^* and T_B^* normalized by their respective maximum, we obtain a curve called a thermal contrast curve, which is a function of the thermophysical parameters of the film (1) and of the substrate (2).

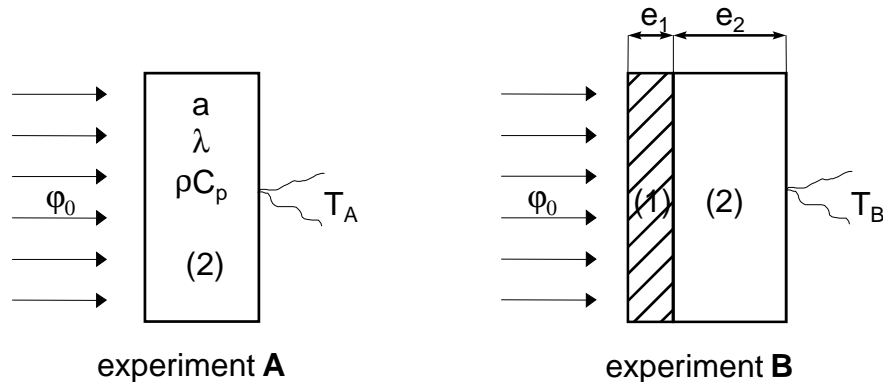


Figure 8 : *Principle of the Method*

The thermal quadrupoles method [7] is very appropriate to find the rear-face temperatures. Taking the Laplace transform of the heat equation yields a linear relationship between the different quantities of the "in" and "out" faces of each layer of the material.

Let $\theta(z, p)$ and $\phi(z, p)$ being the Laplace transforms of the temperature $T(z, t)$ and heat density $\phi(z, t)$ respectively, with z the axis normal to both faces :

$$\theta(z, p) = \mathbf{L} [T(z, t)] = \int_0^{\infty} T(z, t) \exp(-pt) dt \tag{61}$$

and

$$\phi(z, p) = \mathbf{L} [\phi(z, t)] = \int_0^{\infty} \phi(z, t) \exp(-pt) dt \quad \text{with} \quad \phi(z, t) = -\lambda \frac{\partial T}{\partial z} \tag{62}$$

The thermal quadrupoles method allows to linearly link the temperatures and the heat flux densities of a homogeneous layer (numbered i here) without any source term and with zero initial temperature, through a transfer matrix M_i , defined in the following way:

$$\begin{bmatrix} \theta_{i_{in}} \\ \phi_{i_{in}} \end{bmatrix} = \begin{bmatrix} A_i & B_i \\ C_i & D_i \end{bmatrix} \begin{bmatrix} \theta_{i_{out}} \\ \phi_{i_{out}} \end{bmatrix} \tag{63}$$

with the coefficients of the matrix being calculated as:

$$A_i = D_i = \cosh\left(\sqrt{\frac{pe_i^2}{a_i}}\right), B_i = \frac{1}{\lambda \lambda_i \sqrt{\frac{p}{a_i}}} \sinh\left(\sqrt{\frac{pe_i^2}{a_i}}\right) \quad \text{and} \quad C_i = \lambda \lambda_i \sqrt{\frac{p}{a_i}} \sinh\left(\sqrt{\frac{pe_i^2}{a_i}}\right)$$

The subscript (i) is related to the layer (i) : film (1) and substrate (2).

e_i : thickness of the material

- a_i : thermal diffusivity
- λ_i : thermal conductivity
- ρC_{p_i} : specific heat

It is convenient in this 1D transient problem, to notice that time can be made dimensionless with the thermal diffusivity a_2 of the substrate and with its thickness e_2 , to make a Fourier number t^* appear, which will be associated to a reduced Laplace parameter p^* defined as:

$$t^* = \frac{a_2 t}{e_2^2}, \quad p^* = p \frac{e_2^2}{a_2} \quad \text{and} \quad s = \sqrt{p^*} \tag{64}$$

We can then define a reduced Laplace transform $\tilde{\theta}$ as:

$$\tilde{\theta}(z, p^*) = \tilde{\mathcal{L}} [T(z, t^*)] = \int_0^\infty T(z, t^*) \exp(-p^* t^*) dt^* = \frac{a_2}{e_2^2} \theta(z, p) \tag{65}$$

➤ **Flash Experiment on the substrate:**

The expression of the rear face response to a pulsed (Dirac) stimulation $\varphi(t) = Q_2 \delta(t)$, where Q_2 is the energy density (in $J.m^{-2}$) absorbed by the front face, is given by the following relationship:

$$\begin{bmatrix} \theta_{2in} \\ \phi_{2int} = Q_2 \end{bmatrix} = \begin{bmatrix} A_2 & B_2 \\ C_2 & D_2 \end{bmatrix} \begin{bmatrix} \theta_{2out} \\ \phi_{2out} = 0 \end{bmatrix} \tag{66}$$

Hence:

$$\theta_{2out} = \frac{Q_2}{C_2} = \frac{Q_2}{\lambda_2 \sqrt{\frac{p}{a_2}} \sinh\left(\sqrt{\frac{pe_2^2}{a_2}}\right)} \tag{67}$$

Here subscript 'in' designates the front (stimulated) face while subscript 'out' is associated to the rear face, where temperature can be measured. This rear face is supposed to be insulated here ($\phi_{2out} = 0$ in (66)).

Setting $s = \sqrt{p^*}$ and normalizing the thermogram with respect to its maximum that corresponds to the adiabatic temperature: $T_{2\infty} = \frac{Q_2}{\rho_2 C_2 e_2}$ reached for long times for this adiabatic model, we obtain:

$$\theta_{2out}^* = \mathcal{L} \left(\frac{T_2}{T_{2\infty}} \right) = \frac{e_2^2}{a_2} \frac{1}{s \sinh(s)} \tag{68}$$

Using the reduced Laplace transform (65), we can write:

$$\tilde{\theta}_{2out}^* = \tilde{\mathcal{L}} \left(\frac{T_2}{T_{2\infty}} \right) = \frac{1}{s \sinh(s)} \quad (69)$$

➤ **Flash Experiment on the two-layer material:**

The expression of the rear face response of the two-layer material can also be obtained easily through the quadrupoles method:

$$\begin{bmatrix} \theta_{1/2in} \\ \phi_{1/2in} = Q_{1/2} \end{bmatrix} = \begin{bmatrix} A_{eq} & B_{eq} \\ C_{eq} & D_{eq} \end{bmatrix} \begin{bmatrix} \theta_{1/2out} \\ \phi_{1/2out} = 0 \end{bmatrix} \quad (70)$$

where:

$$\begin{bmatrix} A_{eq} & B_{eq} \\ C_{eq} & D_{eq} \end{bmatrix} = \begin{bmatrix} A_1 & B_1 \\ C_1 & D_1 \end{bmatrix} \begin{bmatrix} A_2 & B_2 \\ C_2 & D_2 \end{bmatrix} = \begin{bmatrix} A_1A_2 + B_1C_2 & A_1B_2 + A_2B_1 \\ A_1C_2 + A_2C_1 & A_1A_2 + B_2C_1 \end{bmatrix} \quad (71)$$

and where $Q_{1/2}$ is the energy density absorbed by the front face in this second flash experiment on the two-layer sample.

In the case of good conductive materials with small thicknesses, the Biot number which represents the ratio between the internal resistance and the external resistance is low, which justifies neglecting the heat losses in the model output (rear face temperature) above. The expression of the temperature takes the following form:

$$\theta_{1/2} = \frac{Q_{1/2}}{C_{eq}} = \frac{Q_{1/2}}{A_1C_2 + A_2C_1} \quad (72)$$

Note: If we switch the two layers of the material, it means inverting subscripts 1 and 2, and the expression of the rear-face temperature can be proved to remain unchanged.

$$\theta_{1/2out} = \frac{Q_{1/2}}{\lambda_1 \sqrt{\frac{\rho}{a_1}} \sinh\left(\sqrt{\frac{\rho e_1^2}{a_1}}\right) \cosh\left(\sqrt{\frac{\rho e_2^2}{a_2}}\right) + \lambda_2 \sqrt{\frac{\rho}{a_2}} \sinh\left(\sqrt{\frac{\rho e_2^2}{a_2}}\right) \cosh\left(\sqrt{\frac{\rho e_1^2}{a_1}}\right)} \quad (73)$$

If we now scale the thermogram with the adiabatic temperature of the two-layer material, that is with $T_{1/2\infty} = \frac{Q_{1/2}}{\rho_1 c_1 e_1 + \rho_2 c_2 e_2}$, the expression of the Laplace transform of this reduced temperature $T_{1/2} / T_{1/2\infty}$ takes a simpler form:

$$\theta_{1/2out}^* = \frac{e_2^2}{a_2} \frac{1 + \frac{\rho_1 c_1 e_1}{\rho_2 c_2 e_2}}{s \left[\sqrt{\frac{\lambda_1 \rho_1 c_1}{\lambda_2 \rho_2 c_2}} \sinh\left(\frac{e_1}{e_2} \sqrt{\frac{a_2}{a_1}} s\right) \cosh(s) + \sinh(s) \cosh\left(\frac{e_1}{e_2} \sqrt{\frac{a_2}{a_1}} s\right) \right]} \quad (74)$$

As in section 3.1 two reduced parameters are introduced:

$$K_1 = \frac{e_1}{e_2} \sqrt{\frac{a_2}{a_1}} : \text{ratio of the root of characteristic times}$$

$$\text{or } K_1 = \sqrt{tc_1 / tc_2} \text{ with } tc_i = e_i^2 / a_i \quad \text{for } i=1, 2 \quad (75)$$

$$K_2 = \sqrt{\frac{\lambda_1 \rho_1 c_1}{\lambda_2 \rho_2 c_2}} : \text{ratio of the thermal effusivities}$$

$$\text{or } K_2 = \sqrt{b_1 / b_2} \text{ with } b_i = \sqrt{\lambda_i \rho c_i} \quad \text{for } i=1, 2 \quad (76)$$

We can note that K_1 is a function of the thicknesses of the substrate and coating and K_2 is an intrinsic parameter of the materials. The reduced Laplace transform of the response of the two-layer system can then be written, using (65):

$$\tilde{\theta}_{1/2out}^* = \frac{1}{s} \left[\frac{1 + K_1 K_2}{K_2 \sinh(K_1 s) \cosh(s) + \sinh(s) \cosh(K_1 s)} \right] \quad (77)$$

The heterogeneous nature of the two-layer material system appears here through the expression of the denominator that cannot be simplified: this makes the definition of an equivalent material associated to this two-layer sample impossible.

➤ Contrast Curve:

The contrast curve is obtained by taking the difference between the two thermograms, that is:

$$\Delta \tilde{\theta}_{out}^* = \tilde{\theta}_{1/2out}^* - \tilde{\theta}_{2out}^* = \tilde{\Gamma} (T_{1/2out}^* - T_{2out}^*) = \tilde{\Gamma} (\Delta T^*) \quad (78)$$

The expression of the reduced thermal contrast in the Laplace domain is:

$$\Delta \tilde{\theta}_{out}^* = \frac{1}{s} \left[\frac{1 + K_1 K_2}{K_2 \sinh(K_1 s) \cosh(s) + \sinh(s) \cosh(K_1 s)} - \frac{1}{\sinh(s)} \right] \quad (79)$$

Theoretically, K_1 and K_2 can be measured from an experimental thermal contrast curve through an "inverse" technique. The numerical inversion of the model is implemented by De Hoog algorithm.

From K_1 and K_2 (or by a parameter substitution), it is also possible to calculate the thermal capacity and conductivity of the deposit by the following relations:

$$K_3 = K_1 K_2 = \frac{\rho_1 c_1 e_1}{\rho_2 c_2 e_2} \quad \text{thermal capacities ratio}$$

or $K_3 = C_{t1} / C_{t2}$ with $C_{ti} = \rho c_i e_i$ for $i=1, 2$ (80)

and

$$K_4 = \frac{K_1}{K_2} = \frac{e_1 \lambda_2}{e_2 \lambda_1} \quad \text{thermal resistances ratio}$$

or $K_4 = R_1 / R_2$ with $R_i = e_i / \lambda_i$ for $i=1, 2$ (81)

Another parametrization of the same model consists in writing expression (79) as a function of K_3 and K_4 .

The expression of the theoretical model with reduced parameters clearly shows that the problem is in this case only function of two parameters. This means in particular that the thermophysical properties of the deposit can theoretically be obtained only if the properties of the substrate are known and the thicknesses of each layer as well. Thus, the precision of the measurement also depends on the precision of these known parameters.

In the followings, our attention will be focused on two particular cases. The first one corresponds to a conductive deposit on an insulating material. The second one corresponds to an insulating film on a conductive substrate.

In these two cases, the materials we consider have low thicknesses and are good conductors. So, the Biot number based on the properties of the substrate $Bi = h e_2 / \lambda_2$ is low and it is possible, as a first approximation, to neglect its influence on the measured reduced rear face contrast ΔT^* . It can be shown that even in the presence of heat losses, there is some kind of compensation through the construction of this contrast, which is a difference, which means that the present adiabatic model is a robust one: we will see in a later section that this parameter has a low influence in the estimation of the coating properties. The thicknesses and thermophysical properties are given in **Table 3**.

	Thickness (μm)	a (m^2/s)	λ ($\text{W}/\text{m}\cdot^\circ\text{K}$)	ρC_p ($\text{J}/\text{m}^3\cdot^\circ\text{K}$)
Case 1 :	Aluminium coating on a Cobalt/Nickel substrate			
Film (1)	220	$9.46 \cdot 10^{-5}$	230	$2.43 \cdot 10^6$
Substrate (2)	1 100	$2.36 \cdot 10^{-5}$	84.5	$3.57 \cdot 10^6$
Case 2 :	Insulating film on a Alumina substrate			
Film (1)	247	$6.84 \cdot 10^{-7}$	2.23	$3.26 \cdot 10^6$
Substrate (2)	640	$7.47 \cdot 10^{-6}$	23	$3.08 \cdot 10^6$

Table 3: Thermophysical properties and thicknesses of the materials

The reduced thermograms for the substrate and two-layer material as well as the contrast curve are plotted for the conductive/insulating and insulating/conductive cases in **Figure 9** and **Figure 10** respectively.

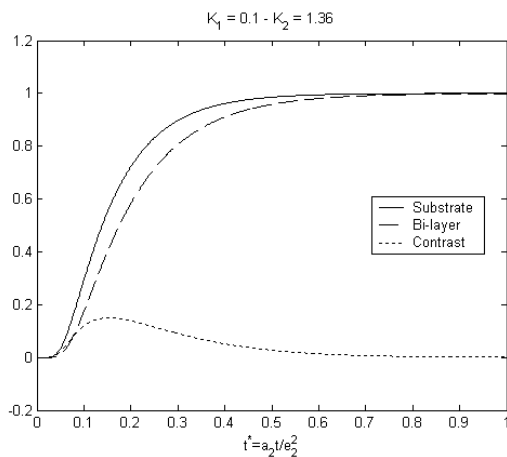


Figure 9 : Case 1 – Conductive coating / Insulating substrate

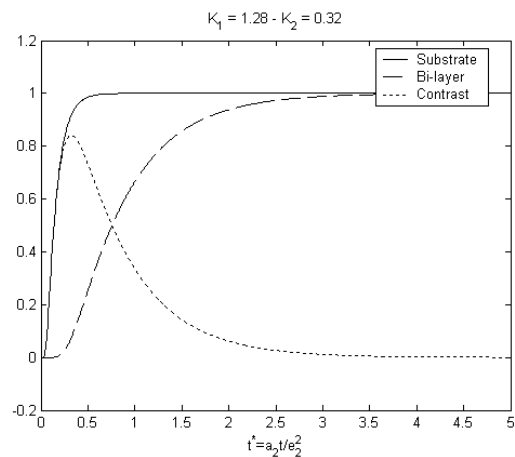


Figure 10 : Case 2 – Insulating film / Conductive substrate

➤ **Sensitivity Study**

The contrast curves and reduced sensitivities to parameters K_1 and K_2 for the two cases considered (conductive and insulating deposits) are plotted in **Figure 11** and **Figure 12**.

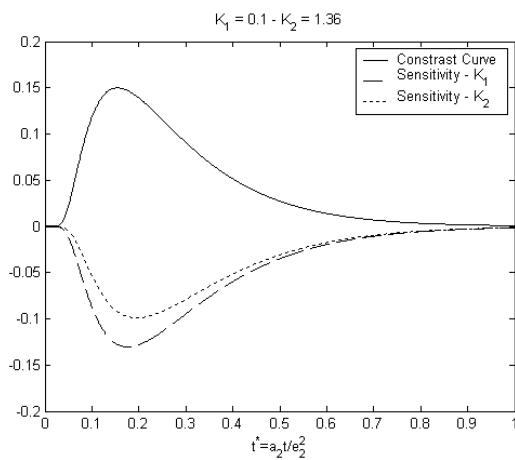


Figure 11 : Contrast curve and reduced sensitivities to K_1 and K_2 (Case 1)

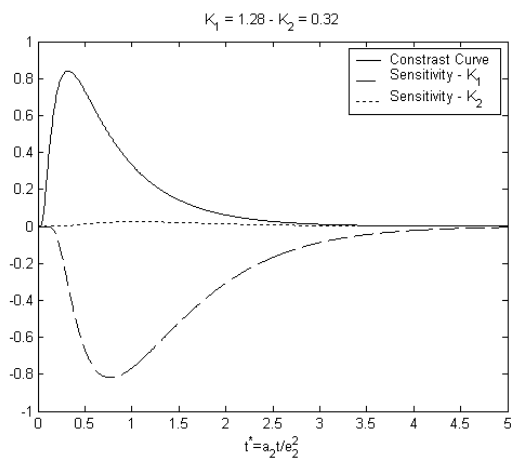


Figure 12 : Contrast curve and reduced sensitivities to K_1 and K_2 (Case 2)

These two examples are representative of most of the cases that can be met. In the first case, both sensitivities are of the same order of magnitude but seem to be strongly correlated: they exhibit a nearly constant ratio, which means that they are proportional. In the second case, one of the sensitivity is low.

➤ **Covariance and correlation matrices**

Table 4 gives the scaled covariance matrix $\text{rcov}(\hat{\mathbf{K}}) = \sigma^2 (\mathbf{S}^T \mathbf{S}^*)^{-1}$ defined in (52b), as well as the correlation matrix $\text{cor}(\hat{\mathbf{K}})$ defined in (15), for the two cases considered (the standard-deviation of noise σ is taken equal to unity here and 1000 points in time are used for the simulation of the thermal contrast curve).

Variance-Covariance	Variance-Covariance
$\begin{matrix} 28.0302 & -35.9846 \\ -35.9846 & 46.6417 \end{matrix}$	$\begin{matrix} 0.1067 & 3.1409 \\ 3.1409 & 99.1677 \end{matrix}$
Correlation	Correlation
$\begin{matrix} 1.0000 & -0.9952 \\ -0.9952 & 1.0000 \end{matrix}$	$\begin{matrix} 1.0000 & 0.9655 \\ 0.9655 & 1.0000 \end{matrix}$
Case 1	Case 2

Table 4 : Reduced covariance and correlation matrices K_1 and K_2 (for $\sigma = 1$)

The most interesting information is given by the reduced variance-covariance matrix $\text{rcov}(\hat{\mathbf{K}})$: it takes into account at the same times the reduced sensitivities through the inversion of the reduced information matrix $\mathbf{S}^T \mathbf{S}^*$ as well as the noise through its standard deviation σ .

We calculate now the square root of the diagonal terms of matrix $\text{rcov}(\hat{\mathbf{K}})$, that is the relative standard deviations of the estimates of each parameter K_1 and K_2 , for a reduced standard deviation of the noise on each of the two T_2^* and $T_{1/2}^*$ scaled thermograms now equal to $\sigma^* = 0.01$. This corresponds to a signal over noise ratio of 100. So measurement of the (experimental) reduced thermal contrast ΔT^{*exp} is affected by a (relative) standard deviation ΔT^* equal to $\sqrt{2} \sigma^*$ (for two independent experiments, because $\text{var}(\Delta T^{*exp}) = \text{var}(T_2^{*exp}) + \text{var}(T_{1/2}^{*exp}) = 2 \sigma^{*2}$), one gets (application of equation (52b) with $\sqrt{2} \sigma^*$ replacing σ):

$$\begin{array}{l}
 \text{- for case 1:} \\
 \sigma_{\hat{K}_1} / K_1 = \sqrt{2} \sigma^* \sqrt{28.0302} = 0.0749 \approx 7.5\% \quad \text{for} \quad K_1 = 0.1 \\
 \sigma_{\hat{K}_2} / K_2 = \sqrt{2} \sigma^* \sqrt{46.6417} = 0.0966 \approx 9.5\% \quad \text{for} \quad K_2 = 1.36
 \end{array} \tag{82a}$$

It is interesting to calculate the singular values of the reduced sensitivity matrix \mathbf{S}^* . They are the square roots of the eigenvalues (equal to the singular values) of the reduced information matrix $\mathbf{S}^{*T} \mathbf{S}^*$ and can also be calculated through the inverse of the eigenvalues of $(\mathbf{S}^{*T} \mathbf{S}^*)^{-1}$:

$$\begin{aligned}
 w_1(\mathbf{S}^*) &= (w_1(\mathbf{S}^{*T} \mathbf{S}^*))^{1/2} = 1 / (w_2((\mathbf{S}^{*T} \mathbf{S}^*)^{-1}))^{1/2} = 2.4347 \\
 w_2(\mathbf{S}^*) &= (w_2(\mathbf{S}^{*T} \mathbf{S}^*))^{1/2} = 1 / (w_1((\mathbf{S}^{*T} \mathbf{S}^*)^{-1}))^{1/2} = 0.1159
 \end{aligned} \tag{82b}$$

This allows to get the condition number of \mathbf{S}^* (see Lecture L3):

$$\text{cond}(\mathbf{S}^*) = w_1(\mathbf{S}^*) / w_2(\mathbf{S}^*) = 21 \tag{82c}$$

We can also calculate the root mean square reduced standard deviation m_q of the estimates of both parameters K_1 and K_2 defined in (55):

$$m_q = \sigma^* \sqrt{2} (1/w_1^2 + 1/w_2^2)^{1/2} = 0.0864 \tag{82d}$$

It is easy to check that this value is simply the root mean square of the relative standards deviations given in (82a).

Let us note that this value (82c) is close to the lower bound of m_q defined in (56), here:

$(\sigma^* \sqrt{2}) / (\sqrt{2} w_2) = \sigma^* / w_2 = 0.0862$. The smallest singular value is mostly responsible for the relative errors on both parameters.

The same calculations can be made for the second case:

$$\begin{array}{l}
 \text{- for case 2:} \\
 \sigma_{\hat{K}_1} / K_1 = \sqrt{2} \sigma^* \sqrt{0.1067} = 0.0046 \approx 0.5\% \quad \text{for} \quad K_1 = 1.28 \\
 \sigma_{\hat{K}_2} / K_2 = \sqrt{2} \sigma^* \sqrt{99.1677} = 0.1408 \approx 14.1\% \quad \text{for} \quad K_2 = 0.32
 \end{array} \tag{83a}$$

and : $w_1(\mathbf{S}^*) = 11.7851 \quad w_2(\mathbf{S}^*) = 0.1004$ (83b)

So, the condition number of \mathbf{S}^* is:

$$\text{cond}(\mathbf{S}^*) = w_1(\mathbf{S}^*)/w_2(\mathbf{S}^*) = 117$$
 (83c)

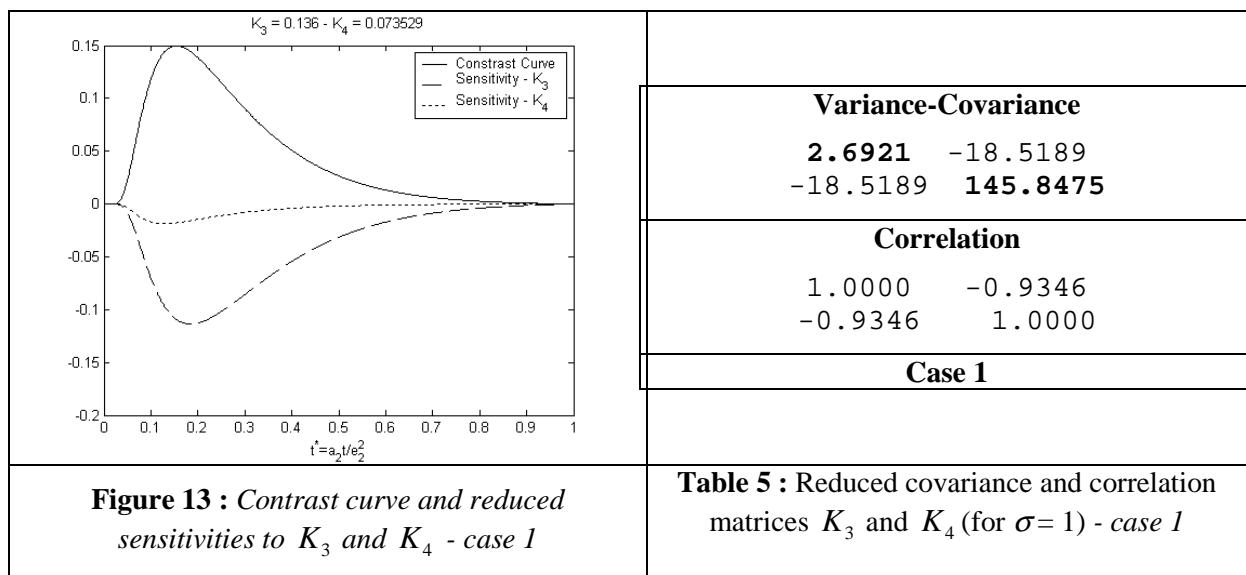
which means that matrix \mathbf{S}^* is more ill-conditioned in the second case with respect to the first one.

One also get here: $m_q = 0.0996$ and lower bound for m_q : $\sigma^* / w_2 = 0.0996$ (83d)

So, returning to case 1, it appears clearly that both the ratios K_1 of the characteristic times and K_2 of the effusivities can be estimated with a relative error nearly equivalent for both parameters (in the 7 to 10 % interval): this was already apparent in **Figure 11** where the reduced sensitivity curves corresponding to both parameters were very close, with a slightly higher absolute value for the sensitivity to K_1 .

For case 2, it is clearly the ratio K_1 of the characteristic times that can be reached, with a very good precision (0.5 % here): this is quite natural since the reduced sensitivity to K_2 in **Figure 12** is close to zero. So, because of the non linear character of this PEP problem, the accessible parameter depends on the location of the (K_1, K_2) parameter vector in the \mathbf{R}^2 plane.

The question that remains is to know if is possible to measure, with higher precisions, two parameters derived from (K_1, K_2) using the experiment corresponding to case 1 for example. Let us introduce for instance the (K_3, K_4) pair instead of (K_1, K_2) in the analytical model.



The thermal contrast is naturally the same (the materials are identical). **Table 5** gives the scaled covariance matrix $\text{rcov}(\hat{\mathbf{K}})$ as well as the correlation matrix $\text{cor}(\hat{\mathbf{K}})$ for the estimator of $\mathbf{K} = [K_3 \ K_4]^T$. The relative standard deviation of both parameters becomes (for $\sigma^* = 0.01$):

$$\begin{array}{l}
 \text{- for case 1: } \\
 \boxed{\begin{array}{l}
 \sigma_{\hat{K}_3} / K_3 = \sqrt{2} \sigma^* \sqrt{2.6921} = 0.0232 \approx 2.3\% \quad \text{for } K_3 = 0.136 \\
 \sigma_{\hat{K}_4} / K_4 = \sqrt{2} \sigma^* \sqrt{145.8475} = 0.1708 \approx 17.1\% \quad \text{for } K_4 = 0.0735
 \end{array}}
 \end{array} \quad (84a)$$

So, when comparing (84a) and (82a), one clearly sees that instead of having (K_1, K_2) with quite poor precisions, the (K_3, K_4) allows to retrieve very precise values for the ratio of volumetric heat capacities K_3 . This was already apparent in **Figure 13**: the relative sensitivity to K_4 was quite low when compared to the one of K_3 , but both minima of the corresponding curves occurred at times far apart, with a degree of colinearity much weaker than in figure 11 (see also section 3.3.2 of this lecture).

This result obtained for the two cases can be explained from the expression of the contrast curve.

$$\Delta \tilde{\theta}^* = \frac{1}{s} \left[\frac{1 + K_1 K_2}{K_2 \sinh(K_1 s) \cosh(s) + \sinh(s) \cosh(K_1 s)} - \frac{1}{\sinh(s)} \right] \quad (84b)$$

In the previous case (conductive coating on an insulating substrate), K_1 is close to zero. A rough approximation can be obtained by setting: $\begin{cases} \sinh(K_1 s) \approx K_1 s \\ \cosh(K_1 s) \approx 1 \end{cases}$

$$\boxed{\Delta \tilde{\theta}^* = \frac{1}{s} \left[\frac{1 + K_3}{K_3 s \cosh(s) + \sinh(s)} - \frac{1}{\sinh(s)} \right]} \quad (84c)$$

We can see then that within this first order approximation, the model is only a function of $K_3 = K_1 K_2$. We can check the other criteria already considered for case 1 with the (K_1, K_2) parameters :

$$w_1(\mathbf{S}^*) = 1.7270 \quad w_2(\mathbf{S}^*) = 0.0821 \quad (84d)$$

So, the condition number of \mathbf{S}^* is:

$$\text{cond}(\mathbf{S}^*) = w_1(\mathbf{S}^*) / w_2(\mathbf{S}^*) = 21 \quad (84e)$$

Compared to the preceding parameterization, the reduced sensitivity matrix \mathbf{S}^* as well as its singular values have changed, but the condition number is the same, see (82c).

One also get here:

$$m_q = 0.1219 \quad \text{and lower bound for } m_q : \sigma^* / w_2 = 0.1218 \quad (84f)$$

When both m_q 's are compared, see (82d), one can say that the global precision of the estimation of the (K_3, K_4) parameterization is lower than the (K_1, K_2) one. However we will see later on that this

superiority of the (K_3, K_4) parameterization is only an apparent one if both thermophysical characteristics of the film are looked for.

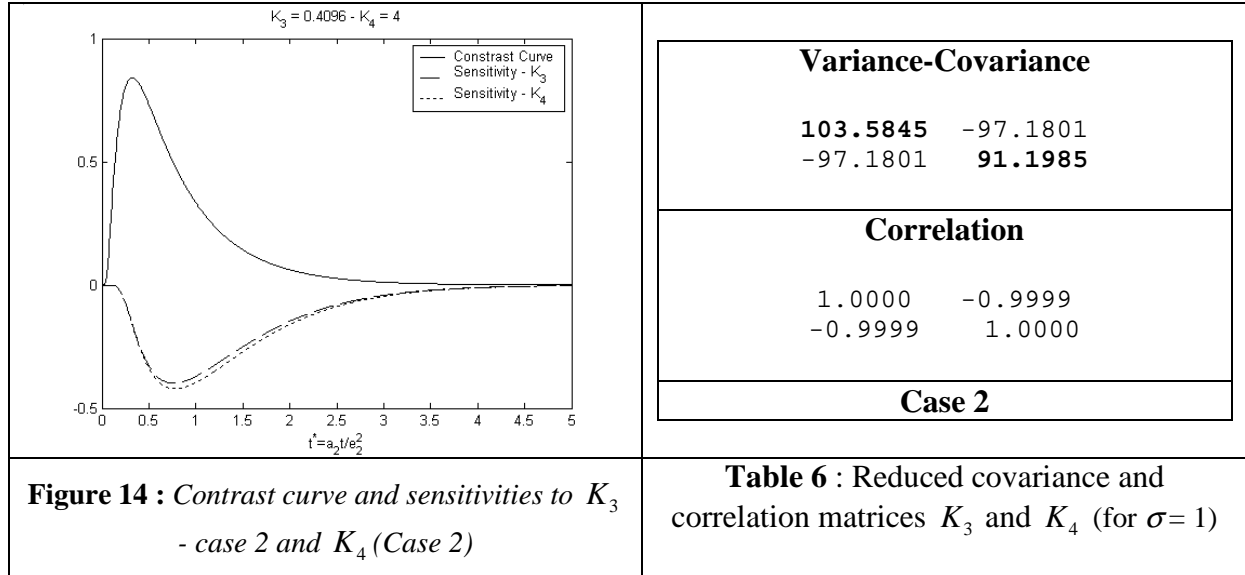


Figure 14 : Contrast curve and sensitivities to K_3 - case 2 and K_4 (Case 2)

Table 6 : Reduced covariance and correlation matrices K_3 and K_4 (for $\sigma = 1$)

In case 2 (insulating coating on a conductive substrate), parameters K_3 and K_4 are strongly correlated and exhibit the same sensitivity curves – see **Figure 14**. This confirms the result we observed previously, that is a thermal contrast mostly sensitive to K_1 .

$$K_3 K_4 = \frac{C_1}{C_2} \frac{R_1}{R_2} = \frac{R_1 C_1}{R_2 C_2} = \frac{tc_1}{tc_2} = K_1^2 \tag{85a}$$

This can be also explained by the fact that K_1 is close to unity :

$$\sinh(K_1 s) \cosh(s) \approx K_1 \sinh(s) \cosh(K_1 s) \tag{85b}$$

This yields:

$$\Delta \tilde{\theta}_{out}^* = \frac{1}{s} \left[\frac{1}{\sinh(s) \cosh(K_1 s)} - \frac{1}{\sinh(s)} \right] \tag{85c}$$

So, the thermal contrast is mainly a function of K_1 . Returning to the same calculation as in the other case, using **Table 6**, one gets:

- for case 2:	$\sigma_{\hat{K}_3} / K_3 = \sqrt{2} \sigma^* \sqrt{103.5845} = 0.1439 \approx 14.4\%$	for $K_3 = 0.4096$	(85d)
	$\sigma_{\hat{K}_4} / K_4 = \sqrt{2} \sigma^* \sqrt{91.1985} = 0.1351 \approx 13.5\%$	for $K_4 = 4$	

The singular values of the reduced sensitivity matrix are:

$$w_1(\mathbf{S}^*) = 8.3624 \quad w_2(\mathbf{S}^*) = 0.0717 \quad (85e)$$

So, the condition number of \mathbf{S}^* is:

$$\text{cond}(\mathbf{S}^*) = w_1(\mathbf{S}^*)/w_2(\mathbf{S}^*) = 117 \quad (85e)$$

We observe here the same thing as for case 2: the condition number of the reduced sensitivity matrix is independent of the parameterization, see (83c).

One also gets here:

$$m_q = 0.1396 \quad \text{and lower bound for } m_q: \sigma^* / w_2 = 0.1395 \quad (85f)$$

When both m_q 's are compared, see (83d), one can say that the global precision of the estimation of the (K_3, K_4) parameterization, which provided an excellent estimation for K_3 , is lower than the (K_1, K_2) one.

4.3 Note on the change of parameters

It has been suggested earlier that some change of parameterization would allow to overcome parameter estimation difficulties such as in the case of high correlation coefficients inducing high variances for the estimated parameters for example. We want here to come back to this discussion to give, very briefly, some precisions and our conclusions.

First, and taking experience of what has been shown previously, if a change of parameterization is made that results in the production of a new parameter of sensitivity close to zero (and thereof excluded from the model), this new parameterization will have a positive effect and will allow to properly estimate the remaining ones. Note that it is the object of Dimensional Analysis to help making such reparameterization efficient.

Second, if all the parameters of the problem have non negligible sensitivities but appear correlated, the question is: is it possible to find a new set of parameters defined from the initial one, to enhance the quality of the estimation process?

The answer is no. It can be demonstrate, see Remy [9] that the sensitivities to a new set of parameters can be derived from the sensitivities of the current set (using the Jacobian of the transformation). The same is true for the variance-covariance matrix and the explanation is obvious from the quantified SVD analysis given above (the same condition number of \mathbf{S}^* is obtained whatever set of parameterization is used) These relationships show that:

- if two parameters appear correlated in a given set of parameters, two parameters of a new set, recombined from the previous ones, will also be correlated.
- if the sensitivity of a parameter is changed with a new parameterization (for example, it is enhanced), this will not change its variance in fine.

For instance, if we keep the parameter K_1 and choose another second parameter instead of K_2 , we can show that the sensitivity curve to K_1 can become higher or lower: we have to remind that the partial derivative that appears in the definition (4) of a sensitivity coefficient is associated to the variation of the output of the model for a variation of a given parameter, which requires that the other ones stay fixed at given values. This means that if the definition of these other parameters is changed, such is also the case for the sensitivity coefficients. So, talking of a sensitivity coefficient to a given parameter does not mean anything if the other parameters in the parameter vector are not specified.

This observation could lead us to consider as theoretically possible to improve the estimation of K_1 by combining this parameter with a particular parameter that can increase its sensitivity. In fact, this is not true because the standard-deviation of the estimates of the parameters not only depend on the sensitivities of parameters but also on the correlation between the estimates of the different parameters.

To show this, we are going to see through an example how the standard-deviations (square roots of variances) of the new set of parameters change when one parameter is kept as for instance parameter $K_1 = K_a = K_1^\alpha K_2^\beta$ with $\alpha=1; \beta=0$ while K_2 is replaced by $K_b = F_b(K_1, K_2)$:

$$\begin{aligned} K_a &= F_a(K_1) = K_1 \\ K_b &= F_b(K_1, K_2) \end{aligned} \tag{86}$$

We have:

$$y_{mo} = \eta(t; \mathbf{K}) \text{ with } \mathbf{K} = \begin{bmatrix} K_1 \\ K_2 \end{bmatrix} \Rightarrow dy_{mo} = \mathbf{S} d\mathbf{K} = \mathbf{S}' d\mathbf{K}' \text{ with } \mathbf{K}' = \begin{bmatrix} K_a \\ K_b \end{bmatrix} \tag{87}$$

where \mathbf{S} is the sensitivity matrix to the old (K_1, K_2) set of parameters and \mathbf{S}' the sensitivity matrix to the new (K_a, K_b) one. This requires the calculation of the Jacobian matrix \mathbf{J} of this transformation since ;

$$d\mathbf{K}' = \mathbf{J} d\mathbf{K} \Rightarrow \mathbf{S} = \mathbf{S}' \mathbf{J} \quad \text{and} \quad \text{cov}(\hat{\mathbf{K}}') = \mathbf{J} \text{cov}(\hat{\mathbf{K}}) \mathbf{J}^T \tag{88}$$

The last equation in (88) stems from the linearization around the exact value of the \mathbf{K} parameter vector:

$$\text{cov}(\hat{\mathbf{K}}) = \text{cov}(d\hat{\mathbf{K}}) \tag{89}$$

with:

$$\mathbf{J} = \frac{D(F_a, F_b)}{D(K_1, K_2)} = \begin{bmatrix} \frac{\partial F_a}{\partial K_1} & \frac{\partial F_a}{\partial K_2} \\ \frac{\partial F_b}{\partial K_1} & \frac{\partial F_b}{\partial K_2} \end{bmatrix} = \begin{bmatrix} 1 & 0 \\ F_{b,1} & F_{b,2} \end{bmatrix} \tag{90}$$

So, the sensitivity matrix to the new parameter set \mathbf{K}' is:

$$\mathbf{S}' = [\mathbf{S}_a \quad \mathbf{S}_b] = \mathbf{S} \mathbf{J}^{-1} = [\mathbf{S}_1 \quad \mathbf{S}_2] \begin{bmatrix} 1 & 0 \\ -F_{b,1}/F_{b,2} & 1/F_{b,2} \end{bmatrix} = [\mathbf{S}_1 - (F_{b,1}/F_{b,2})\mathbf{S}_2 \quad (1/F_{b,2})\mathbf{S}_2] \quad (91)$$

Here the old sensitivity column vectors \mathbf{S}_1 and \mathbf{S}_2 , as well as the new ones \mathbf{S}_a and \mathbf{S}_b , have been explicitly written in the corresponding sensitivity matrices, \mathbf{S} and \mathbf{S}' respectively.

Application of (88) allows the calculation of the variances and covariance of the estimators of the new set of parameters (K_a, K_b) :

$$\text{cov}(\hat{\mathbf{K}}') = \begin{bmatrix} \text{var}(\hat{K}_a) & \text{cov}(\hat{K}_a, \hat{K}_b) \\ \text{cov}(\hat{K}_a, \hat{K}_b) & \text{var}(\hat{K}_b) \end{bmatrix} = \begin{bmatrix} 1 & 0 \\ F_{b,1} & F_{b,2} \end{bmatrix} \begin{bmatrix} \text{var}(\hat{K}_1) & \text{cov}(\hat{K}_1, \hat{K}_2) \\ \text{cov}(\hat{K}_1, \hat{K}_2) & \text{var}(\hat{K}_2) \end{bmatrix} \begin{bmatrix} 1 & F_{b,1} \\ 0 & F_{b,2} \end{bmatrix} \quad (92)$$

that is:

$$\begin{aligned} \text{var}(\hat{K}_a) &= \text{var}(\hat{K}_1) \\ \text{var}(\hat{K}_b) &= F_{b,1}^2 \text{var}(\hat{K}_1) + F_{b,2}^2 \text{var}(\hat{K}_2) + 2 F_{b,1} F_{b,2} \text{cov}(\hat{K}_1, \hat{K}_2) \\ \text{cov}(\hat{K}_a, \hat{K}_b) &= F_{b,1} \text{var}(\hat{K}_1) + F_{b,2} \text{cov}(\hat{K}_1, \hat{K}_2) \end{aligned} \quad (93a)$$

We can see that even if the change of parameters modifies the sensitivity to parameter K_a , which replaces parameter K_1 in the new set of parameters, the variance of this parameter remains unchanged whatever the choice of the second parameter.

This means that the variance of a given parameter (and consequently the error on this parameter) is independent on the choice of the second parameter. Thus, identifying the parameter K_1 from the (K_1, K_2) pair is equivalent to estimating K_1 from the (K_1, K_3) or (K_1, K_4) pairs.

Similarly, we can show that aiming at estimating parameters (K_3, K_4) either through the parameterization (K_1, K_2) or directly is strictly the same.

The conclusion is that the interest of a change of parameters is justified only when an improved estimation of a particular parameter of interest is looked for.

Whatever the parameterization, if the thicknesses of both layers are known, as well as the thermophysical properties of the substrate, we have:

$$\begin{aligned} \sigma_{\rho \hat{c}_1} / \rho c_1 &= \sigma_{\hat{K}_3} / K_3 = 2.3 \% \quad \text{for case 1} \\ \sigma_{\hat{a}_1} / a_1 &= \sigma_{\hat{K}_1} / K_1 = 0.4 \% \quad \text{for case 2} \end{aligned} \quad (93b)$$

So, this rear face thermal contrast technique allows estimation of the capacity of the film for a case 1 and of its diffusivity in case 2, for high enough signal over noise ratios.

In case of very low sensitivity to a given parameter, it is possible to fix the value of the corresponding parameter to its nominal values. So, if the number of parameters that are looked for is reduced, then the stochastic errors on the remaining parameters (reduced standard deviations) go

down. However, their estimation becomes biased and leads to a systematic error on each estimated parameter such as:

$$b_{\hat{\beta}_r} = E(\hat{\beta}_r) - \beta_r = -(\mathbf{S}_r^T \mathbf{S}_r)^{-1} \mathbf{S}_r^T \mathbf{S}_c (\beta_c^{nom} - \beta_c^{exact}) \tag{93c}$$

Here the initial parameter vector has been decomposed into two parts $\beta = \begin{bmatrix} \beta_r \\ \beta_c \end{bmatrix}$, where β_r gathers the parameters that are looked for and its complementary part β_c is supposed to be known, that is its value is blocked to a nominal value $\beta_c = \beta_c^{nom}$ which differs from its exact value β_c^{exact} . Equation (94), which has already been derived in the case of a linear model in lecture L2 of this series (see also [1]), corresponds here to a linearization in the neighborhood of the exact value of β .

This technique, which consists in reducing the number of parameters that are looked for, presents an interest only if the bias caused by the reduction of the number of parameters and its associated standard deviations are much lower than the initial stochastic error as illustrated in **Figure 15**.

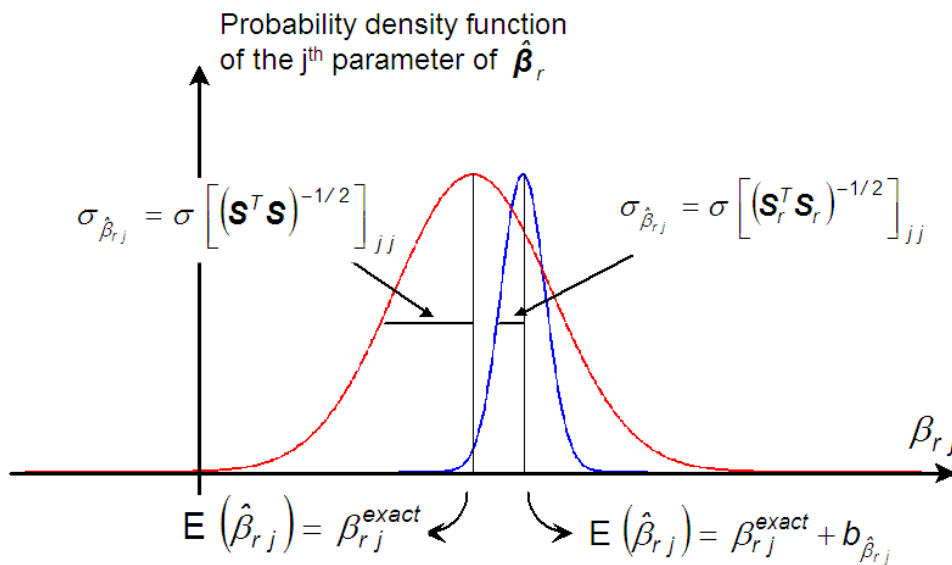


Figure 15 : Comparison between the probability density distributions of the j^{th} parameter of the parameter vector for two different estimators 1) all the parameters in β are estimated altogether (red) or 2) only the components of one of its part β_r (blue) are estimated while its complementary part β_c are blocked to its nominal value. **NB:** here one assumes that index j in β and in β_r are the same ($\beta_{r,j} = \beta_j$) and that the scale of the vertical axis is different for both distributions for practical plotting reasons (the area below both distributions should be equal to unity)

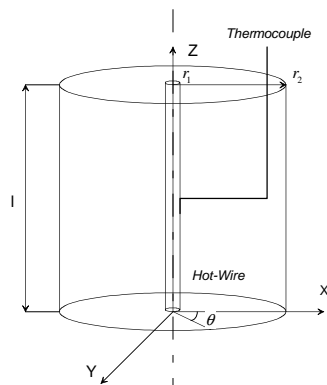
5. Models with different numbers of parameters: the hot wire case

5.1 Different models for thermal characterization by the hot wire method

The Hot-Wire technique [8] consists in a constant heat power generation by Joule effect through a thin cylindrical wire embedded in the material that is assumed to be a semi-infinite medium (no heat losses), see **Figure 16**. The transient temperature rise of this wire is measured by a thermocouple (crossbar technique).

5.1.1 The standard hot wire model: model 0

At longer times, the Hot-Wire temperature evolution (asymptotic expansion) is only a function of the thermal conductivity of the material and is given by the following expression (this model will be called model 0 now on):



$$\theta_1(r_1, t) = \frac{\Phi_1}{4\pi l \lambda} \ln(t) + C^{St} \tag{94}$$

- r_1 and l : Hot-Wire radius and length
- r_2 : medium radius
- θ_1 and Φ_1 : temperature and flux (Power dissipation in watts) in $r = r_1$
- λ_1 : thermal conductivity of the material/powder
- C^{St} : arbitrary constant

Figure 16: Theoretical model in cylindrical coordinates system

In a semilog time plot, the temperature rise, equation (94) in **Figure 16**, is then linear. Knowing the heat power dissipation, the heat conductivity of the material can be determined from the slope.

5.1.2 The finite hot wire model: model 1

A quadrupole approach [7] can be efficiently used to build this model in which hot-wire (modelled by a resistance R between average wire temperature and the lineic power dissipation at its output radius r_1 and by a thermal capacity C) and medium (through Z_1 , Z_2 and Z_3 impedances) thermal properties, contact resistance between Hot-Wire and material (R_c) and convective resistance (heat losses) with the surrounding environment (R_{conv}) will be taken into account. This method allows us to represent each part of the system by a transfer matrix that linearly links in Laplace domain the temperature/flux in or out each material or interface, see [8].

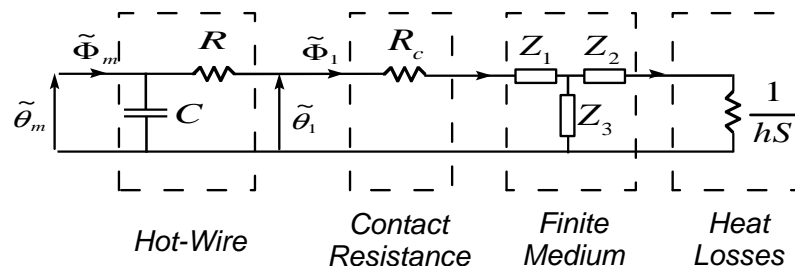


Figure 17: Schematic representation of the Hot-Wire / Medium system - Model 1

Let $\tilde{\theta}_m$ and $\tilde{\Phi}_m$ be the Laplace transforms of the Hot-Wire mean temperature variation and mean power dissipation respectively.

Their expressions are given by:

$$\tilde{\theta}_m = \frac{1}{V_1} \int_0^{r_1} \theta \cdot 2\pi r l dr = \frac{2}{r_1^2} \int_0^{r_1} \theta r dr \quad (95a)$$

and by:
$$\tilde{\Phi}_m = V_1 G_0(\rho) \quad \text{with : } V_1 = \pi r_1^2 l \quad (95b)$$

where $G_0(\rho) = L(g_0(t))$ is the Laplace transform of the volumetric Hot-Wire heat dissipation g_0 (W.m⁻³).

$\tilde{\theta}_1$ and $\tilde{\Phi}_1$ represent the Laplace transforms of temperature and flux in $r = r_1$ (the inverse Laplace transform is implemented through a numerical algorithm)

$$\tilde{\theta}_1 = \frac{\tilde{\Phi}_m}{\left(\frac{1+RC \cdot \rho}{R_c + Z'} \right) + C \cdot \rho} \quad \text{with : } Z' = Z_1 + \frac{Z_3(Z_2 + R_{conv})}{(Z_2 + Z_3 + R_{conv})} \quad (96)$$

The expressions of Z_1, Z_2 and Z_3 are given by:

$$Z_1 = \frac{A-1}{C'}, Z_2 = \frac{D-1}{C'} \quad \text{and} \quad Z_3 = \frac{1}{C'} \quad (97)$$

with:

$$\begin{aligned} A &= k r_2 (K_1(k r_2) \cdot I_0(k r_1) + K_0(k r_1) \cdot I_1(k r_2)) \\ B &= \frac{1}{2\pi \lambda l} (K_0(k r_1) \cdot I_0(k r_2) - K_0(k r_2) \cdot I_0(k r_1)) \\ C' &= -2\pi \lambda l k^2 r_1 r_2 (K_1(k r_2) \cdot I_1(k r_1) - K_1(k r_1) \cdot I_1(k r_2)) \\ D &= k r_1 (K_0(k r_2) \cdot I_1(k r_1) + K_1(k r_1) \cdot I_0(k r_2)) \end{aligned} \quad (98)$$

where $k = \sqrt{\rho/a_{medium}}$ (ρ being the Laplace variable and a_{medium} the heat diffusivity of the material) and $K_n(.)$ and $I_n(.)$ are the modified Bessel functions

The Hot-Wire resistance R and capacity C can be easily obtained from these general expressions of by assuming that the Hot-Wire response time and size are small when compared to the medium ones (i.e. $\rho \rightarrow 0$ and $r_1 \ll r_2$).

We obtain for the "hot" wire ([7]):

$$R = \frac{1}{8\pi \lambda_{wire} l} \quad : \text{Resistance} \qquad C = \pi r_1^2 l (\rho C_p)_{wire} \quad : \text{Capacity (99)}$$

The heat loss resistance is given by (r_2 being here the radius of the sample):

$$R_{conv} = \frac{1}{hS_2} \quad \text{with:} \quad S_2 = 2\pi r_2 l \qquad (100)$$

Knowing the mean heat power dissipation Φ_m , this model perfectly describes the real time evolution of the hot-wire temperature θ_1 that is measured by the thermocouple.

5.1.3 The semi-infinite hot wire model: model 2

In the case of a semi-infinite medium where $kr_2 \gg 1$, we show that Z_2 and Z_3 tend to zero and Z_1 to a very simple expression, called model 2 now on, see **Figure 18**:

$$Z_1 \rightarrow Z_{1\infty} = \frac{1}{2\pi\lambda l} \frac{K_0(kr_1)}{kr_1 \cdot K_1(kr_1)} \qquad (101)$$

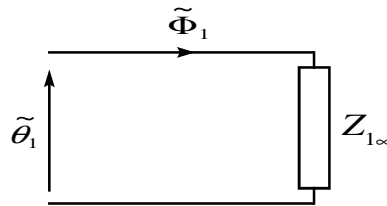


Figure 18 : *Quadrupole formulation of a semi-infinite medium - Model 2*

5.2 Sensitivity study

In **Figure 19**, the reduced sensitivity curves are plotted in the cases of the semi-infinite (model 2) and finite (model 1) samples, and the corresponding correlation matrices $\text{cor}(\hat{\beta})$, for the following parameters:

- Hot-Wire Conductivity, λ_{wire}
- Hot-Wire Diffusivity, a_{wire} written as $\lambda_{wire} / (\rho C_p)_{wire}$ in the sensitivity calculations
- Medium Conductivity, λ_{medium}
- Medium Diffusivity, a_{medium}
- Contact resistance between Hot-Wire and medium, R_c
- Convective Resistance (Heat Losses with the surrounding), R_{conv}

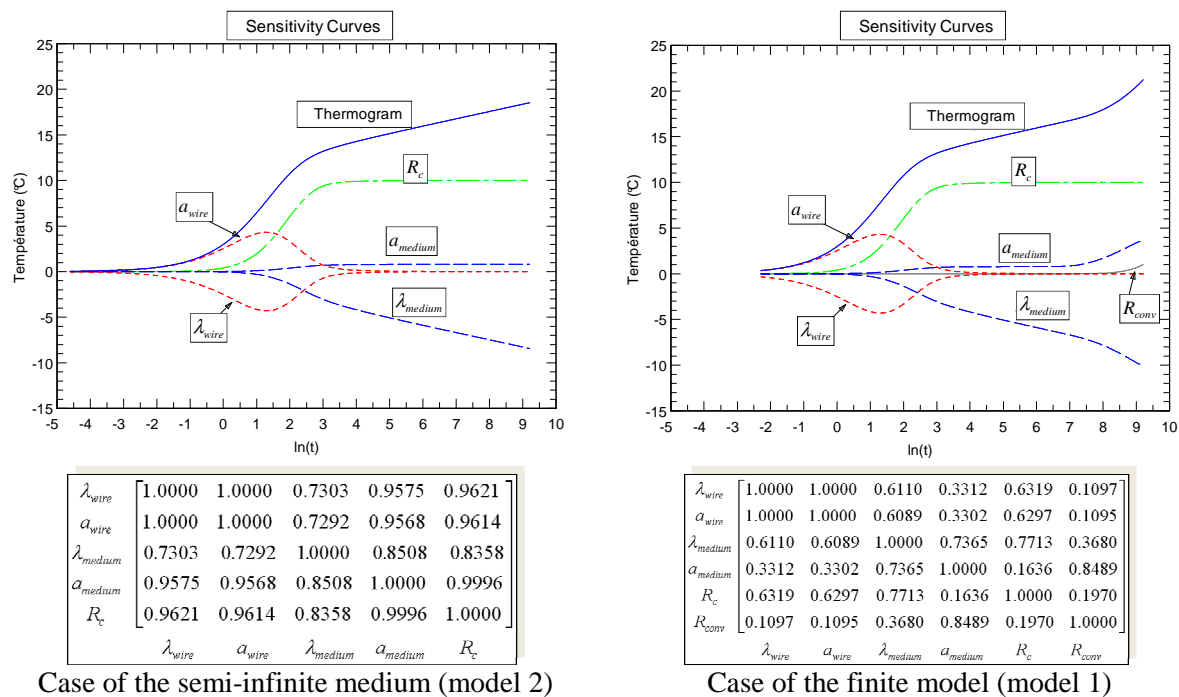


Figure 19: Sensitivity curves and correlation matrices in the case of the semi-infinite (2) and finite (1) models

In the case of the semi-infinite material (model 2), we can observe that the sensitivity curves to Hot-Wire conductivity and diffusivity exhibit the same shape with opposite signs. Such is also the case for the sensitivities to the contact resistance and to the medium diffusivity within a proportionality factor. The sensitivity curve to the medium conductivity is increasing with time and exhibits the same type of variation as the temperature response of the wire, while the others rapidly tend to zero or to an asymptotic value. This also clearly shows that the $(\lambda_{wire}, a_{wire})$ and (R_c, a_{medium}) pairs are correlated and that the more sensitive and non-correlated parameter is the thermal conductivity λ_{medium} of the material, the parameter we are seeking for.

The sensitivity coefficients obtained in the case of a material of finite size (model 1) are also shown in **Figure 19**. They are similar except for longer times. The $(\lambda_{wire}, a_{wire})$ pair remains correlated but because of the introduction of a new parameter R_{conv} , the contact resistance R_c and the medium diffusivity a_{medium} become non correlated while R_{conv} appears to be correlated with a_{medium} and λ_{medium} . All the previous remarks can be quantitatively confirmed by evaluating the correlation parameters shown in the matrices in **Figure 19**.

This validates the thermal conductivity measurement by the inverse method presented here. To perform a good measurement, we have then to consider an acquisition time large enough to reduce the Hot-Wire convection effect (thermal properties) and small enough to avoid the boundary effect (heat losses). Plotting sensitivity curves allows to determine the best estimation interval over which the asymptotic model 0 can be applied (lower bound chosen to prevent the effects of the Hot-Wire properties and of the contact resistance and upper bound to prevent the convective resistance effect).

5.3 Model Reduction using fewer parameters

We can observe that in the two cases we considered, the $(\lambda_{wire}, a_{wire})$ pair is always correlated, see **Figure 19**. A close examination of the analytic form of the temperature response shows that, after simplification, that only the ratio $\lambda_{wire} / a_{wire} = \rho C_{p wire}$ appeared : this explains the fact that their scaled sensitivities to these two coefficients are equal, with opposite signs.

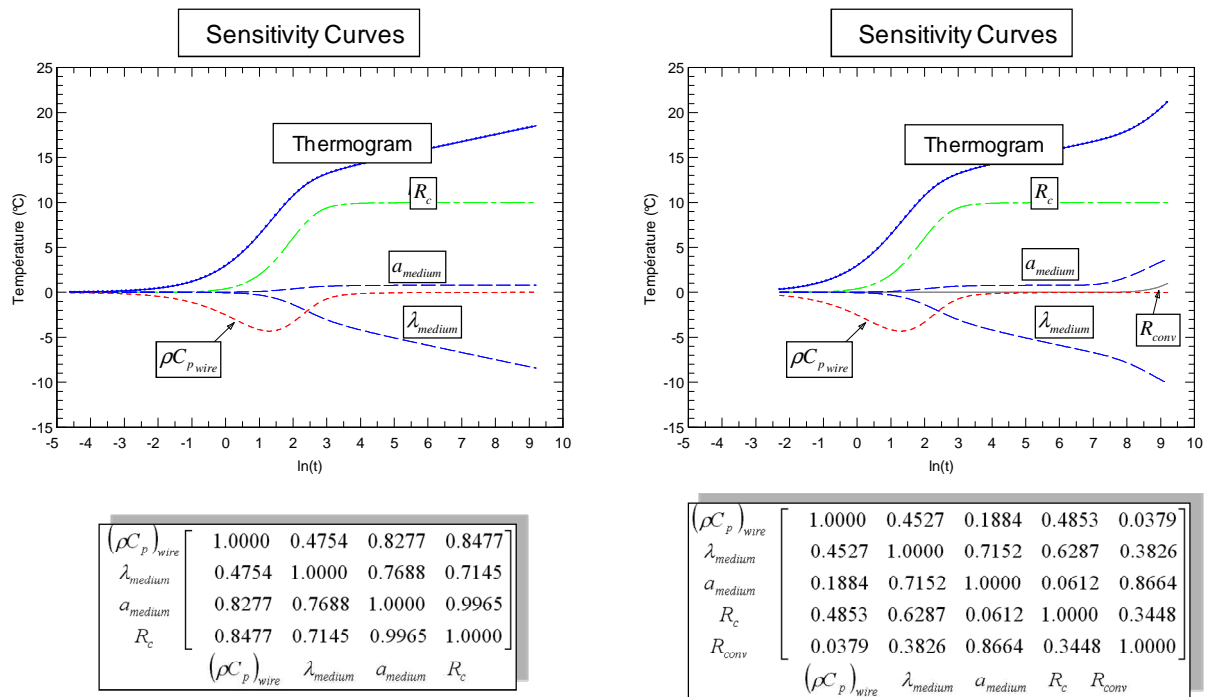


Figure 20: Sensitivity curves in the case of the semi-infinite and finite models (Reduced Models (1') right and (2') left)

So, the previous finite (1) and semi-infinite (2) models are replaced now by the corresponding models, noted (1') and (2'), with a conductivity for the wire that is supposed to be known and that is consequently fixed to its nominal value $\rho C_{p wire} = \rho C_{p wire}^{nom}$. The scaled sensitivity curves of reduced models (1') and (2'), as well as the corresponding correlation matrices $cor(\hat{\beta})$, are shown in **Figure 20**.

This reduction (one parameter is removed) is of great interest because it allows to reduce the computation time and to increase the precision on the estimated parameters (the sensitivity matrix is better conditioned).

The fact that in this case the estimation of the thermal conductivity of the medium is less affected by the others parameters can be shown through direct simulations. Figure 21 shows the different thermograms obtained for different values of the contact resistance (left) and of "hot" wire volumetric heat (right) respectively for model (2').

We can show that the slope of the curve which is directly proportional to the inverse of the thermal conductivity of the medium and is not affected by the values of these two parameters.

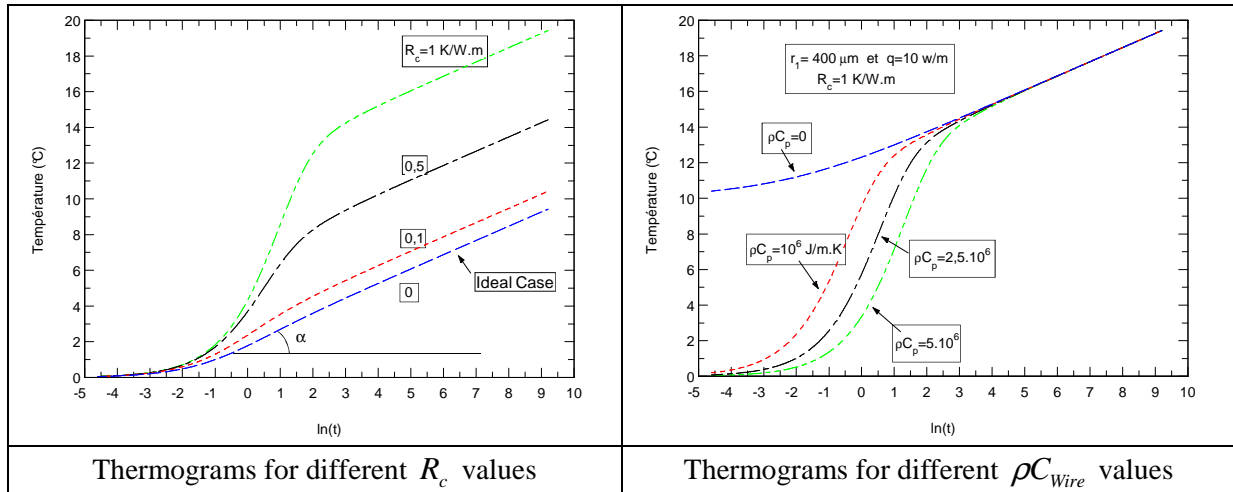


Figure 21: Thermograms for a given thermal conductivity versus R_c and ρC_{Wire}

As explained in section 3.3 of this lecture, reducing the number of degrees of parametric freedom of the model allows to improve the estimation. We will present the case of a three layer system next.

6. Design optimization: flash experiment for thermal characterization of a liquid

6.1 Modelling

The problem is described in **Figure 22**. It consists of a liquid layer in between two cylindrical walls. If the liquid layer thickness is small with respect to its inner radius modelling in a plane geometry becomes justified. A pulse heat flux is absorbed by the front face (inner surface).

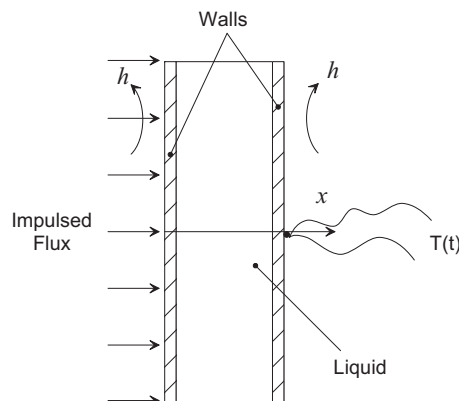


Figure 22: Model of flash experiment for thermal characterization of a liquid

The implementation of the analytical model is simplified by the use of thermal quadrupoles [7]. After a Laplace transform on the problem, our model is given by a chain of quadrupoles. A diagram of the system is given in **Figure 23**.

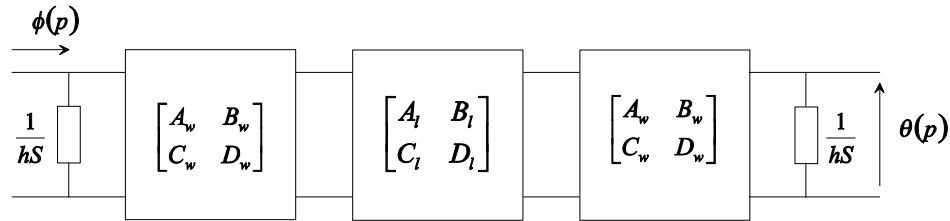


Figure 23: *Quadrupole representation*

with:

- $1/hS$ being the resistance of the convective heat losses with the surrounding inside and outside environments;
- A, B, C and D being the coefficients of the inverse transfer matrices for the walls and the liquid. Their expressions are given by:

$$A_i = D_i = \cosh\left(\sqrt{\frac{\rho e_i^2}{a_i}}\right), B_i = \frac{1}{\lambda_i S \sqrt{\frac{\rho}{a_i}}} \sinh\left(\sqrt{\frac{\rho e_i^2}{a_i}}\right) \text{ and } C_i = \lambda_i S \sqrt{\frac{\rho}{a_i}} \sinh\left(\sqrt{\frac{\rho e_i^2}{a_i}}\right) \quad (102)$$

(lower subscript i indifferently refers to the fluid or to the wall layers)

and:

- e_i : thickness of the material
- a_i : thermal diffusivity
- λ_i : thermal conductivity

6.2 Solution

The rear-face temperature $\theta(p)$ is then given by:

$$\theta(p) = \frac{\phi(p)}{C + 2A hS + B(hs)^2} \quad (103)$$

A, B and C represent the coefficients of the transfer matrix obtained by taking the product of the transfers matrices for the three materials:

$$\begin{bmatrix} A & B \\ C & D \end{bmatrix} = \begin{bmatrix} A_w & B_w \\ C_w & A_w \end{bmatrix} \begin{bmatrix} A_l & B_l \\ C_l & A_l \end{bmatrix} \begin{bmatrix} A_w & B_w \\ C_w & A_w \end{bmatrix} \quad (104)$$

with:

$$\begin{aligned} A &= (A_w A_l + B_w C_l) A_w + (A_w B_l + B_w A_l) C_w \\ B &= (A_w A_l + B_w C_l) B_w + (A_w B_l + B_w A_l) A_w \\ C &= (C_w A_l + A_w C_l) A_w + (C_w B_l + A_w A_l) C_w \end{aligned}$$

By assuming that the heat pulse $\phi(t)$ absorbed by the system ($W.m^{-2}$) is infinitely short (Dirac of flux), then its transform $\phi(p) = Q/S$ is equal to the pulse energy Q per unit area of the front face S .

For $h = 0$, the temperature at long times is obtained by:

$$T_\infty = \lim_{t \rightarrow \infty} T(t) = \lim_{p \rightarrow 0} p\theta(p) \quad (105)$$

Thus,

$$T_\infty = \lim_{p \rightarrow 0} \frac{p\phi(p)}{C(p)} \quad (106)$$

and:

$$T_\infty = \frac{Q}{S(2\rho c_w e_w + \rho c_l e_l)} \quad (T_\infty \text{ is called the adiabatic temperature}) \quad (107)$$

In the general case (for any t), the inverse Laplace transform of relation (109) is implemented numerically. We use several algorithms which gives the same results, either the Stehfest algorithm [10] the De Hoog algorithm or a numerical Inverse Fast Fourier Transform (I.F.F.T).

Figure 24 gives an example of the results obtained for two liquids (water and oil) and two different thicknesses of both walls (0,5 and 2 mm). The thermophysical properties used for the simulations are:

- $e_l = 4.5 \text{ mm}$, $h = 5 \text{ W.m}^{-2}.\text{K}^{-1}$.
- Water: $\lambda_l = 0.597 \text{ W.m}^{-1}.\text{K}^{-1}$, $a_l = 1.43.10^{-7} \text{ m}^2.\text{s}^{-1}$
- Oil: $\lambda_l = 0.132 \text{ W.m}^{-1}.\text{K}^{-1}$, $a_l = 7.33.10^{-8} \text{ m}^2.\text{s}^{-1}$
- Walls (copper): $\lambda_w = 395 \text{ W.m}^{-1}.\text{K}^{-1}$, $a_w = 1.15.10^{-4} \text{ m}^2.\text{s}^{-1}$
- $e_w = 0.5 \text{ or } 2 \text{ mm}$
- $Q/S = 4.10^4 \text{ J.m}^{-2}$

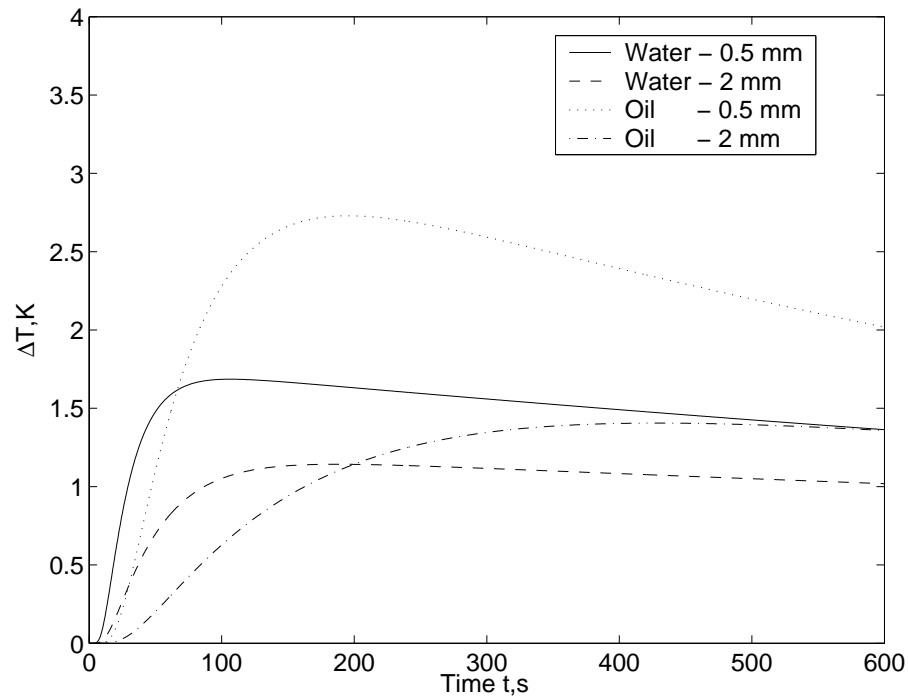


Figure 24: Simulation examples (Pulsed responses)

6.3 Sensitivity study

The model depends on several parameters. Some of them are supposed to be exactly known and the others will be identified. The initial goal is to thermally characterize the fluid, i.e. to estimate two quantities, its thermal diffusivity and conductivity (or any other set of parameters as the effusivity or the specific heat). Assuming the thermal properties of the walls and the geometry of the system known, the model is a function of four unknown parameters:

$$\begin{aligned}
 * \beta_1 &= e_1 / \sqrt{a_1} & * \beta_2 &= e_1 / \lambda_1 & (108) \\
 * \beta_3 &= Q/S & * \beta_4 &= h
 \end{aligned}$$

One can wonder here whether simultaneous estimation of these four parameters is possible. So, a sensitivity study has to be implemented.

Let β being the unknown parameter vector, the temperature response of the rear face is:

$$T = f(t; \beta_1, \beta_2, \beta_3, \beta_4) = f(t; \beta) \tag{109}$$

The experimental temperature being disturbed, one can assume an additive noise

$$y_i = T(t_i; \beta) + \varepsilon_i \tag{110}$$

ε_i being the random noise, associated with the measurement y_i at the time t_i .

The sensitivity coefficient of the response T to parameters β_j at time t is defined by:

$$S_j(t, \beta) = \frac{\partial T}{\partial \beta_j}(t, \beta) \tag{111a}$$

Thereafter, we will use the reduced sensitivity coefficients which are easier to compare:

$$S_j^*(t, \beta) = \beta_j \frac{\partial T}{\partial \beta_j}(t, \beta) \tag{111b}$$

The estimation problem is non-linear. Thus, the sensitivity curves and consequently the estimation will depend on the nominal values of the unknown parameters but also on the known parameters and the geometry of the system. This is the reason why for instance, an optimum on the walls thicknesses exists.

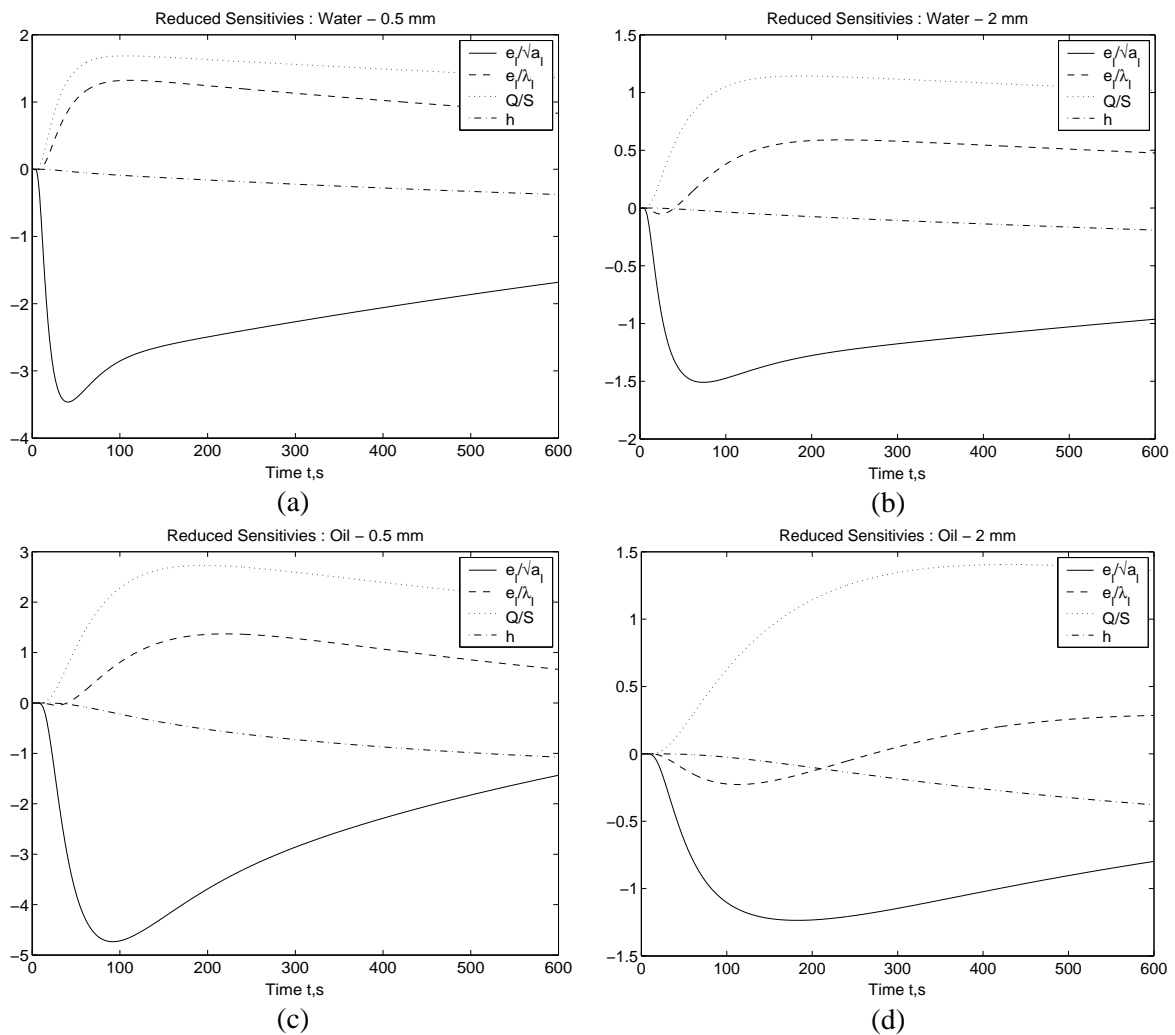


Figure 25: Sensitivity curves for Water and Oil (0.5 mm and 2 mm)

As an example,

Figure 25 gives the sensitivity functions for water and oil with 0.5 mm and 2 mm walls thicknesses respectively. The whole set of curves shows that some parameters are more or less correlated (proportional sensitivities), particularly $\beta_1 (e_i/\sqrt{a_i})$ and $\beta_3 (Q/S)$ or β_1 and $\beta_2 (e_i/\lambda_i)$, which would not allow the simultaneous estimation of these parameters and consequently of the thermal diffusivity.

In addition, one can notice that for times larger than twice the time of the maximum response, the parameters are strongly correlated. In fact, the system cooling seems to occur at a quasi-uniform temperature. The thermogram is a pure exponential which only depends on one parameter, the time-constant of the system $(2\rho c_w e_w + \rho c_l e_l)/h$. This remark suggests a limitation of the estimation interval to short times. We have chosen to work between $t = 0$ and $t = 1.5 t_{max}$ here.

The high number of parameters (4) and their correlations make the reading and the interpretation of the sensitivity curves difficult. A stochastic study will allow a better comprehension of this problem.

Useful measurements imply small variances associated to correlation coefficients far from unity. The reduced covariance matrix $rcov(\hat{\beta})$, for a unit standard deviation of the noise ($\sigma = 1^\circ C$) and the correlation matrix corresponding to the four preceding parameters are given in **Table 7** and **Table 8**.

From the reduced covariance matrices $rcov(\hat{\beta})$, one can notice that the relative variance of β_1 is the smallest one, which shows that the thermal diffusivity will be better identified than the thermal conductivity. In the same way, the estimation will be better for oil than for water. Later on, one will consider the water as a fluid test knowing that for less conducting fluids, the results will be better. Finally, one can observe that the variances strongly vary with the thickness of the walls which have thus to be optimised.

From the correlation matrices, one can note that β_3 is correlated with β_1 and β_2 in most cases, particularly for water, which confirms the preceding results. In case 4 (oil, 2 mm), one can notice that the parameters are less correlated. It will thus be possible to estimate a and λ at the same time, if the thickness of the walls is chosen in an optimal way.

One can also notice that the estimation problem is strongly non-linear since the four studied cases exhibit very different covariance and correlation matrices.

Table 7: Reduced variance-covariance Matrices (1°C standard deviation for the noise)

Water – 0,5 mm				Water – 2 mm			
0.3394	-2.3464	2.4913	1.4724	0.3218	-0.8419	0.7528	-0.5216
-2.3464	16.5302	-17.4179	-9.4267	-0.8419	2.4531	-2.0146	2.5528
2.4913	-17.4179	18.4144	10.4120	0.7528	-2.0146	1.7770	-1.3092
1.4724	-9.4267	10.4120	9.7216	-0.5216	2.5528	-1.3092	8.7357
Oil – 0,5 mm				Oil – 2 mm			
0.0649	-0.2870	0.2533	0.1216	0.1920	-0.4540	0.1500	-0.2349
-0.2870	1.3529	-1.1408	-0.4388	-0.4540	1.3544	-0.2825	1.0794

0,2533	-1,1408	0,9958	0,4599	0,1500	-0,2825	0,1413	-0,0219
0,1216	-0,4388	0,4599	0,3979	-0,2349	1,0794	-0,0219	1,4113

Table 8: Correlation Matrices

Water – 0,5 mm				Water – 2 mm			
1,0000	-0,9907	0,9966	0,8106	1,0000	-0,9476	0,9954	-0,3111
-0,9907	1,0000	-0,9983	-0,7436	-0,9476	1,0000	-0,9649	0,5514
0,9966	-0,9983	1,0000	0,7782	0,9954	-0,9649	1,0000	-0,3323
0,8106	-0,7436	0,7782	1,0000	-0,3111	0,5514	-0,3323	1,0000
Oil – 0,5 mm				Oil – 2 mm			
1,0000	-0,9685	0,9965	0,7569	1,0000	-0,8903	0,9104	-0,4512
-0,9685	1,0000	-0,9829	-0,5981	-0,8903	1,0000	-0,6457	0,7807
0,9965	-0,9829	1,0000	0,7305	0,9104	-0,6457	1,0000	-0,0491
0,7569	-0,5981	0,7305	1,0000	-0,4512	0,7807	-0,0491	1,0000

In all cases, it seems difficult to estimate the two parameters β_1 and β_2 simultaneously, because of the large relative standard deviation $\sigma_{\hat{\beta}_2} / \beta_2 = \sigma_{\hat{\lambda}} / \lambda = \left([\text{rcov}(\hat{\beta})]_{22} \right)^{1/2}$ of β_2 in each of the four cases.

6.4 Simplified study with a two-parameter model

To simplify, let us consider the case with no heat loss ($h = 0$). Since the heat losses are completely uncorrelated with the other parameters at short times (until the maximum of the thermogram). So, introduction of the heat loss coefficients will have no consequences in the estimation of the two parameters which are looked for the liquid.

To get rid of the influence of the parameter Q/S , which acts as a proportionality constant in model (104), we will work with the reduced thermogram defined by:

$$\theta(t, \beta_1, \beta_2) = \frac{T(t, \beta_1, \beta_2, \beta_3)}{T_{\max}(\beta_2, \beta_3)} \tag{112}$$

The four examples previously presented are given in **Figure 26** and

Table 9.

In some cases, the correlation between the parameters β_1 and β_2 is large (greater than 0.99). The first idea is to seek a new couple of parameters which would be less correlated and thus could be estimated under better conditions but it is unfortunately impossible as shown in the previous section.

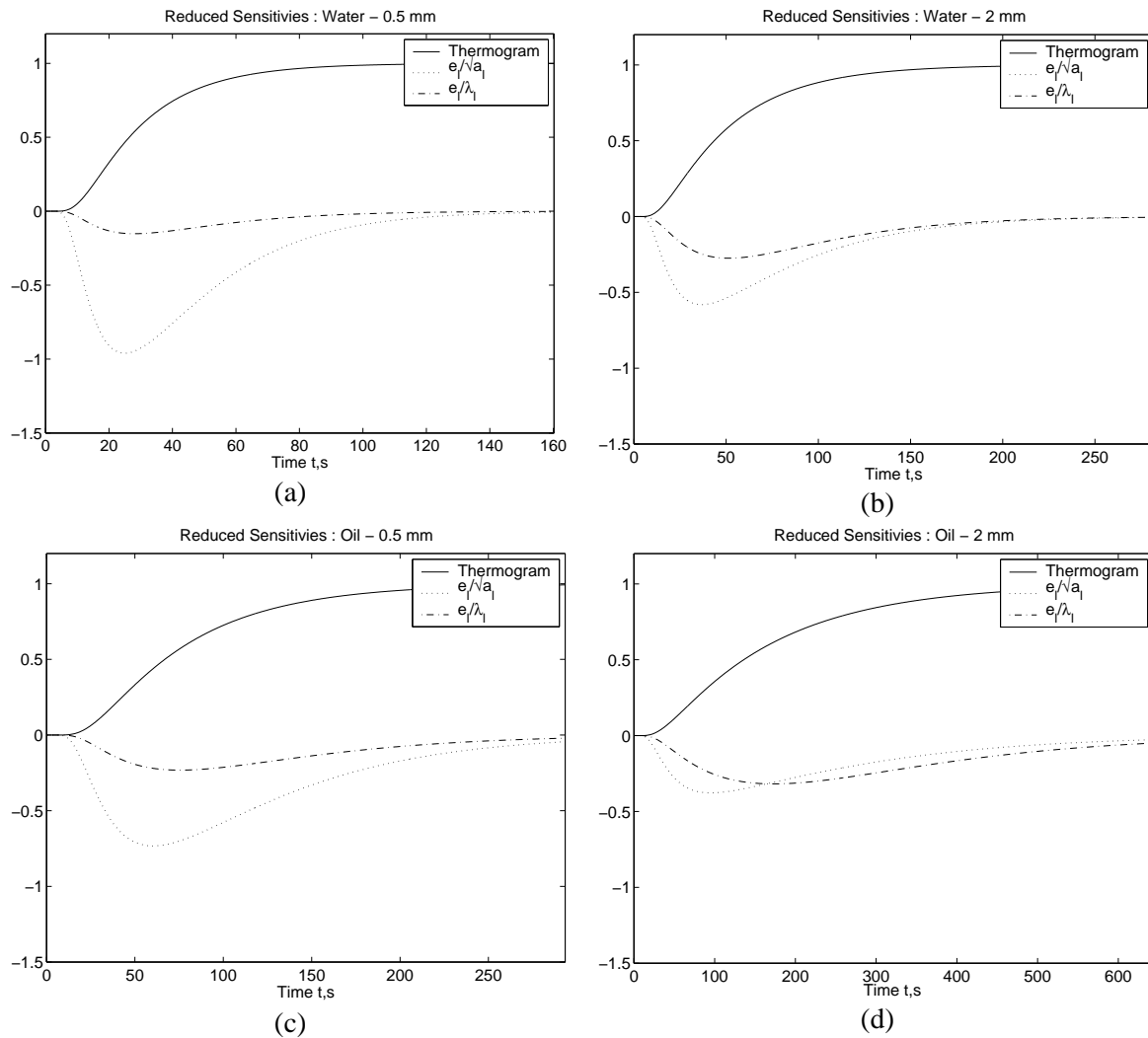


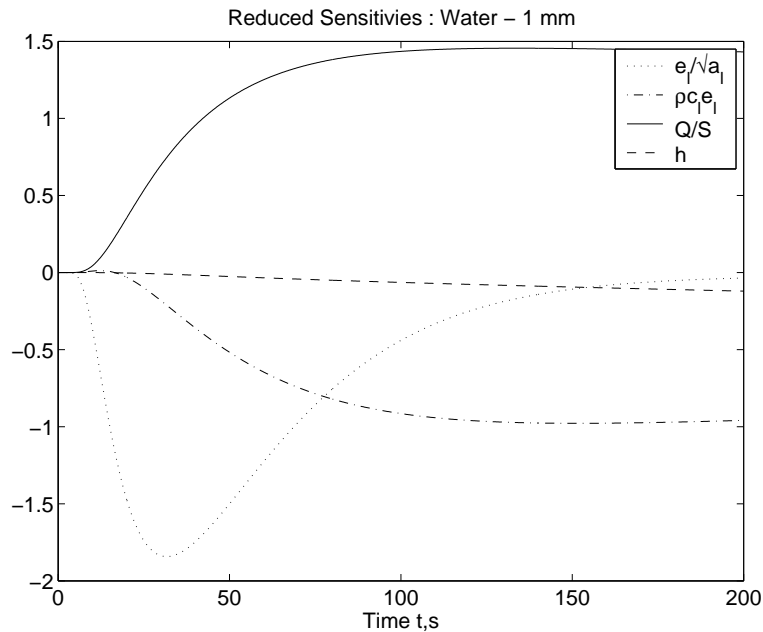
Figure 26: *Reduced Thermograms and Sensitivity curves of the two-parameter model for Water and Oil (0,5 mm and 2 mm)*

Table 9: Covariance and Correlation Matrices - two-parameter model

Water				Oil			
0,5 mm		2 mm		0,5 mm		2 mm	
Covariance				Covariance			
0.5007	-3.0373	0.2369	-0.4378	0.1911	-0.5548	0.1977	-0.1851
-3.0373	18.6223	-0.4378	0.8622	-0.5548	1.6662	-0.1851	0.1979
Correlation				Correlation			
1.0000	-0.9947	1.0000	-0.9688	1.0000	-0.9832	1.0000	-0.9358
-0.9947	1.0000	-0.9688	1.0000	-0.9832	1.0000	-0.9358	1.0000

6.5 Change in the definition of the parameters

However, there is a physical limitation with this theoretical approach. The parameter $\beta_2 = e_l/\lambda_l$ is unknown since it is the quantity that one seeks to measure. Then, it seems to be more relevant, if necessary, to introduce a parameter that one will be able to measure in an additional experiment, for instance $\rho c_l e_l$ here.



Fluid (Water) [$e_f=4.5$ mm, $\lambda_f = 0.597$ W.m⁻¹.K⁻¹, $a_l=1.43.10^{-7}$ m².s⁻¹, $\rho c_l = 4.17.10^6$ J.m⁻³.K⁻¹]
 Walls (Copper) [$e_w=1$ mm, $\lambda_w=395$ W.m⁻¹.K⁻¹, $a_w=1.15.10^{-4}$ m².s⁻¹, $\rho c_w = 3.43.10^6$ J.m⁻³.K⁻¹]
 $H=5$ W.m⁻².K⁻¹ – $Q/S=4.10^4$ J.m⁻²

Figure 27: Sensitivity curves - dimensional signal with the β' parameter vector

As it is impossible in all cases to eliminate a parameter and knowing that the parameters substitution does not have any influence on the quality of the estimation (if one keeps the same number of parameters), one chooses now:

$$\beta' = [\beta_1' = \beta_1 = e_l / \sqrt{a_l} \quad \beta_2' = \rho c_l e_l \quad \beta_3' = \beta_3 = Q/S \quad \beta_4' = \beta_4 = h]^T$$

In difficult cases, one will fix β_2 to its nominal value (as the standard deviation on β_2 is too large).?

Figure 27 gives an example of sensitivity curves obtained from the four parameters ($e_l/\sqrt{a_l}$, $\rho c_l e_l$, Q/S and h) β' dimensional model and the three parameters (β_2 being fixed in this case) models. **Table 10** gives the corresponding covariance and correlation matrices. One can observe that the variances and the correlations are strongly improved as β_2 is fixed.

Table 10: Reduced covariance and correlation matrices

Water – 1 mm							
4 parameters: $e_i/\sqrt{a_i}$, $\rho c_i e_i$, Q/Sand h				3 parameters ($\rho c_i e_i$ fixed): $e_i/\sqrt{a_i}$, Q/Sand h			
Covariance				Covariance			
0.2567	1.5697	1.0776	0.0993	0.0057	0.0094	0.1353	
1.5697	9.8171	6.6809	-0.2249	0.0094	0.0208	0.3121	
1.0776	6.6809	4.5673	0.1590	0.1353	0.3121	4.8955	
0.0993	-0.2249	0.1590	4.9007				
Correlation				Correlation			
1.0000	0.9888	0.9952	0.0886	1.0000	0.8596	0.8074	
0.9888	1.0000	0.9977	-0.0324	0.8596	1.0000	0.9777	
0.9952	0.9977	1.0000	0.0336	0.8074	0.9777	1.0000	
0.0886	-0.0324	0.0336	1.0000				

As shown in this section, by fixing parameters, we can improve the estimation of a particular parameter. By reducing the number of parameters, we have improved the estimation of the remaining parameters but we have also introduced a systematic error. We will show in the next and last section how it is possible to estimate this bias by taking it into account, to reduce the corresponding systematic errors on the estimated parameters.

7. Taking the bias into account to reduce the variances on estimated parameters: case of the flash method [1]

In this section, we will show through a simple example how it is possible to reduce the variances on estimated parameters by taking into account the bias caused by the use of a reduced model. We have already shown in Section 3.3.4 that in the case of a biased model, where the structure (58) of the model is wrong (a drift $b_y(t)$ in the recording system base line there), the estimated parameters are biased and the residuals curve is signed. We also have shown that the bias on the estimated parameters depends on the length of the time interval. The idea is then to estimate the bias on the estimated parameters from the residuals curve using a time variable estimation interval: it will concern either the case of an error in the structure of the model, or the case of an error on the nominal value of a subset of parameters of the parameter vector. In this last case only a part of the parameter vector is estimated while its complementary part is assumed to be known and taken equal to its nominal value that differs from its exact value.

7.1 Modelling

The Flash experiment consists in a uniform in space heat pulse stimulation of a sample with a very short duration (Dirac). The rear face temperature evolution is then considered and allows the estimation of the thermal diffusivity. Different non-ideal aspects as heat losses with the surrounding are then considered. The sample is assumed cylindrical with a thickness e and a radius R . This sample is submitted to an impulsed flux: $\varphi(t) = Q \delta(t)$, where Q is the energy absorbed by unit area of the front face absorbed energy ($W.m^{-2}$).

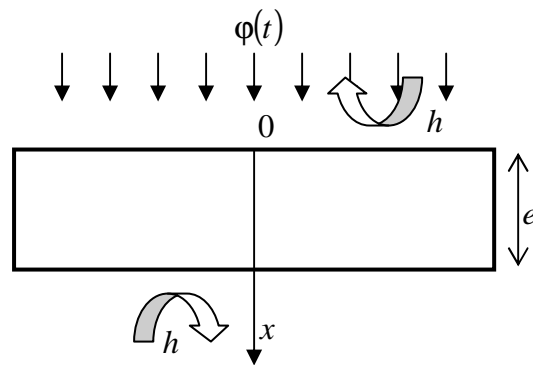


Figure 28: Principle of the Flash Method

Heat transfer in 1D is given by :

$$\frac{\partial^2 T}{\partial x^2} = \frac{1}{a} \frac{\partial T}{\partial t} \tag{113}$$

with the following boundary conditions:

$$\begin{cases} \text{at } t = 0, & T = 0 \\ \text{in } x = 0, & \lambda \frac{\partial T}{\partial x} = hT - \varphi(t) \\ \text{in } x = e, & -\lambda \frac{\partial T}{\partial x} = hT \end{cases} \tag{114}$$

The solution can be easily obtained using a Laplace transform and is a function of two independent parameters:

$$T(t; \boldsymbol{\beta}) = \frac{Q}{\rho c e} f\left(\frac{a}{e^2} t, \frac{he}{\lambda}\right) \text{ or } \mathbf{L} [T(x, t; \boldsymbol{\beta})] = \frac{Q}{C + 2hA + h^2 B} \tag{115a}$$

with $A = \cosh(e\sqrt{p/a})$ $B = \frac{1}{\lambda\sqrt{p/a}} \sinh(e\sqrt{p/a})$ $C = \lambda\sqrt{p/a} \sinh(e\sqrt{p/a})$

The “unknown” parameters are:

- the **characteristic frequency** (inverse of the characteristic time t_c): $\nu = \frac{a}{e^2}$, $t_c = 1/\nu$
- the **Biot number** (heat losses): $Bi = \frac{he}{\lambda}$

The “unknown “ parameters” vector is defined by : $\boldsymbol{\beta} = \begin{pmatrix} \nu \\ Bi \end{pmatrix}$

A third parameter is present in the response (116), the adiabatic asymptotic temperature, $T_{adia} = \frac{Q}{\rho c e}$, which is the maximum temperature that can be reached if no losses occur in the experiment, that is if $Bi = 0$.

In order to get a simpler model, a normalization is made here, using the maximum temperature T_{max} of the thermogram, which can be evaluated on an experimental basis:

$$T_{max} = T_{adia} f(\nu t_{max}, Bi) \quad \text{with} \quad \nu t_{max} = F(Bi) \quad (115b)$$

where t_{max} is the time this maximum occurs and F a function defining the corresponding Fourier number νt_{max} . This allows to get a scaled temperature model T^* , with only two parameters:

$$T^* = \frac{T}{T_{max}} = \frac{T_{adia} f(\nu t, Bi)}{T_{adia} f(\nu t_{max}, Bi)} = \frac{f(\nu t, Bi)}{f(F(Bi), Bi)} = g(\nu t, Bi) \quad (116)$$

We will assume now on that the exact values of these parameters are :

$$\nu^{exact} = 0.1 \text{ s}$$

$$Bi^{exact} = 0.05$$

7.2 Estimation with no bias

The results of an inversion with a pseudo-experimental measurement are shown in **Figure 29**. Temperature T has been calculated by application of model (115a) for a simulated acquisition time step $\Delta t = 0.01 \text{ s}$, that is for $m = 1000$ measurement $t_i = i \Delta t$ with $i \in [1 m]$, with the exact values of β . This temperature theoretical signal is then scaled by division by its maximum to get the scaled temperature T_i^* at any time t_i , which has been corrupted by an additive independent noise ε_i of standard deviation $\sigma = 0.01$ to get a simulated experimental thermogram $y_i = T_i^* + \varepsilon_i$.

Let us note that this scaled standard deviation corresponds in fact to the inverse of the signal over noise ratio of the original temperature signal. The recalculated scaled temperature $T_i^* = g(\hat{\nu} t_i, \hat{Bi})$ as well as the corresponding residuals $r_i = y_i - T_i^*$, are shown in Figure 29.

The following estimates have been obtained through normalized least squares:

$$\begin{bmatrix} \hat{\nu} \\ \hat{Bi} \end{bmatrix} = \begin{bmatrix} 0.099998 \text{ s}^{-1} \\ 0.049987 \end{bmatrix} \quad (117)$$

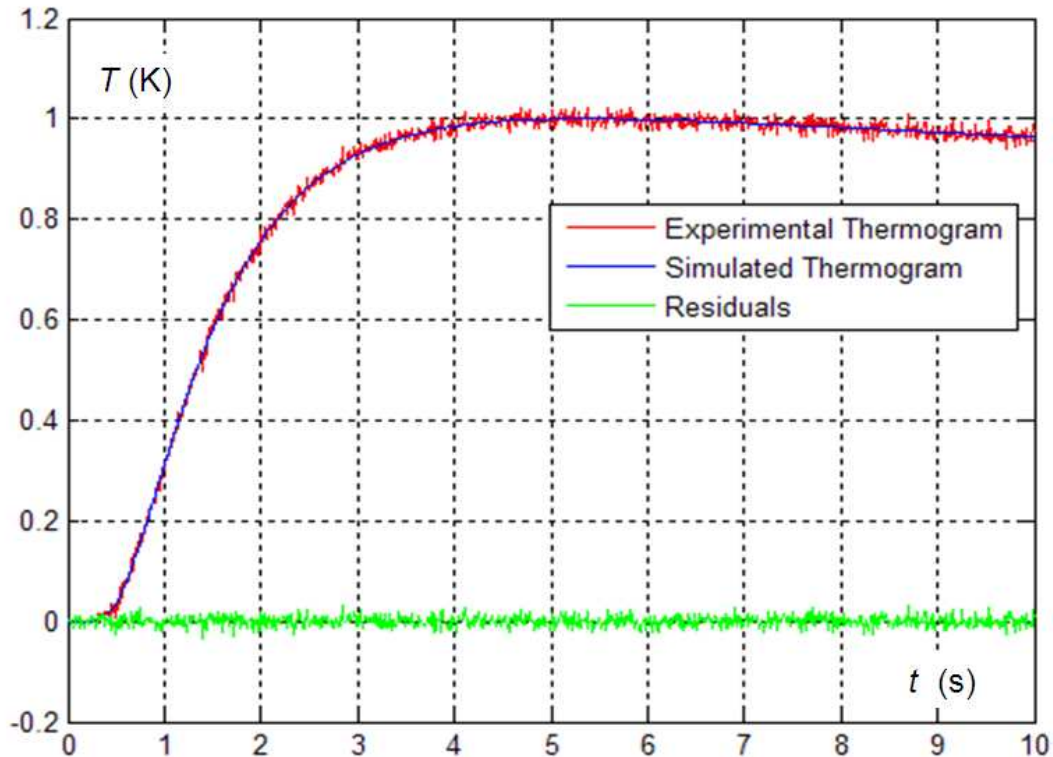


Figure 29: Estimation from a thermogram corrupted by noise

Figure 29 Comparison of the recalculated thermogram (calculated from the estimated values of the « unknown » parameters given by a Levenberg-Marquardt algorithm: O.L.S minimization) with the (synthetic noised thermogram indicated as "experimental" in the plot) and residual plot in green (difference between direct exact model corrupted by noise of standard deviation and recalculated thermogram).

The errors (absolute and relative) on both parameters can be calculated. They are quite low:

$$\begin{bmatrix} e_v = \hat{v} - v^{exacy} \\ e_{Bi} = \hat{Bi} - Bi^{exact} \end{bmatrix} = \begin{bmatrix} 2 \cdot 10^{-6} \text{ s}^{-1} \\ 1.3 \cdot 10^{-5} \end{bmatrix} \Rightarrow \begin{bmatrix} e_v / v^{exact} \\ e_{Bi} / Bi^{exact} \end{bmatrix} = \begin{bmatrix} 0.002 \% \\ 0.026 \% \end{bmatrix} \quad (118)$$

These errors can be still reduced by repetition of experiments and calculation of the corresponding statistical deviations of the corresponding estimations, since there is no bias in the model:

$$E(\hat{\beta}) = \beta^{exact} \quad (119)$$

It is also possible to compare them to their corresponding stochastic levels using the variance-covariance matrix of the OLS estimator:

$$\begin{aligned} \begin{bmatrix} \text{var}(\hat{v}) \\ \text{var}(\hat{Bi}) \end{bmatrix} &= \sigma^2 \text{diag}((\mathbf{S}^T \mathbf{S})^{-1}) = \begin{bmatrix} 0.0243 \cdot 10^{-9} \text{ s}^{-2} \\ 0.9003 \cdot 10^{-9} \end{bmatrix} \Rightarrow \begin{bmatrix} \sigma_{\hat{v}} \\ \sigma_{\hat{Bi}} \end{bmatrix} = \begin{bmatrix} 4.9 \cdot 10^{-6} \text{ s}^{-1} \\ 3 \cdot 10^{-5} \end{bmatrix} \\ &\Rightarrow \begin{bmatrix} \sigma_{\hat{v}} / v^{exact} \\ e_{Bi} / Bi^{exact} \end{bmatrix} = \begin{bmatrix} 0.005 \% \\ 0.060 \% \end{bmatrix} \end{aligned} \quad (120)$$

7.3 Estimation with a bias: whole domain approach

Even if the previous estimation is excellent, in terms of estimation errors, we will try now to reduce the number of “unknown” parameters involved in the theoretical model by setting the second parameter Bi to a nominal value Bi^{nom} that differs from its exact value. So the same technique already presented in section 3, with a decomposition of the parameter vector into two parts:

$$\boldsymbol{\beta} = \begin{bmatrix} \boldsymbol{\beta}_r \\ \boldsymbol{\beta}_c \end{bmatrix} \quad \text{with} \quad \boldsymbol{\beta}_r = [v] \quad \boldsymbol{\beta}_c = [Bi] \quad (121)$$

Only the first part $\boldsymbol{\beta}_r$, which is composed of r parameters, will be estimated while its complementary part, composed of $n - nr$ parameters, is supposed to be known. This second part will be blocked to a wrong nominal value $\boldsymbol{\beta}_c^{nom} = Bi^{nom} = 0.04$ here. So a deterministic error $\mathbf{e}_{\boldsymbol{\beta}_c} \equiv \boldsymbol{\beta}_c^{nom} - \boldsymbol{\beta}_c^{exact}$ will add its effect to the noise, in the $\boldsymbol{\beta}_r$ estimation process.

This means that estimation of $\boldsymbol{\beta}_r$ will be made with a biased model $\mathbf{y}_{mo}^{biased}(\mathbf{t}; \boldsymbol{\beta}_r) = \mathbf{T}^*(\mathbf{t}; \boldsymbol{\beta}_r, \boldsymbol{\beta}_c^{nom})$ instead of the right one, $\mathbf{y}_{mo}(\mathbf{t}; \boldsymbol{\beta}_r) = \mathbf{T}^*(\mathbf{t}; \boldsymbol{\beta}_r, \boldsymbol{\beta}_c^{exact})$, which means that an output bias appears:

$$\mathbf{b}_y(\mathbf{t}) \equiv \mathbf{y}_{mo}^{biased}(\mathbf{t}; \boldsymbol{\beta}_r) - \mathbf{y}_{mo}(\mathbf{t}; \boldsymbol{\beta}_r^{exact}) \approx \mathbf{S}_c \mathbf{e}_{\boldsymbol{\beta}_c} \quad \text{with} \quad \mathbf{t} = [t_1 \quad t_2 \quad \dots \quad t_m]^T \quad (122a)$$

The last approximation derives from a first order approximation around the nominal values of both $\boldsymbol{\beta}_r$ and $\boldsymbol{\beta}_c$. So, at a given time, the experimental signal can be written the following way:

$$y_i = y_{mo}(t_i; \boldsymbol{\beta}_r) + \varepsilon_i = y_{mo}^{biased}(t_i; \boldsymbol{\beta}_r) - b_y(t_i) + \varepsilon_i \quad (122b)$$

The corresponding deterministic error $\mathbf{e}_{\boldsymbol{\beta}_c}$ for this parameter will produce a bias $\mathbf{b}_{\hat{\boldsymbol{\beta}}_r}$ for the estimation of $\boldsymbol{\beta}_r$, see equation (93c), which is recalled here:

$$\mathbf{b}_{\hat{\boldsymbol{\beta}}_r} = -(\mathbf{S}_r^T \mathbf{S}_r)^{-1} \mathbf{S}_r^T \mathbf{b}_y(\mathbf{t}) \quad \text{with} \quad \mathbf{b}_{\hat{\boldsymbol{\beta}}_r} \equiv \mathbb{E}(\hat{\boldsymbol{\beta}}_r) - \boldsymbol{\beta}_r^{exact} \quad \text{and} \quad \mathbf{b}_y(\mathbf{t}) = \mathbf{S}_c \mathbf{e}_{\boldsymbol{\beta}_c} \quad (122c, d, e)$$

Up to now it has been assumed that the structure of the model is known (sensitivity to both set of parameters $\boldsymbol{\beta}_r$ and $\boldsymbol{\beta}_c$ are available) and that the estimation bias for $\boldsymbol{\beta}_r$ stems from an error of the parameters $\boldsymbol{\beta}_c$ that are supposed to be known and that are fixed to a wrong value $\boldsymbol{\beta}_c^{nom}$. Equation

(122c to e) corresponds to a generalization of this approach: one considers now that the error lies in the structure of the model, without any specific reference to the fixed parameters.

In order to analyse the effect of estimating with a biased model, synthetic measurements, using the exact model (116), $T^* = g(v^{exact} t; B_i^{exact}) = y_{mo}(t; \beta_r, \beta_c)$ have been generated on the [0 10 s] time interval, in the absence of noise ($\sigma = 0$) and an OLS estimation of $\beta_r = v$, using the same model (116), but with the nominal value of $\beta_c = B_i^{nom}$ has been implemented: this means that the biased model has been used for inversion. OLS estimation over this time interval yields $\hat{\beta}_r = 0.101096 \text{ s}^{-1}$, that is a bias $b_{\beta_r} = 0.001096 \text{ s}^{-1}$ hence, through application of its definition (122d).

Direct application of (122c and e) for $e_{\beta_c} = -0.01$ yields $b_{\hat{\beta}_r} = 0.01095 \text{ s}^{-1}$, that is $E(\hat{\beta}_r) = 0.101095 \text{ s}^{-1}$, which is a value quite close to $\hat{\beta}_r$.

The corresponding simulated 'experimental' biased residuals $y_{mo}(t_i; \hat{\beta}_r, \beta_c^{nom})$ (red line) as well as the residuals of the unbiased estimation (green line), are plotted in **Figure 30**. The corresponding theoretical bias $b_y(t)$, calculated using equation (122e) is also plotted (blue line): this constitutes a validation of this equation.

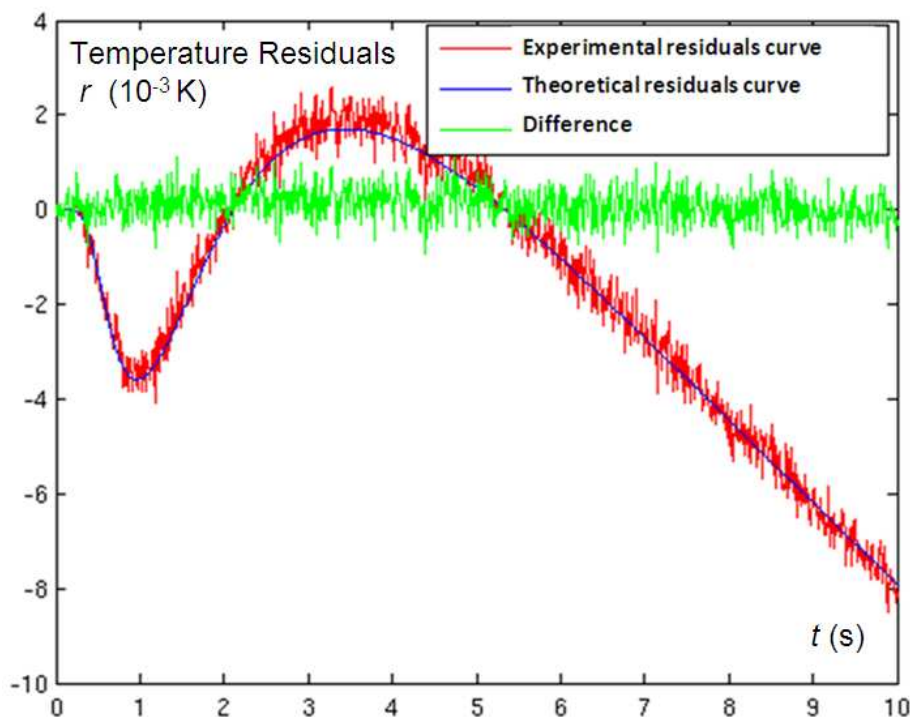


Figure 30: Residuals curve in the case of the biased (red) or a unbiased (green) model and theoretical biased residuals (blue, equation 112e)

In case of noisy measurements (independent and identically distributed noise, with a standard deviation σ), it is very useful to look for the expression of the estimation error. It is a column vector defined as:

$$\mathbf{e}_{\hat{\beta}_r} = \hat{\beta}_r - \beta_r^{exact} = \hat{\beta}_r - E(\hat{\beta}_r) + E(\hat{\beta}_r) - \beta_r^{exact} = \hat{\beta}_r - E(\hat{\beta}_r) + \mathbf{b}_{\hat{\beta}_r} \quad (123)$$

So the estimation error for $\hat{\beta}_r$ is composed of a stochastic part $\hat{\beta}_r - E(\hat{\beta}_r)$ caused by noise $\boldsymbol{\varepsilon}$ in the measurement output temperature signal, and of a deterministic part, the previous bias $\mathbf{b}_{\hat{\beta}_r}$, caused by the error \mathbf{e}_{β_c} on the fixed nominal value β_c^{nom} in the non estimated part of the parameter vector.

The magnitude of this error can be quantified if the expectancy of the square of its "length" (or of its norm, if all the parameters present in the original parameter vectors have the same unit):

$$E(\mathbf{e}_{\hat{\beta}_r}^t \mathbf{e}_{\hat{\beta}_r}) = E(\hat{\beta}_r - E(\hat{\beta}_r))^2 + \mathbf{b}_{\hat{\beta}_r}^T \mathbf{b}_{\hat{\beta}_r} = \text{cov}(\hat{\beta}_r) + \mathbf{b}_{\hat{\beta}_r}^T \mathbf{b}_{\hat{\beta}_r} \quad (124)$$

Using equations (122a) and the expression (14) of the variance-covariance matrix of an unbiased estimator:

$$E(\mathbf{e}_{\hat{\beta}_r}^t \mathbf{e}_{\hat{\beta}_r}) = \sigma^2 (\mathbf{S}_r^t \mathbf{S}_r)^{-1} + \mathbf{e}_{\beta_c}^T \mathbf{S}_c^T \mathbf{S}_r (\mathbf{S}_r^T \mathbf{S}_r)^{-2} \mathbf{S}_r^T \mathbf{S}_c \mathbf{e}_{\beta_c} \quad (125)$$

In the present case, both β_r and β_c are scalars and this equation corresponds to a "modified" variance of the estimation error:

$$\text{mvar}(\hat{\nu}) = E((\hat{\nu} - \nu^{exact})^2) = \text{var}(\hat{\nu}) + b_{\hat{\nu}}^2 = \frac{\sigma^2}{\mathbf{S}_r^t \mathbf{S}_r} + b_{\hat{\nu}}^2 \quad (126)$$

In case of a noise of standard deviation $\sigma = 0.01$ K and an estimation over the [0 10 s] time interval, the value of this modified variance is $\text{mvar}(\hat{\nu}) = 1.2031 \cdot 10^{-6} \text{ s}^2$, with a stochastic component $\text{var}(\hat{\nu}) = 1.4 \cdot 10^{-11} \text{ s}^2$ and a deterministic component $b_{\hat{\nu}}^2 = 1.2031 \cdot 10^{-6} \text{ s}^2$: the bias is then the dominant component of the estimation error, with a relative error $\sqrt{\text{mvar}(\hat{\nu})} / \nu^{exact} \approx b_{\hat{\nu}} / \nu^{exact} = 1.1 \%$.

It is possible to link the residual vector to the preceding systematic error \mathbf{e}_{β_c} and to the noise, using now the more general notation $T = y_{mo}(t; \beta_r, \beta_c)$, instead of (116) for the model output :

$$\begin{aligned} r &= \mathbf{y} - \mathbf{y}_{mo}(t; \hat{\beta}_r, \beta_c^{nom}) = \mathbf{y}_{mo}(t; \beta_r^{exact}, \beta_c^{exact}) + \boldsymbol{\varepsilon} - \mathbf{y}_{mo}(t; \hat{\beta}_r, \beta_c^{nom}) \\ r &= \boldsymbol{\varepsilon} - \mathbf{S}_r(\hat{\beta}_r - \beta_r^{exact}) - \mathbf{S}_c(\beta_c^{nom} - \beta_c^{exact}) \\ \text{with } \mathbf{S}_r &= \mathbf{S}_r(t; \hat{\beta}_r, \beta_c^{nom}) \text{ and } \mathbf{S}_c = \mathbf{S}_c(t; \hat{\beta}_r, \beta_c^{nom}) \text{ and } \mathbf{S} = [\mathbf{S}_r \ \mathbf{S}_c] \\ r &= \boldsymbol{\varepsilon} - \mathbf{S}_r(\hat{\beta}_r - E(\hat{\beta}_r) + \mathbf{b}_{\hat{\beta}_r}) - \mathbf{S}_c \mathbf{e}_{\beta_c} \end{aligned} \quad (127)$$

Use of equation (122) and the fact that the stochastic part of the error in $\hat{\beta}_r$ is:

$$\hat{\beta}_r - E(\hat{\beta}_r) = (\mathbf{S}_r^T \mathbf{S}_r)^{-1} \mathbf{S}_r^T \boldsymbol{\varepsilon} \quad (128)$$

yields:

$$\mathbf{r} = \left(\mathbf{I} - \mathbf{S}_r (\mathbf{S}_r^T \mathbf{S}_r)^{-1} \mathbf{S}_r^T \right) (\boldsymbol{\varepsilon} - \mathbf{S}_c \mathbf{e}_{\beta_c}) \quad (129)$$

Taking the expectancy of this expression of the residual vector yields:

$$E(\mathbf{r}) = \mathbf{A} (-\mathbf{S}_c \mathbf{e}_{\beta_c}) \quad \text{with} \quad \mathbf{A} = \mathbf{I} - \mathbf{S}_r (\mathbf{S}_r^T \mathbf{S}_r)^{-1} \mathbf{S}_r^T \quad (130)$$

This equations shows that the modelled residual vector is a linear function of the deterministic error $\mathbf{S}_c \mathbf{e}_{\beta_c} = \mathbf{y}(\mathbf{t}; \boldsymbol{\beta}_r^{\text{exact}}, \boldsymbol{\beta}_c^{\text{nom}}) - \mathbf{y}(\mathbf{t}; \boldsymbol{\beta}_r^{\text{exact}}, \boldsymbol{\beta}_c^{\text{exact}})$ for the temperature output induced by the error in the nominal value of the fixed part $\boldsymbol{\beta}_c^{\text{nom}}$ of the parameter vector $\boldsymbol{\beta}$. However, it is not possible to use this model to estimate $\mathbf{S}_c \mathbf{e}_{\beta_c}$ because matrix $\mathbf{A} = \mathbf{I} - \mathbf{S}_r (\mathbf{S}_r^T \mathbf{S}_r)^{-1} \mathbf{S}_r^T$ is idempotent (the corresponding linear operator is also called a projector):

$$\mathbf{A} = \mathbf{A}^2 = \mathbf{A}^3 = \dots$$

Since matrix \mathbf{A} is idempotent, it is also singular and its inverse does not exist. This forbids the use of model (130) to estimate the error $\mathbf{S}_c \mathbf{e}_{\beta_c}$ and hence to correct $\boldsymbol{\beta}_c$.

However, interesting conclusions can be drawn from equations (122a) and (130):

- if $\mathbf{e}_{\beta_c} = \mathbf{0}$ then the residuals are not signed: $E(\mathbf{r}) = \mathbf{0}$ and the bias $\mathbf{b}_{\hat{\beta}_r}$ is equal to zero.
- if $\mathbf{e}_{\beta_c} \neq \mathbf{0}$ then the residuals are signed: $E(\mathbf{r}) \neq \mathbf{0}$
- if $\mathbf{S}_r^T \mathbf{S}_c = \mathbf{0}$, the sensitivities to the parameter present in $\boldsymbol{\beta}_r^{\text{nom}}$ are completely uncorrelated with those present in $\boldsymbol{\beta}_c^{\text{nom}}$ (the corresponding two subspaces of \mathbf{R}^{nr} and \mathbf{R}^{n-nr} are orthogonal) and there is no bias for $\hat{\beta}_r$, whatever the error for $\boldsymbol{\beta}_c^{\text{nom}}$. In this case, the residuals are still signed, with an expectancy $E(\mathbf{r}) = -\mathbf{S}_c \mathbf{e}_{\beta_c}$.

The residual curves for OLS estimations with $t_{\text{end}} = t_m = 10 \text{ s}$ using either the unbiased model (green, already shown in figure 29) or the biased one (red) are shown in **Figure 30**.

7.4 Estimation with a bias: use of a variable estimation time interval

In the discussion of the different cases presented above, one can see that if either the sensitivities to the parameters present in β_r^{nom} are linearly independent of those present in β_c^{nom} (case where $S_r^T S_c = 0$ which implies $E(r) = -S_c e_{\beta_c}$ and $b_{\hat{\beta}_r} = 0$), or if there is no error for β_c^{nom} ($e_{\beta_c} = 0$ which implies $E(r) = 0$ and $b_{\hat{\beta}_r} = 0$) the residuals do not depend on the estimation time interval considered.

So, in the general case where these two assumptions do not hold, the estimate of β_r depends on this interval: one can thus vary the length of the time interval (initial value $[t_1 \ t_m]$) which can become $[t_1 \ t_p = t_{end}]$ with $p \leq m$. So this estimate, that can be noted $\hat{\beta}_r(t_{end})$ depends on the final time t_{end} of the estimation interval considered.

Consequently model (122a) is recast for the bias:

$$b_{\hat{\beta}_r}(t_{end}) = E(\hat{\beta}_r(t_{end})) - \beta_r^{exact} = -\left(S_r^T(t_{end}) S_r(t_{end})\right)^{-1} S_r^T(t_{end}) S_c(t_{end}) e_{\beta_c} \quad (131)$$

and it can be written for two final times $t_{end} = t_a$ and $t_{end} = t_b$, with $t_b > t_a$. Subtracting the corresponding two equations allows to get a model whose output, the expectancy of the difference of the two estimates, can be evaluated:

$$\Delta b_{\hat{\beta}_{r,ab}} = E(\hat{\beta}_{r,b} - \hat{\beta}_{r,a}) = -\left[\left(S_{r,b}^T S_{r,b}\right)^{-1} S_{r,b}^T S_{c,b} - \left(S_{r,a}^T S_{r,a}\right)^{-1} S_{r,a}^T S_{c,a}\right] e_{\beta_c} \quad (132)$$

where $S_{r,k} = S_r(t_{end,k})$; $S_{c,k} = S_c(t_{end,k})$ and $\hat{\beta}_{r,k} = \hat{\beta}_r(t_{end,k})$ for $k = a$ or b

Writing the two sensitivity matrices over the two intervals $[t_1 \ t_a]$ and $[t_1 \ t_b]$ yields:

$$S_{r,b} = \begin{bmatrix} S_{r,a} \\ S_{r,ab} \end{bmatrix} \quad \text{and} \quad S_{c,b} = \begin{bmatrix} S_{c,a} \\ S_{c,ab} \end{bmatrix} \quad \Rightarrow \quad S_{r,b}^T S_{c,b} = S_{r,a}^T S_{c,a} + S_{r,ab}^T S_{c,ab} \quad (133)$$

where $S_{r,ab}$ and $S_{c,ab}$ are the sensitivity to both parameter sets over the $[t_{a+1} \ t_b]$ interval. Substitution of this equation into (132) yields:

$$\Delta b_{\hat{\beta}_{r,ab}} = -\left[\left(S_{r,b}^T S_{r,b}\right)^{-1} - \left(S_{r,a}^T S_{r,a}\right)^{-1}\right] S_{r,a}^T S_{c,a} + \left(S_{r,b}^T S_{r,b}\right)^{-1} S_{r,ab}^T S_{c,ab} e_{\beta_c} \quad (134)$$

If t_a and t_b are very close, it is possible to neglect the first difference in the bracket, since $\left(S_{r,b}^T S_{r,b}\right)^{-1} \approx \left(S_{r,a}^T S_{r,a}\right)^{-1}$, which yields:

$$\Delta b_{\hat{\beta}_{r,ab}} \approx -\left(S_{r,a}^T S_{r,a}\right)^{-1} S_{r,ab}^T S_{c,ab} e_{\beta_c} \quad (135)$$

If we take $b = a + 1$ and introduce the sensitivities \mathbf{S}_r of the output to the n_r parameters present in $\boldsymbol{\beta}_r$ at a single time \bar{t}_{ab} (\mathbf{S}_r is a line vector), as well as its counterpart \mathbf{S}_c for the n_c parameters present in $\boldsymbol{\beta}_c$ at the same time, the above equation becomes:

$$\Delta \mathbf{b}_{\hat{\beta}_r, ab} = -(\mathbf{S}_{r_a}^T \mathbf{S}_{r_a})^{-1} \mathbf{S}_r^T(\bar{t}_{ab}) \mathbf{S}_c(\bar{t}_{ab}) \mathbf{e}_{\beta_c} = -(\mathbf{S}_{r_a}^T \mathbf{S}_{r_a})^{-1} \mathbf{S}_r^T(\bar{t}_{ab}) b_y(\bar{t}_{ab}) \quad \text{with} \quad \bar{t}_{ab} = t_a + \Delta t / 2 \quad (136)$$

Here the bias $b_y(\bar{t}_{ab})$ in the model output defined in (122c) appears explicitly. So, the above equation can be recast under the following form:

$$\mathbf{S}_r^T(\bar{t}_{ab}) b_y(\bar{t}_{ab}) = -\mathbf{S}_{r_a}^T \mathbf{S}_{r_a} \Delta \mathbf{b}_{\hat{\beta}_r, ab} \quad (137)$$

It is possible to get a realization of $\Delta \mathbf{b}_{\hat{\beta}_r, ab}$ which is simply the difference of the two estimated values $\hat{\boldsymbol{\beta}}_{r_b}$ and $\hat{\boldsymbol{\beta}}_{r_a}$. Equation (137) corresponds to a system of n_r equations with a single unknown $b_y(\bar{t}_{ab})$. Its solution can be found in the ordinary least squares sense:

$$\hat{b}_y(\bar{t}_{ab}) = -\frac{1}{\sum_{j=1}^{n_r} \mathbf{S}_{r_j}^2(\bar{t}_{ab})} \mathbf{S}_r(\bar{t}_{ab}) \mathbf{S}_{r_a}^T \mathbf{S}_{r_a} (\hat{\boldsymbol{\beta}}_{r_b} - \hat{\boldsymbol{\beta}}_{r_a}) \quad (138)$$

If we go back to the preceding example (biased model of the flash experiment with a single parameter ν), one has $n_r = 1$ and equation (138) becomes:

$$\hat{b}_y(\bar{t}_{ab}) = \frac{\hat{\nu}_a - \hat{\nu}_b}{\mathbf{S}_\nu(\bar{t}_{ab})} \sum_{i=1}^a \mathbf{S}_\nu^2(t_i) \quad (139)$$

where $\hat{\nu}_a$ is the characteristic frequency estimated over the $[t_1 \ t_a]$ interval and $\hat{\nu}_b$ over the $[t_1 \ t_{a+1}]$ using biased model $y_{mo}^{biased}(t; \boldsymbol{\beta}_r) = g(\nu t; \mathbf{B}i^{nom}) = y_{mo}(t; \boldsymbol{\beta}_r, \boldsymbol{\beta}_c^{nom})$.

It is thus possible to plot the $\hat{b}_y(\bar{t}_{ab})$ using (139) with a varying from 2 to $m-1$.

An alternate expression of the output bias estimation (139) can be implemented with a difference $k = b - a$ larger than 1, in order to smooth the noise in the $(\hat{\nu}_b - \hat{\nu}_a)$ difference (a kind of "moving average filtering"). In this case, the estimated bias becomes:

$$\hat{b}_y(\bar{t}_{ab}) = \frac{\hat{\nu}_a - \hat{\nu}_b}{(b-a) \mathbf{S}_\nu(\bar{t}_{ab})} \sum_{i=1}^a \mathbf{S}_\nu^2(t_i) \quad \text{with} \quad \bar{t}_{ab} = \frac{t_a + t_b}{2} \quad (140)$$

Once the output bias $\hat{b}_y(t)$ estimated for each of the possible pair of intervals of the form:

$$[t_1 \ t_a] \text{ and } [t_1 \ t_{a+k}] \quad \text{for} \quad a = 2 \text{ to } m - k \quad (141)$$

one can build an output bias vector the components of which are the $m - (k + 1)$ possible times \bar{t}_{ab}

$$\hat{\mathbf{b}}_y = [\hat{b}_y(\bar{t}_{2 \ 2+k}) \ \hat{b}_y(\bar{t}_{3 \ 3+k}) \ \dots \ \hat{b}_y(\bar{t}_{m-k \ m})]^T \quad (142a)$$

and application of equation (122c), with sensitivities to the components of $\boldsymbol{\beta}_r$ calculated on the corresponding values of \bar{t}_{ab} yields a corrected value of the preceding estimator:

$$\hat{\boldsymbol{\beta}}_r^{corrected} = \hat{\boldsymbol{\beta}}_r(t_m) - \hat{\mathbf{b}}_{\hat{\boldsymbol{\beta}}_r} = \hat{\boldsymbol{\beta}}_r(t_m) + (\mathbf{S}_r^T \mathbf{S}_r)^{-1} \mathbf{S}_r^T \hat{\mathbf{b}}_y \quad (142b)$$

The first components of the estimation of the output bias vector $\hat{\mathbf{b}}_y$ are characterized by a high stochastic error, because their estimations are derived by a low number of measurement points. So, it is more interesting to use the last components, for example $\hat{b}_y(\bar{t}_{m-k \ m})$, for the estimation of the estimation bias thanks to the expectancy of the scalar form (122b) written for $\boldsymbol{\beta}_r = \hat{\boldsymbol{\beta}}_r$:

$$E(r_i) = E(y_i) - E(y_{mo}^{biased}(t_i; \hat{\boldsymbol{\beta}}_r)) = y_{mo}(t_i; \boldsymbol{\beta}_r^{exact}) - E(y_{mo}^{biased}(t_i; \boldsymbol{\beta}_r^{exact} + (\hat{\boldsymbol{\beta}}_r - \boldsymbol{\beta}_r^{exact}))) \quad (143a)$$

A first order expansion of the last expression yields:

$$E(r_i) = -\mathbf{S}_{r \ i} E(\hat{\boldsymbol{\beta}}_r - \boldsymbol{\beta}_r^{exact}) - \mathbf{S}_{c \ i} \mathbf{e}_{\beta_c} = -\mathbf{S}_{r \ i} \mathbf{b}_{\hat{\boldsymbol{\beta}}_r} - b_y(t_i) \quad (143b)$$

Once an estimation of the output bias available, for $t_i = \bar{t}_{ab} = \bar{t}_{m-k \ m}$, an observation of the residual at the same time on the $[t_1 \ t_m]$ interval yields a relationship between the estimates of $b_y(t_i)$ and of $\mathbf{b}_{\hat{\boldsymbol{\beta}}_r}$:

$$r_i = -\mathbf{S}_{r \ i} \mathbf{b}_{\hat{\boldsymbol{\beta}}_r} - \hat{b}_y(t_i) \quad (143c)$$

If one single parameter is estimated, that is if $n_r = 1$, the preceding sensitivity line vector $\mathbf{S}_{r \ i}$ at time t_i becomes a scalar, which allows an estimation $\hat{\mathbf{b}}_{\hat{\boldsymbol{\beta}}_r}$ of the estimation bias and hence the definition of a corrected estimator for $\boldsymbol{\beta}_r$:

$$\hat{\mathbf{b}}_{\hat{\boldsymbol{\beta}}_r} = -\frac{\hat{b}_y(t_i) + r_i}{\mathbf{S}_{r \ i}} \quad \Rightarrow \quad \hat{\boldsymbol{\beta}}_r^{corrected} = \hat{\boldsymbol{\beta}}_r + \frac{\hat{b}_y(t_i) + r_i}{\mathbf{S}_{r \ i}} \quad (143d)$$

Let us remind that all the previous expressions for the output bias b_y are based on the assumption associated with equation (135):

$$(t_b - t_a) / t_a \ll 1 \tag{143e}$$

7.5 Correction of the bias using a variable estimation time interval: application to the flash method

To illustrate these results, we consider the case of the Flash method. As previously shown, this problem involves two parameters: the characteristic frequency and the Biot number (heat losses).

For the simulation of an experimental curve, the following exact values are considered:

$$\begin{aligned} \nu^{exact} &= 0.1 \text{ s} \\ Bi^{exact} &= 0.05 \end{aligned}$$

To simulate a bias on this detailed model, we consider the heat losses as a “known” parameter. The value of the Biot number is fixed to a nominal value $Bi^{nom} = 0.03$. To simplify, we will consider the signal without noise (only the determinist component of the error is considered).

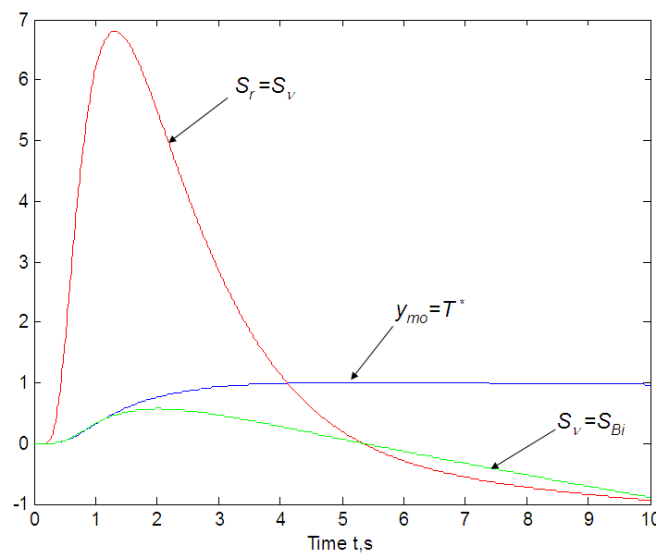


Figure 31: Thermogram with heat loss and scaled sensitivities

Theoretical thermogram (detailed model) and scaled sensitivities to “unknown” (S_r) and assumed to be “known” (S_c) parameters are plotted in **Figure 31**.

The sensitivity curves show that the thermogram is sensitive to $\beta_r = \nu$. This parameter has been estimated by an O.L.S method with the biased model. The solution is presented in **Figure 32**. It is clear that the estimated value is different of the nominal value.

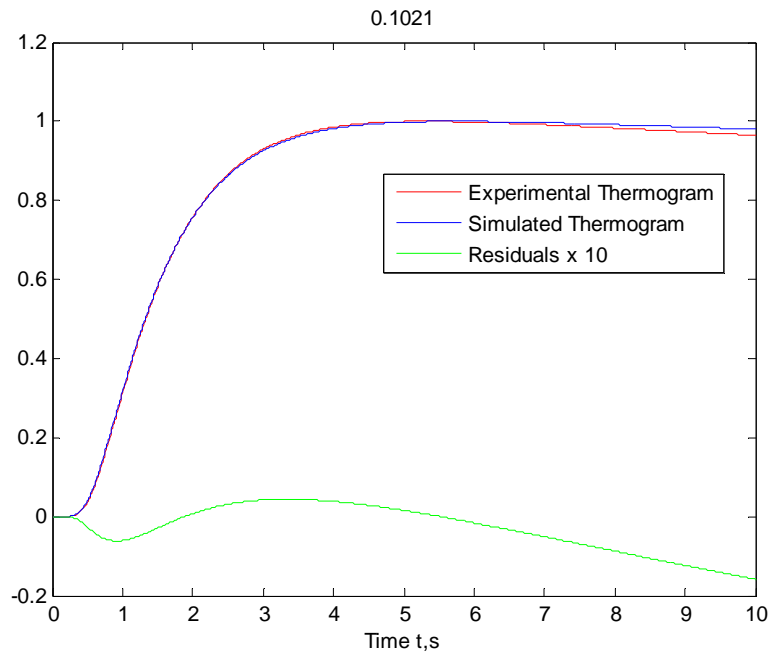


Figure 33: Original (experimental) thermogram and recalculated thermogram with $\hat{\beta}_r = \hat{\nu} = 0.1021 \text{ s}^{-1}$ and $\beta_c = \hat{B}i^{nom} = 0.03$ and residuals

If we then try to perform this estimation for different time interval lengths t_p , we can observe as illustrated in **Figure 33** a variation of the estimated characteristic frequency $\hat{\nu}(t_p)$ with the estimation duration t_p . This means, as explained before, that a bias $b_{\hat{\beta}_r} = b_{\hat{\nu}}$ exists for the estimated parameter.

This information can be used for the determination of $b_y(t_i) = S_{c i} e_{\beta_c}$. Only one point in time is required to determinate the value of the β_r parameter and consequently the bias on the estimated parameter.

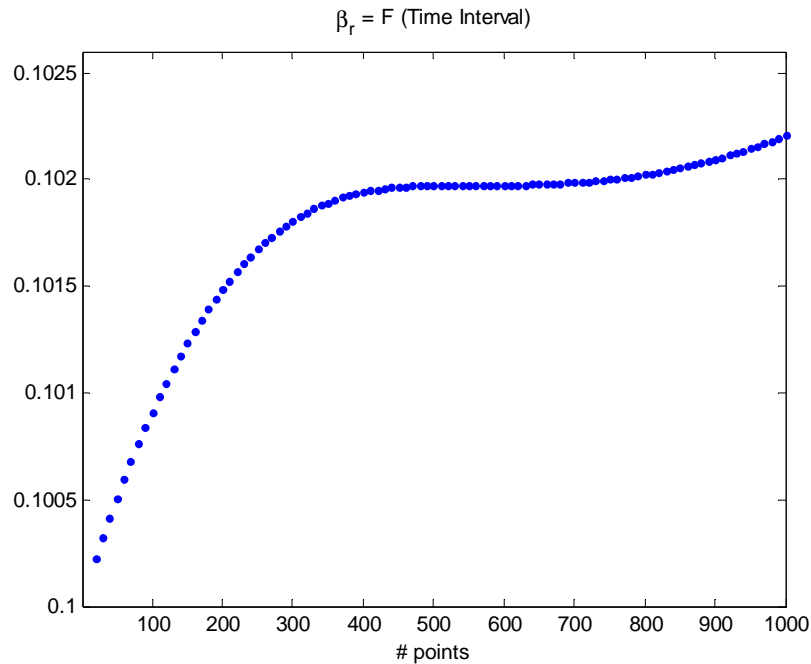


Figure 33: Evolution of estimated diffusivity $\hat{v}(t_p)$ over the $[t_1 \ t_p]$ time interval versus duration t_p for $p = 1$ to $m=1000$

In **Figure 34**, after an estimation of the output bias $\hat{b}_y(\bar{t}_{900 \ 1000}) = \hat{b}_y(t_{950} = 9.5 \text{ s})$ using equation (140), the estimation bias $b_{\hat{\beta}_r} = b_{\hat{v}} = 0.0022186 \text{ s}^{-1}$ has been calculated thanks to equation (143d). This yields a corrected estimation $\hat{\beta}_r^{\text{corrected}}$ equal to:

$$\hat{\beta}_r^{\text{corrected}} = \hat{\beta}_r - \hat{b}_{\hat{\beta}_r} = 0.10214 - 0.00222 = 0.09992 \text{ s}^{-1}$$

that is a 0.08 % difference with the exact value.

At this same time the output bias is plotted (blue point) in figure 34. This operation has been repeated for each time t_i using a moving average (140) with $k = a - b = 100$ (blue solid line).

This estimation output bias has been compared to the theoretical one $b_y(t_i) = S_{c_i} e_{\beta_c} = -0.03 S_{Bi}(t_i)$ (red solid line) which is known here. Both curves are quite similar with a time lag that probably stems from the fact that the upper bound in the summation (140) is a and not $(a+b)/2$.

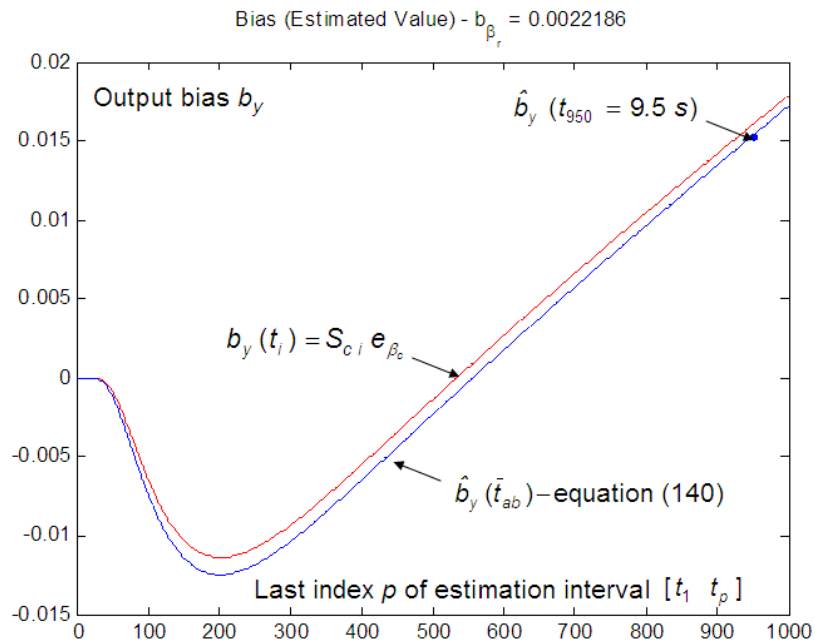


Figure 34: Comparison between theoretical and estimated output bias curves

So this method allowing the estimation of the bias on estimated parameters obtained by an inverse technique using a biased model seems to be validated by this example.

8. Conclusion

Useful tools have been introduced for the analysis of estimations (variance-covariance matrix) and the detection of the ill-conditioned character of the Parameter Estimation Problem (PEP). Different techniques have been presented for tracking the true degrees of freedom of a given PEP (matrix rank, correlations between parameters, SVD, ..). If we want to enhance the estimation of a given parameter, one solution is to use a reduced model. This reduced model can be either unbiased or biased. It is of particular interest to know if a reduced model is biased or not.

We have proposed, in the last section of the lecture, to work with a variable estimation time interval in order to evaluate the systematic error caused in the estimated parameters. We hope that the different "realistic" examples of thermal metrology presented in this lecture will help the reader to master the corresponding tools to get good estimates in a PEP.

References

- [1] Chapter 9: Nonlinear estimation techniques, B. Rémy, S. André, in *Thermal Measurements and Inverse Techniques*, 2011, Orlande H R.B., Fudym O, Maillet D and Cotta R M editors, CRC Press, Series: Heat Transfer, 770p.
- [2] J.V. Beck, K..J. Arnold, *Parameter Estimation in Engineering and Science*, John Wiley & Sons, 1977.
- [3] K. Levenberg, A method for the solution of certain problems in Least Squares, *Quart. Appl. Math.* 2, 164-168, 1944.

- [4] Gallant, A.R., 1975, Nonlinear regression, *Am. Stat.*, 29:73-81.
- [5] Andre S, Serra JJ, Cella N and Silva Neto AJ, Parameter Estimation of Thermo-optical Glass Properties From Experimental Phase Lag Signals Obtained Through Periodic Heat Flux Excitation, *Proc. 4th International Conference on Inverse Problems in Engineering: Theory and Practice*, Mai 26-31, 2002, Angra dos Reis, Brasil.
- [6] The Physical Basis of dimensional analysis, Ain A. Sonin, MIT course manuscript, 2001 <http://me.mit.edu/people/sonin/html>
- [7] Maillet D., André S., Batsale J.C., Degiovanni A. and Moyne C., *Thermal Quadrupoles : Solving the Heat equation Through Integral Transforms*, Chichester, PA: John Wiley & Sons Ltd, 2000.
- [8] B. Remy and A. Degiovanni, "*Inverse Method Applied to the Measurement of the Thermal Conductivity of Powders by a Hot Wire Technique*", ITCC26-ITES14 – 9th Int. Thermal Conductivity Conference, Boston, U.S.A (6-8 Août 2001), Vol. 19, n°3, pp. 332-340.
- [9] B. Remy and A. Degiovanni, "*Parameters Estimation and Measurement of Thermophysical Properties of Liquids*", *International Journal of Heat & Mass Transfer – Vol. 48, Issues 19-20, Septembre 2005*), pp 4103-4120.
- [10] Stehfest, H., Remarks on Algorithm 368 - Numerical Inversion of Laplace Transforms, *Communications of the ACM*, (1970) 13, pp. 624.